GEOLOGICAL, HYDROGEOLOGICAL AND GEOCHEMICAL ANALYSES OF THE GEOTHERMAL SYSTEMS IN THE BÜYÜK MENDERES GRABEN

A THESIS SUBMITTED TO
THE GRADUATE SCHOOL OF NATURAL AND APPLIED SCIENCES
OF
MIDDLE EAST TECHNICAL UNIVERSITY

BY

HATİCE GÜDÜCÜ

IN PARTIAL FULFILLMENT OF THE REQUIREMENTS
FOR
THE DEGREE OF MASTER OF SCIENCE
IN
GEOLOGICAL ENGINEERING

SEPTEMBER 2012

Approval of the thesis

GEOLOGICAL, HYDROGEOLOGICAL AND GEOCHEMICAL ANALYSES OF THE GEOTHERMAL SYSTEMS IN THE BÜYÜK MENDERES GRABEN

submitted by **HATİCE GÜDÜCÜ** in partial fulfillment of the requirements for the degree of **Master of Science in Geological Engineering, Middle East Technical University** by,

Prof. Dr. Canan Özgen
Dean, Graduate School of **Natural and Applied Sciences** _____

Prof. Dr. Erdin Bozkurt
Head of Department, **Geological Engineering** _____

Prof. Dr. Nurkan Karahanoğlu
Supervisor, **Geological Engineering, METU** _____

Examining Committee Members:

Prof. Dr. Mahmut Parlaktuna
Petroleum and Natural Gas Engineering, METU _____

Prof. Dr. Nurkan Karahanoğlu
Geological Engineering Dept., METU _____

Prof. Dr. Nilgün Güleç
Geological Engineering Dept., METU _____

Prof. Dr. Erdin Bozkurt
Geological Engineering Dept., METU _____

Assoc. Prof. Dr. Bora Rojay
Geological Engineering Dept., METU _____

Date: 28.09.2012

I hereby declare that all information in this document has been obtained and presented in accordance with academic rules and ethical conduct. I also declare that, as required by these rules and conduct, I have fully cited and referenced all material and results that are not original to this work.

Name, Last name: Hatice Güdücü

Signature :

ABSTRACT

GEOLOGICAL, HYDROGEOLOGICAL AND GEOCHEMICAL ANALYSES OF THE GEOTHERMAL SYSTEMS IN THE BÜYÜK MENDERES GRABEN

Güdücü, Hatice
M.Sc., Department of Geological Engineering
Supervisor: Prof. Dr. Nurkan Karahanoğlu

September 2012, 118 Pages

Geothermal reservoirs have become very popular in the last decades due to their renewable energy contents. Turkey has a high geothermal energy potential; especially Western Anatolia is a promising region in terms of its highest energy. Büyük Menderes Graben system is a tectonically active extensional region and is undergoing a N–S extension leading to form geothermal fields in the graben. In the last decade, geothermal exploration, investigations and investments have been increased rapidly through the law related to geothermal energy assigned.

The aim of this study is to analyze the geothermal fields located in the graben system in order to investigate their geological, hydrogeological and geochemical features and reservoir characteristics. A data set is compiled from the accessible archives, published papers and documents and several variables have been searched at every field in the graben. The variables include the fluid temperature, the distance to sea, the depth to the reservoir, the reservoir lithology, the chemical constituents, etc. In view of these variables the fields are compared and constrasted and their common

characterisrics have been noted. Interpretation of the data set reveals that the fields have some common features and characters however some fields have got notable differences.

Keywords: Büyük Menderes Graben, Geology, Hydrogeology, Hydrogeochemistry, Well Data

ÖZ

BÜYÜK MENDERES GRABEN SİSTEMİNDEKİ JEOTERMAL SAHALARIN JEOLOJİK, HİDROJEOLOJİK VE JEOKİMYASAL ANALİZİ

Güdücü, Hatice
Yüksek Lisans, Jeoloji Mühendisliği Bölümü
Tez Yöneticisi: Prof. Dr. Nurkan Karahanoğlu

Eylül 2012, 118 sayfa

Jeotermal rezervuarlar yenilenebilir enerji içeriklerinden dolayı, son yıllarda çok popüler olmuştur. Türkiye büyük bir potansiyele sahiptir; özellikle Batı Anadolu, Türkiye'de en yüksek potansiyele sahip olması açısından gelecek vadeden bir bölgedir. Büyük Menderes Graben sistemi tektonik olarak aktif bir açılma bölgesidir ve jeotermal sahaların oluşmasını sağlayan K-G doğrultusunda açılma geçirmektedir. Son on yılda, jeotermalle ilgili kanunun yürürlüğe jeotermal aramalar, incelemeler ve yatırımlar çok hızlı yükselmiştir.

Bu çalışmanın amacı, graben sisteminde yeralan jeotermal alanları jeolojik, hidrojeolojik ve hidrojeokimyasal özellikleri ve rezervuar karakteristikleri açısından analiz etmektir. Ulaşılabilen arşivlerden, yayınlan makalelerden ve dokümanlardan bir veri grubu oluşturulmuştur ve birçok değişken, grabende bulunan her sahada araştırılmıştır. Değişkenler, akışkan sıcaklığı, denize olan uzaklık, rezervuar derinliği, rezervuar litolojisi, kimyasal bileşenler ve benzeri gibi parametreleri içermektedir. Bu değişkenler göz önünde tutularak sahalar arasındaki benzerlikler ve

farklılıklar karşılaştırılmış ve genel karakteristikleri belirtilmiştir. Veri grubunun yorumlanması göstermektedir ki, sahalar bir takım ortak özellik ve karaktere sahiptir fakat bazı sahalar dikkate değer farklılıklara sahiptir.

Anahtar Sözcükler: Büyük Menderes Grabeni, Jeoloji, Hidrojeoloji, Hidrojeokimya, Veri Grubu

To My Family

ACKNOWLEDGEMENTS

It is an honor for me to express my admiration and esteem to my supervisor Prof. Nurkan KARAHANOĞLU for his understanding, continuous support, unlimited trust, supervision and patience throughout the study. His intervention on crucial points rendered the thesis a worthwhile work.

I would like to thank The General Directorate of Mineral Research and Exploration (MTA) and İzmir Directorate of Mineral Research and Exploration for the major contribution during the data compilation.

I would especially express my thanks to my dear cats, Erik and Ceviz, for their motivation and cheerful existence.

I would like to thank to my director and my co-workers for their support.

I would also like to thank to my dear friends Balkar Erdoğan, Bulut Aslan and Özge Tığlı for their contributions for the improvement of the document and any support.

I would like to express my special thanks to my family who always support and motivate me and who truly merit the dedication of this thesis.

TABLE OF CONTENTS

LIST OF TABLES

LIST OF FIGURES

FIGURES

CHAPTER 1

INTRODUCTION

“Geothermal” comes from the Greek words of geo (earth) and thermal (heat). Geothermal energy is basically interior heat of the earth. The volcanoes, hot springs, and other thermal phenomena were revealed that the interior of the Earth is hot. When the first mines were excavated to a few hundred meters below ground level in the sixteenth and seventeenth century, it was concluded that the Earth’s temperature increased with depth (Armstead, 1983). Moreover, a geothermal system can be described as ‘convecting water in the upper crust of the Earth, which, in a confined space, transfers heat from a heat source to a heat sink, usually the free surface (Hochstein, 1990).

Geothermal energy has been produced commercially for nearly a century and on scale of hundreds of MW for over four decades both for electricity generation and direct use. Geothermal resources have been identified in over 80 countries and there are quantified records of geothermal utilization in 58 countries in the world in 2000 (Çakın, 2003).

Geothermal energy is a renewable, sustainable and environmentally friendly. Moreover, it is a cheap energy type compared to fossil fuels and other renewable energy sources. Although the long-term effects are not known, it is very pleasurable energy in short-term. It is very popular at several countries and Turkey in recent years. Turkey has a great potential of geothermal energy. As it is a promising energy type, the utilization rate is accelerating.

The temperature increases with respect to increasing depth. As the depth increases about 100 m, the temperature increases about 10 ^{o}C. This is the first source of heat in earth. Other than that, geothermal energy utilized is mainly fed on hydrothermal sources. Hydrothermal sourced geothermal energy system can be comprehensively defined as a system with components, a heat source, a mobile carrier, a cap rock and a reservoir. A heat source can be volcanoes, magma or radioactive decay. The carrier is generally water through a fault zone or fractures and also the carrier can be steam. Cap rock is generally impervious rocks or layers. Reservoir is an aquifer which is porous and permeable and bearing water and steam. On the other hand, hot dry rock is a newly discovered geothermal energy source type. There is no carrier or path for the liquid in these type geothermal energy systems. The path of liquid is made artificially and the water is sent to depths more than 5 km.

Büyük Menderes graben is an E–W trending depression, over 150 km long and 10-20 km wide, bounded by active normal faults. The graben changes its direction in Ortaklar, extends NE-SW through Söke, it also intersects with Gediz graben in the east of Buldan and turns to Denizli basin from Sarayköy (Özgür, 2003). In Aydın and Denizli provinces, which are located in the Aegean Region and within the borders of Büyük Menderes graben, many geothermal fields were discovered. These are Kızıldere, Tekkehamam, Gölemezli, Yenice, Buldan areas in Denizli and Hıdırbeyli, Ömerbeyli, Bozköy, Yılmazköy, İmamköy, Salavatlı, Ilıcabaşı, Umurlu, Atça and Pamukören areas in Aydın (Karamanderesi & Ölçenoğlu, 2005).

1.1 Purpose and Scope of the Thesis

The Western Anatolia region has the greatest potential geothermal energy in Turkey. The General Directorate of Mineral Research and Exploration had started the exploration in 1960s. Countless geothermal wells had been drilled in the Büyük Menderes Graben. Several scientific researches had been done about this region for long years. After the admission of Law on Geothermal Resources and Natural Mineral Water in 2007, several companies started to explore and produce energy in Büyük Menderes Graben.

The purpose of this thesis is to compile the studies and works done about geothermal energy regions in the Büyük Menderes Graben and investigate the relationships between the fields based on their geological, hydrogeological and hydrogeochemical features.

This thesis is comprised of six chapters. Chapter 1 comprises introduction part involving purpose and scope, location of study area and a brief history of studies conducted in Büyük Menderes Graben geothermal system. Geology and tectonic evolution of Büyük Menderes Graben are described in Chapter 2. Chapter 3 presents methodology of study that involves the brief information about geothermal parameters and used parameters in this thesis. Moreover, the resource of data analyzed is mentioned in third chapter. Geological, hydrogeological, hydrogeochemical and other data are analyzed in Chapter 4. In Chapter 5, analyzed data is interpreted, different location data are compared and contrasted. Lastly, the conclusion part covers the assessment of the study and results are stated.

1.2 Geographical Setting of Study Area

The Büyük Menderes Graben System lies within Aegean Region. Graben system begins with Pamukkale – Karahayıt geothermal field at the east and ends with Söke – Davutlar geothermal field at the east. It comprises two cities, Denizli and Aydın which have several geothermal fields. The location map of Denizli and Aydın is shown in Figure 1-1.

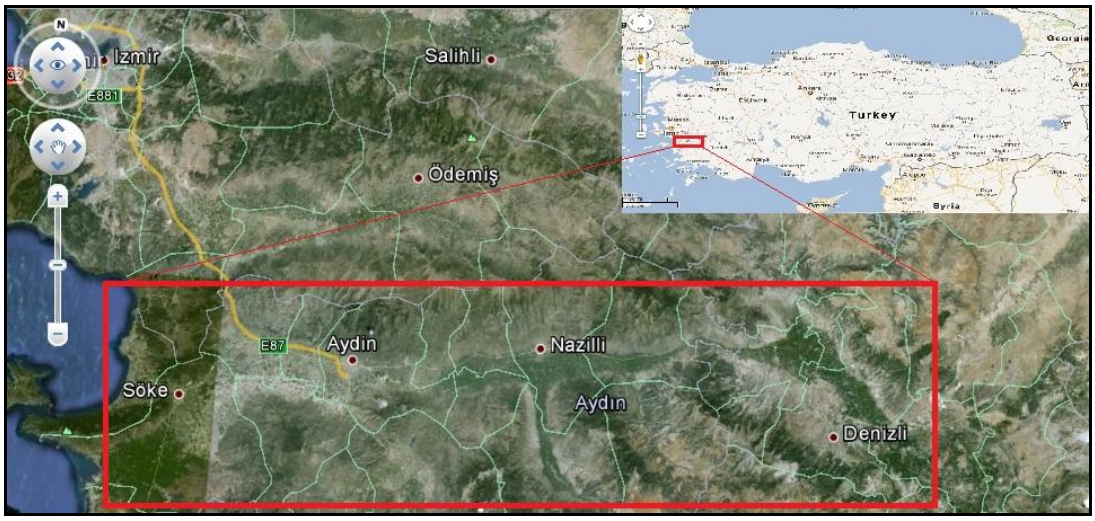

Figure 1-1: The location map of the study area.

1.3 A Brief History and Present Status of Study Area

As mentioned before, Turkey has an important geothermal energy potential. 187 geothermal fields that contain geothermal fluid with more than 40°C temperature were discovered by investigations in Turkey (Mertoğlu et al., 2010).

Between 2005 and 2009, a total of about 256 geothermal explorations and production wells were drilled for electricity production and direct use purposes (Mertoğlu et al., 2010). Especially in the Büyük Menderes Graben and Gediz Graben geothermal systems, new geothermal fields have been explored by MTA. The total geothermal potential in Turkey is estimated to be about 31,500 MWt (Dağıstan et al., 2010).

Western Anatolia has the greatest potential energy in Turkey. Büyük Menderes geothermal systems have high enthalpy reservoirs with temperature range of 120-240 ^{o}C (Öngür, 2010).

Mineral Research and Exploration Institute of Turkey defines eighteen geothermal fields and anomalies along the Büyük Menderes graben (Serpen et al., 2010). Except for one field (Tekkehamam) which is located in the southern margin of the graben, most fields and anomalies occur at the northern margin, and distributed along E-W-trending margin-boundary normal fault systems.

There are several hot springs from its eastern end (from Pamukkale-Karahayıt systems) to Söke at the western end; extensive engineering investigation and resource development works have been performed at these geothermal fields up to now (Öngür, 2010). The most important fields with high temperatures are Kızıldere, Ömerbeyli – Alangüllü, Salavatlı – Sultanhisar and Pamukören.

Geothermal explorations and investigations in Turkey started at Balçova, İzmir by General Directorate of Mineral Research and Exploration (MTA) in Turkey in 1962. The first well was drilled in 1963 and geothermal fluid at a temperature of 124 ^{o}C was obtained (Aksoy & Serpen, 2005).

In 1965, Kızıldere geothermal field in the Büyük Menderes Graben system was discovered by MTA. Kızıldere field is the first geothermal field that was discovered with highest temperatures obtained. Moreover, electricity generation from geothermal energy was firstly accomplished in Kızıldere field with an installed capacity of 0.5 MWe. The capacity of Kızıldere Geothermal Power Plant was increased to 17.4 MWe in 1984 (Kindap et al., 2010). The reservoir has a temperature of 242 °C and contains % 1.5 noncondensable gases. A liquid CO_2 and dry ice production factory is integrated to this power plant which produces 120,000 tons of liquid carbon dioxide and dry ice annually. After 2008, the Kızıldere field was privatized. According to company's research studies, the possibility of an undiscovered reservoir with a temperature varying between 250 – 260 ^{o}C is very high and the target of the company is to reach the capacity of a 60 MWe power plant in the near future (Kindap et al., 2010).

After the Kızıldere field, MTA discovered Germencik geothermal field. The first geothermal research on Germencik field was done in 1967 and continued with deep well drilling in 1982-1986 (Hamendi, 2009). In 2007 Germencik Field was assigned to GÜRMAT A.Ş. The construction of power plant had been completed at the end of 2008 after drilling new production wells and completing production tests (Tekin, 2010). According to 2009 data, the temperature of the reservoir is 232 ^{o}C and the capacity of power plant is 47.4 MWe. The Gürmat plant has been running since 2009 and the total installed capacity is aimed to reach 100 MWe.

Discovery of the Salavatlı field followed Kızıldere and Germencik fields. A couple of deep wells were drilled by MTA in 1987 and 1988. Nearly 7.35 MWe installed capacity Binary Cycle Power Plant, which is the first private owned plant, has been running since May 2006 (Serpen & Aksoy, 2010). The temperature of geothermal water is 167 °C. A second 9.7 MWe capacity power plant was constructed in 2010 and is producing electricity.

Exploration wells were drilled in 1989 to a depth of 200 – 471 m on Aydın – Ilıcabaşı geothermal field which is located in the city center of Aydın (Şimşek, 2003a). Moreover, Yılmazköy – İmamköy geothermal field is located at 5 km east of city center and an exploration well was drilled at Yılmazköy in 1999 at a depth of 1500 m (Toksoy & Aksoy, 2003).

After 2005, the geothermal investigations gained speed and Aydın – Umurlu (150 °C), Aydın – Sultanhisar (146 °C), Aydın – Bozköy (143 °C), Aydın – Atça (124 °C) and Aydın – Pamukören (188 °C) geothermal fields which are suitable for electricity generation are discovered (Dağıstan et al., 2010).

Through the law assigned in 2007, privatization of the fields was undertaken. Moreover, a lot of companies started to research and working in Büyük Menderes Graben geothermal fields.

CHAPTER 2

GEOLOGY

2.1 Tectonic Setting of Büyük Menderes Graben

The Aegean region is one of the most active extensional regions in the world and is undergoing a current N–S extension (Dewey & Şengör, 1979). The origin and age of extensional activity in the Aegean have been subjects of discussions for many years. There are four models suggested to explain the origin of extension. They are the tectonic escape model, the back-arc spreading model, the orogenic collapse model and episodic, two-stage graben model (Koçyiğit et al., 1999; Bozkurt, 2000; Bozkurt & Sözbilir, 2004; Bozkurt & Rojay, 2005; Rojay et al., 2005; Gürer et al., 2009).

1) *The tectonic escape model* is the westward escape of the Anatolian block along its boundary structures, the dextral North and sinistral East Anatolian faults, since the Late Serravalian (12 Ma) (e.g. Dewey & Şengör, 1979).
2) *The back-arc spreading model* is the back-arc extension caused by inception of subduction rollback process and consequent southwestward migration of the southern Aegean Arc (Mckenzie, 1978; Avigad et al., 1997).
3) *The orogenic collapse model* is localized extension is caused by the spreading and thinning of over-thickened crust after the latest Paleocene collision across Neotethys along the İzmir-Ankara-Erzincan Suture Zone during the Late Oligocene–Early Miocene (Seyitoğlu & Scott, 1992; Mcclusky et al., 2000).
4) *The episodic, two-stage graben model*, which involves westward escape of the Anatolian block following orogenic collapse (Koçyiğit et al., 1999;

Yılmaz et al., 2000; Bozkurt & Oberhänsli, 2001; Bozkurt & Sözbilir, 2004; Bozkurt, 2004; Bozkurt & Rojay, 2005).

The active N–S extension in the Aegean region including western Anatolia is defined by two tectonic phenomena: the roll-back of the subducting African plate and the west-southwestward escape of the Anatolian block along its boundary faults, North Anatolian and East Anatolian fault systems (Taymaz, Jackson & McKenzie, 1991; Okay & Satır, 2000; Flerit et al. 2004).

In the region, different tectonic processes during Neogene-Quaternary times produced a network of fault systems dominated by an array dominant E to NE and NW tendency normal fault (Gürer et al., 2009).

There are two systems of faults recognized: (1) approximately NE- and NW-trending subvertical oblique faults adjacent to Unit A; (2) E–W faults adjacent to units B and C (Gürer et al., 2009). The second system can be subdivided into: (a) a major E trending low-angle fault, the Büyük Menderes detachment fault, and (b) secondary listric high-angle faults, segmented for distances over 10 km (Gürer et al., 2009).

NE- and NW- trending oblique fault systems are responsible for the development of the Early–Middle Miocene deposits of Unit A (Gürer et al., 2009) consists of clastic sediments which uncormably rest on Menderes Massif metamorphics (Bozkurt, 2000).

E–W faults are dominant structural features of the region and confined mostly to the northern margin, which is defined by a S-dipping detachment fault, the Büyük Menderes detachment fault, and high-angle normal faults. The Büyük Menderes detachment fault runs along the northern sector of the graben and can be traced in an E–W direction for several tens of kilometres (Gürer et al., 2009). The subunit B1 and part of subunit B2, which overlie Unit A with an angular unconformity, are bounded by the Büyük Menderes Detachment Fault (Gürer et al., 2009). The high-angle normal faults occur in a step-like pattern and this fault system consists of S-dipping

sub-parallel faults that systematically tilt the beds to the north with roll-over deformation along the northern margin (Gürer et al., 2009). These faults, most of which are active, controlled the deposition of the mostly Unit C and partly subunit B2 and they initiated the elevation of the southern margin and created the steep topography of the northern margin (Gürer et al., 2009).

2.2 Geology of the Büyük Menderes Graben

The Büyük Menderes Graben is a structure with dimensions of about 160 km long and 8-12 km wide and one of the major east-west grabens in western Anatolia. Menderes Massif metamorphic rocks which comprise most of the western part of Turkey are the oldest rocks host as basement rock in the graben (Bozkurt, 2000). Menderes Massif has been separated into three submassifs, Northern Menderes Massif, Central Menderes Massif and Southern Menderes Massif involving active Büyük Menderes graben (Yılmaz et al., 2000; Bozkurt, 2001). Menderes Massif is a dome-like structure, interpreted as an "onion-shaped" structure, with a Precambrian 'augen gneiss core' at the base, a Paleozoic 'schist envelope' covering the gneiss core, and a Mesozoic-Cenozoic 'marble envelope' overlying both, with metamorphism increasing towards the core (Bozkurt & Oberhänsli., 2001; Gürer et al., 2009). The core rocks are composed of augen gneisses, metagranites, schists, paragneisses and metagabbros (Gürer et al., 2009). "Cover" is represented by a Palaeozoic schist envelope and a Mesozoic to Cenozoic marble envelope. The Palaeozoic schist envelope comprises garnet, kyanite, staurolite-bearing micaschists, graphite-rich quartzitic phyllite schists, garnet amphibolites, and marble intercalations while the thick marble envelope of the cover series overlie the schist sequence (Süer, 2010 and references therein).

Hovewer, the age of the core has been the subject of considerable debate during the last decade. There are two interpretations about the age of core series of Southern Menderes massif metamorphics. The first interpretation is that the protolith of the augen gneisses intruded as granitoids into the metasediments during the Tertiary time (Bozkurt & Oberhänsli, 2001; Whitney & Bozkurt, 2002; Erdoğan & Güngör, 2004; Bozkurt, 2004, 2007). The second interpretation suggests that the granitic protolith

intruded during Late Precambrian and Early Cambrian times based on geochronological data (Gessner et al., 2001).

Moreover, recent field studies in the southern Menderes Massif revealed that the ‘core’ of the massif comprises two distinct types of granitoid rocks: an orthogneiss (traditionally known as augen gneisses) and leucocratic metagranite, where the latter is intrusive into the former and the structurally overlying ‘cover’ schists (Bozkurt, 2004, 2007). The orthogneisses, widely known as ‘augen gneisses’, in the study area are typical L-S tectonites characterized by a well-developed, penetrative mylonitic foliation and pronounced NE-trending mineral stretching lineation (Bozkurt, 2004). The leucocratic metagranite is a greyish to white colour fine-grained, equigranular rock which composed of feldspars, quartz, muscovite and biotite as essential minerals, whereas tourmaline, zircon, rutile, monozite and opaques comprise the accessories (Bozkurt, 2004).

The contact between the orthogneisses and overlying schists is a major structural discontinuity named the ‘southern Menderes shear zone; the origin and nature of shear zone have been a controversy for over a decade. Some suggest that the contact is a S-facing high-angle Alpine extensional shear zone (Whitney & Bozkurt, 2002; Bozkurt, 2004, 2007; Seyitoğlu, Işık & Çemen, 2004). Some stand up for a S-facing thrust fault (Gessner et al., 2001).

Menderes Massif rocks are unconformably overlain by Neogene sediments. Fluvio-lacustrine sediments are exposed in a wide zone in the Büyük Menderes Graben. There are three main lithostratigraphic units based on their distinct structure in the graben (Bozkurt, 2000; Gürer et al., 2009). They are northwards tilted sediments (unit A); almost flat-lying, terraced sediments (unit B); and marginal alluvial fans and present-day graben-floor sediments (unit C) (Bozkurt, 2000).

Unit A can be subdivided into the Lower subunit (A1) and Upper subunit (A2) (Gürer et al., 2009). Unit A consists mainly of northwards tilted continental clastic sediments delimited by NNW- and NW-trending faults (Bozkurt, 2000; Gürer et al., 2009). Lower subunit (A1) consist of coarse-grained, well cemented conglomerate at

the basement Above the conglomerates (A1), Upper subunit (A2) passes upward into inter-fingering sandstone, mudstone, shale and marls; locally they contain thin coal seams (Gürer et al., 2009). Unit A is dated as Late Early Miocene–Late Middle Miocene, based on the small mammal associations and is overlain by Unit B with an angular unconformity (Gürer et al., 2009).

Unit B comprises cobble to boulder conglomerates with alternations of sandstone, siltstone, mudstone and claystone which are delimited in the north by the Büyük Menderes Detachment Fault (Bozkurt, 2000; Gürer et al., 2009). Unit B is subdivided into two subunits which are subunit B1and subunit B2. Subunit B1 is composed mostly of fluvial orange-red conglomerates, grey to greenish grey sandstones and subordinate mudstones and marls while subunit B2 light yellow-coloured cobble to pebble conglomerates with alternations of sandstone, siltstone and mudstone (Gürer et al., 2009). Subunit B2 rests on the metamorphic rocks, Unit A and locally on subunit B1 with an unconformity (Gürer et al., 2009). It is overlain unconformably by the present-day grabenfloor deposits (unit C) and bounded either by the detachment fault or high-angle faults (Gürer et al., 2009).

Unit C is composed mainly of marginal alluvial fan and graben-floor sediments (Bozkurt, 2000). Unit C sediments developed by the active normal faults are represented by fan deposits and fluvial deposits (Gürer et al., 2009).The alluvial fans grade into fine-grained basin-floor sediments along the Büyük Menderes River (Bozkurt, 2000).

The general geology of Western Anatolia and Büyük Menderes Graben is shown in Figure 2-1 while generalized stratigraphic columnar section of the Büyük Menderes Graben is shown in Figure 2.2.

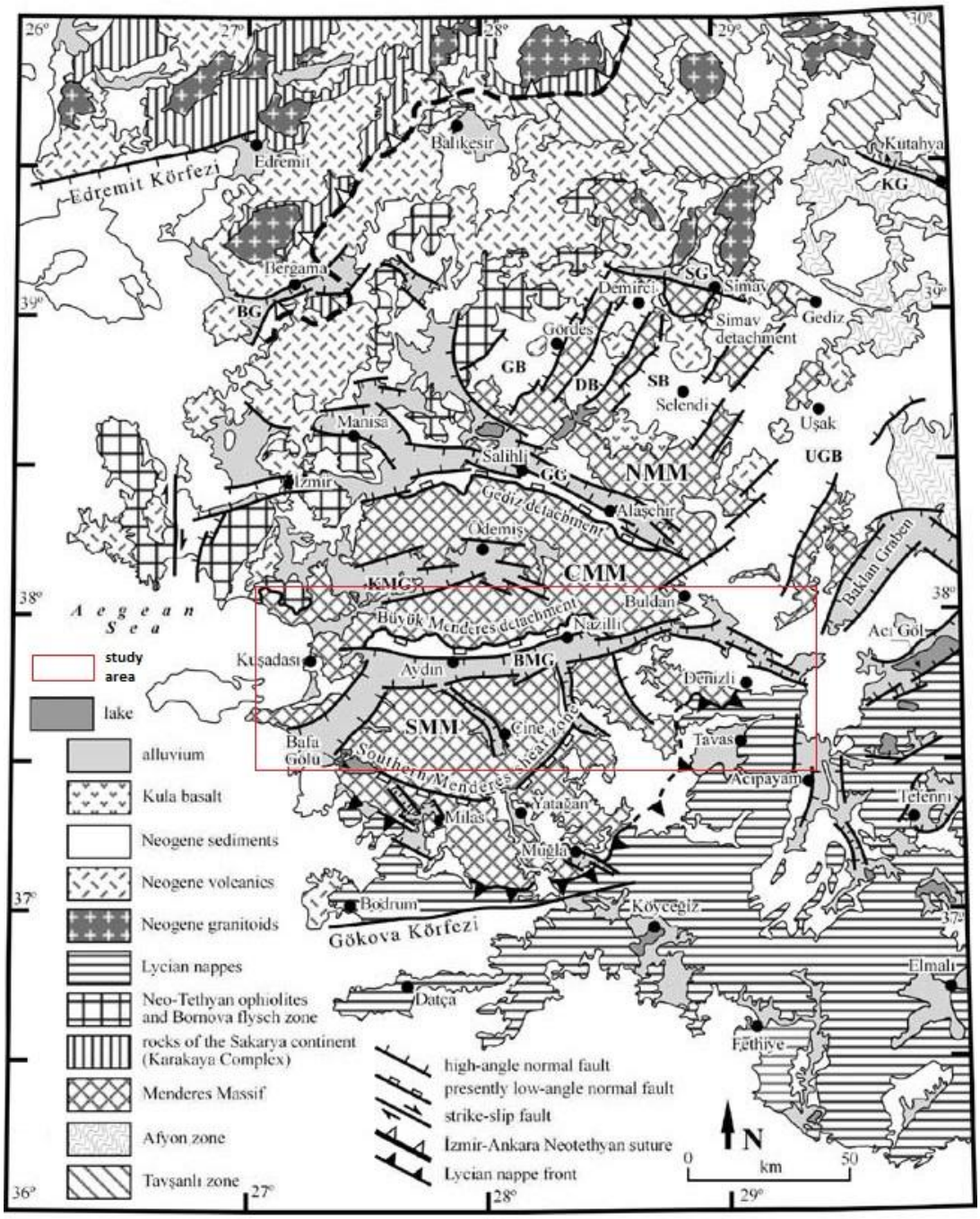

Figure 2-1: Geological map of Western Anatolia and Büyük Menderes Graben (Bozkurt, 2007). BG – Bakırçay Graben; DB – Demirci Basin; GB – Gördes Basin; GG – Gediz Graben; KG – Kütahya Graben; SB – Selendi Basin; SG – Simav Graben; BMG – Büyük Menderes Graben; CMM – Central Menderes Massif; KMG – Küçük Menderes Graben; NMM – Northern Menderes Massif; SMM – Southern Menderes Massif; UGB – Uşak-Güre Basin.

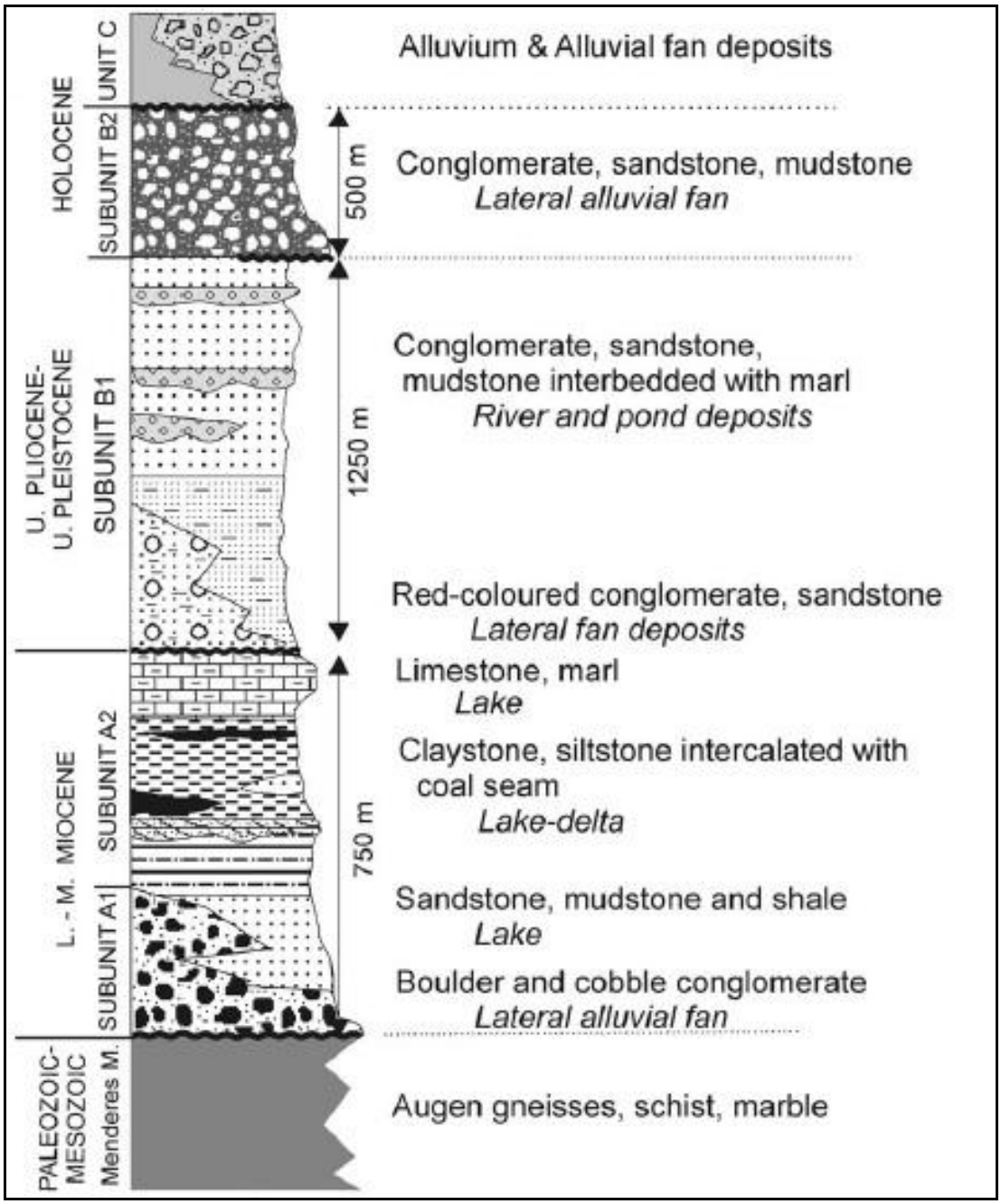

Figure 2-2: Generalized stratigraphic columnar section of the Büyük Menderes Graben (Gürer et. al, 2009).

CHAPTER 3

METHODOLOGY

3.1 Methodology Description

The literature, the scientific papers, well reports, etc., about Büyük Menderes Graben system was compiled during long months. The major part of the data was provided from MTA explored most of the geothermal fields in the region. The well reports inform about geology, hydrogeology and geochemistry were obtained and studied. Moreover, thesis, articles, bulletins, annual reports of public institutions are compiled and examined.

Furthermore, it should be indicated that the most of the geothermal fields in the graben have been transferred to private companies. During to data collection, it was a complication to reach to data due to ownership of the fields. So, only the public data could be used in this thesis.

Geological and tectonic setting, hydrogeology, geochemistry and wellbore data of each geothermal field were examined in detail as far as possible. Stratigraphy and faults cut were compiled for a specific wellbore in a specific gothermal field. In addition, the trends of faults for each field were examined.

Reservoir number, reservoir and cap-rock formations, wellbore depth were analyzed. Furthermore, the distance of the wells to the sea assumed as a reference point to consider the relations of the fields. The depth to the thermal water (the reservoir

depth) and production zone were noted. Besides, temperature values of the reservoir, geothermal water type, water origin and chemical compounds were studied.

Some geothermal parameters were chosen through the accessible data to be analyzed. Geothermal parameters used are listed below in Table 3-1. Each geothermal field was studied as much as possible basen on the available data.

Table 3-1: Geothermal parameters used in the study.

Well depth (m)
Well temperature (^{o}C)
Well distance to sea (m)
Presence of fault cut
Reservoir unit
Cap rock
Water ion (anion, cation) content (mg/l)
Mineral content (mg/l)
Total dissolved solids (mg/l)
Geothermal water type
Water origin
pH
Electrical conductivity (µmho/cm)

3.2 Geothermal Parameter Definitions

Geological features, lithology, tectonic activity, faults and their relationships with geothermal energy are used in this study. The lithology of a rock unit is a description of its physical characteristics visible at outcrop, in hand or core samples or with low magnification microscopy, such as colour, texture, grain size, or composition (Bates & Jackson, 1984). Tectonic activity is the process of global forces that cause folding and faulting of the Earth's crust; the fault is a result of driving mechanism of tectonic activity and is basically the fracture in the rock that makes movement. The tectonic activity which triggers the heat exposure and the fault which provides circulation and paths carrying fluid are essential for a geothermal system.

Hydrogeological features such as reservoir, production zone and surface manifestations were analyzed and contrasted in the thesis. Geothermal reservoir includes heated and pressurized water and/or vapor accumulations, with defined boundary conditions, from which heat can be extracted from the underground to the

surface (Ledru & Frottier 2010). Reservoir has two main members, aquifer and cap-rock. Aquifer is the medium which is generally composed of sedimentary formations with high porosity and permeability. Cap rock can be defined as a holder that formed from impermeable rocks overlying the permeable rock, generally the sediments. Production zone is the fractured zone in the reservoir where the hot water can be stored and extracted. Geological surface manifestations include hot springs, fumaroles, geysers, travertine deposits, chemically altered rocks, or sometimes, no surface manifestations (a blind resource) (Lund, 2007). Surface manifestations can be the indicators of geothermal reservoirs and can delineate reservoirs. They can be correlated with other geologic features (e.g. whether the concentration of hot-springs occurs where the faults are concentrated). Temperatures and flow rate amounts of surface waters like fumaroles, geysers, springs can give an idea about the reservoir water temperature and discharge amounts. Reservoir pressure is the water pressure of reservoir and is generally measured in Bar. The high pressure rates mean the high discharge amounts. So the high pressured reservoir systems are more efficient.

Hydrogeochemical characteristics have the features related to water chemistry such as chemical compounds and chemical amount, geothermal water type, water origin, thermal water temperature and pressure and geothermal alteration-alteration minerals. The geochemistry involves study of the chemical composition of the Earth, chemical processes and reactions that govern the composition of rocks, water, and soils. Geochemistry is used to evaluate the origin and type of the water, to estimate underground temperature, characterize the reservoir chemistry (Gunnlaugsson, 2008). Chemical compounds are the minerals found in the geothermal liquid. The chemical components of geothermal fluids are determined by their source, the rock types with which they have reacted along their flowpath, the temperature of those interactions, and the chemistry of the fluid. The main chemical components in geothermal water are silica (SiO_2), sodium (Na), potassium (K), calcium (Ca), magnesium (Mg), carbonate (total CO_2), hydrogen sulphide (H_2S), sulphate (SO_4), chloride (Cl) and fluoride (F) (Gunnlaugsson, 2008). Fluid composition in many geothermal fields worldwide appears to closely approach chemical equilibrium with secondary minerals for all major aqueous components except Cl and B (Giggenbach, 1980; Michard, 1991). Hydrothermal alteration is a change in the mineralogy as a

result of interaction of the rock with hot water fluids, called “hydrothermal fluids” (Lagat, 2010). Primary minerals usually tend to alter to secondary (hydrothermal alteration) minerals that are stable. The temperature, permeability, pressure, fluid composition, initial composition of the rock and the duration of the hydrothermal activity specify the formation of hydrothermal alteration minerals; the main hydrothermal minerals in the geothermal field are albite, amphibole (actinolite), biotite, calcite, chlorite, chalcedony, epidote, fluorite, garnet, illite, K-feldspar (adularia), mordenite, secondary Fe-Ti oxides, sulfides (pyrite), titanite (sphene) and quartz (Lagat, 2010). Water origin is inception of reservoir water source. Water origin can be generally meteoric, and magmatic, connate or oceanic. Reservoir temperature is the fluid temperature of reservoir and is generally measured in Celsius. According to reservoir temperature, the types of reservoir are identified. During the exploration phase, geothermometry is used to estimate the subsurface temperatures expected to be encountered by drilling, using the chemical and isotopic composition of hot spring or shallow well discharges (Güleç, 2005).

Geological, geochemical and hydrogeolocical informations about the field can be provided by a wellbore data. In other words, wellbore data help to distinguish the field through output of drilling year, well depth, well formations, formation thicknesses and reservoir type, reservoir units, temperature and pressure, mineral content, faults cut.

3.3 Literature Utilized as Data Source

The investigations, exploration workouts, researches, studies, experimental or pilot workings done by governmental institutions, universities or/and companies are the resource of this study. General Directorate of Mineral Research and Exploration (MTA) is the most competent unit at geothermal systems and investigations in Turkey. So, most of the geothermal field were explored by MTA. The literature of MTA was frequently used in this study. MTA has worked in the Büyük Menderes Graben for years; a lot of fields were investigated and several boreholes were drilled by MTA. Besides, the researches done by universities for thesis’ works or some projects were utilized. Another resource involved in this study was that the private

sector investigations, field works, research studies which are not confidential, open to public.

3.4 Geothermal Fields Studied

In this study, geothermal fields located at Aydın and Denizli provinces were examined (Figure 3-1). Geothermal fields located on the eastern segment of the graben are Pamukkale, Karahayıt, Gölemezli, Yenice, Tekkehamam, Gerali and Kızıldere. The others are Pamukören, Nazilli, Sultanhisar, Salavatlı, İmamköy-Yılmazköy, Ilıcabaşı, Bozköy, Ömerbeyli, Hıdırbeyli and Gümüşköy from east to west. Apart from these, westernmost segment of the graben, which trend in NE-SW, comprises Davutlar-Söke field. Gerali and Tekkehamam fields are located on the southern margin of the graben. All other fields occur on the northern margin.

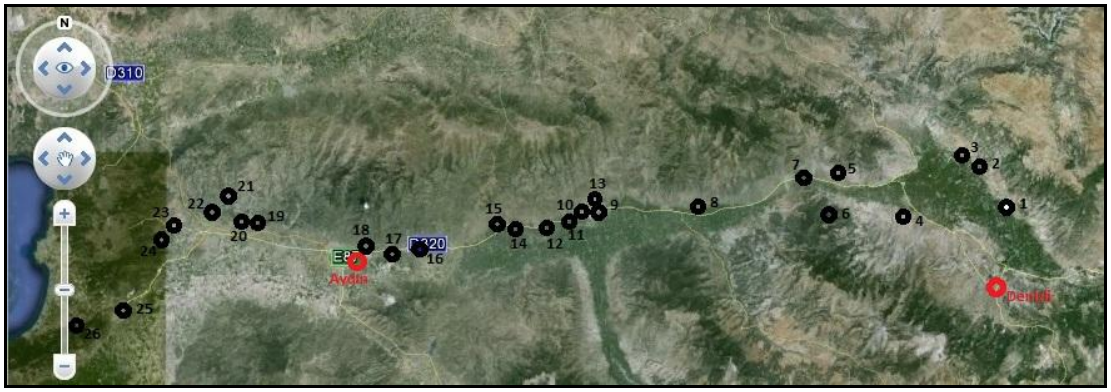

Figure 3-1: Geothermal fields located at Aydın and Denizli provinces. 1-Pamukkale, 2-Karahayıt, 3-Gölömezli, 4-Gerali, 5-Kızıldere, 6-Tekkehamam, 7-Buharkent-Ortakçı, 8-Pamukören, 9-Güzelköy, 10-Nazilli, 11-İsabeyli, 12-Atça, 13-Bozyurt, 14-Sultanhisar, 15-Salavatlı, 16-Umurlu, 17-Yılmazköy-İmamköy, 18-Kalfaköy, 19-Ömerbeyli, 20-Alangüllü, 21-Bozköy, 22-Hıdırbeyli, 23-Ortaklar, 24-Gümüşköy, 25-Söke, 26-Davutlar.

Pamukkale, famous for snow white travertines in the world and Karahayıt geothermal fields are available on the easternmost part of the study area; geographically they are in the border of Denizli province. There a lot of hot springs around Pamukkale and Karahayıt but the temperatures are generally low. The waters emerge as springs reaching throughout the normal faults have about 35 ^{o}C temperatures. The drilled wells are KH1, KH2 and KH3, production wells, at about 500 m in Karahayıt field with about 60 ^{o}C reservuar temperatures (Gökgöz et al., 2010).

Gölemezli and Yenice fields are also in the borders of Denizli. Five wells, DG 1, DG 2, DG 3, DG 4, DG 5, with depths changing between 549 m and 1289 m were drilled in Gölemezli field at the beginning of 2000s (Kahraman, 2003; Tamgaç, 2010). The reservoir temperatures are variable between 62 ^{o}C and 95 ^{o}C (Kahraman, 2003; Tamgaç, 2010). There are three production wells in Yenice geothermal field with reservoir temperatures of 53 ^{o}C, 63 ^{o}C and 38 ^{o}C (Şimşek, 2003b). The reservoir units of Gölemezli and Yenice geothermal fields are Menderes metamorphics.

Gerali geothermal field located on the southern margin of the graben close to Tekkehamam is one of the exceptions in Büyük Menderes Graben system. There is only one well for which the data could be obtained. It has a depth of 1143 m and a reservoir temperature of 125 ^{o}C (Karamanderesi & Ölçenoğlu, 2005).

Kızıldere and Tekkehamam geothermal fields in the Denizli province are located on the northern and southern margins of the graben, respectively. Kızıldere geothermal has the highest reservoir temperature explored in Turkey till now. There are 22 wells drilled since 1965 (Özkaya, 2007; Süer, 2010). Five are observation wells and one is for reinjection. The depths of the wells vary between 370 m and 2260 m and the temperature of the water varies between 157 ^{o}C and 242 ^{o}C (Yeltekin & Akın, 2006; Demirel et al., 2007; Özkaya, 2007; Kaya & Kindap, 2009; Kindap et al., 2010; Süer, 2010). There are two reservoir units and a possible third one. First reservoir occurs with a limestone unit of Pliocene Sazak Formation while the deeper reservoir is located within Menderes metamorhics such as marble, quartzite and schist. Normal faults are penetrated by many well bores in the Kızıldere geothermal field. Moreover, Tekkehamam geothermal field occurs on the southern margin of the graben. There are six wells drilled in the Tekkehamam field with a maximum bottom hole temperature of 170 ^{o}C (Süer, 2010). The depths of the wells range between 115 m and 2001 m (Süer, 2010). All of them are production wells. The reservoir units are the same as Kızıldere field. The power plant constructed in 1984 has been operating with a generator output of 15 MWe in Kızıldere (Kindap et al., 2010). Furthermore, another plant construction with a capacity of 75 MWe is in progress.

Pamukören geothermal field is in Aydın province. The explorations and drillings have been done in very recent years. There are 3 wells drilled by MTA (Atmaca, 2010). Moreover, private companies have been working in the Pamukören field. As these studies showed, the Pamukören geothermal field is a promising one. The reservoir temperature of the field is more than 180 ^{o}C.

The city of Nazilli is located somewhere between Aydın and Denizli (almost same distance to both cities) and has a number of geothermal wells around. Some hot springs exist in İsabeyli, Bozyurt and Atça towns and environs. A number of geothermal fields were drilled in Atça, İsabeyli and Nazilli by MTA. The depth of wells range from about 1000 m to 2000 m while the reservoir temperatures are between about 80 ^{o}C and 140 ^{o}C (Güdücü, 2008; Karahan, 2010a; Karahan, 2010b; Purtul, 2010).

Salavatlı geothermal field has, apart from Kızıldere and Ömerbeyli fields, the highest reservoir temperature explored in third order in the Büyük Menderes Graben. There are 6 production wells and 3 reinjection wells in the field (Serpen & Aksoy, 2010). Power plants, DORA 1 and DORA 2, are running with a capacity of 7.36 and 9.7 MWe (Özdemir et al., 2012). The reservoir temperatures of the production wells are about 160 ^{o}C and 180 ^{o}C while the depths range between about 900 m and 1500 m, reaching the reservoir rocks of the Menderes metamorphics (Karamanderesi, 1987; Demirel, 2005; Bülbül, 2008; Serpen & Aksoy, 2010). In Sultanhisar, there have been two production wells drilled very recently where reservoir temperature is 145 ^{o}C and the depths of wells are about 1000 m (Karahan, 2007).

İmamköy, Yılmazköy and Ilıcabaşı locations are very close to Aydın province. There are some hot springs at temperatures of about 35 ^{o}C. Two wells in Yılmazköy, one well in İmamköy and four wells in Ilıcabaşı areas are present (Şimşek, 2003b; Toksoy & Aksoy, 2003; Yurttaş, 2008). The depths of the wells vary between 200 m and 1500 m (Candaş, 2002; Yolal & Karahan, 2010).

Ömerbeyli geothermal field has the highest capacity, 47.4 MWe, of geothermal power plant in Turkey. In 1980s, MTA drilled nine production wells in Ömerbeyli. In addition, the company running the prospect, drilled nine production and

reinjection wells in 2007-2008. The highest temperature is 232 ^{o}C; and they form the highest temperatures reached in the Menderes metamorphics (Özgür at al., 1998; Filiz et al., 1999, 2000; Şimşek, 2003b; Karakuş, 2010; Tekin, 2010). Alangüllü geothermal field is included in Ömerbeyli prospect. One production well was drilled by MTA in Alangüllü at a depth of 962 m and the hot water temperature is 172 ^{o}C; it was reached in marble units (Ceyhan, 2000). Moreover, the company drilled new wells in Ömerbeyli and Alangüllü.

Hıdırbeyli geothermal field has been also running by private sector. After the two production wells were drilled by MTA, several production and reinjection wells were drilled by the company. The downhole temperatures are over 120 ^{o}C, even reaching 170 ^{o}C in wells (Karahan, 2008; Söğüt, 2011). The depths of the wells are generally over 2000 meters. An operating power plant with a capacity of 18 MWe was built in 2011 (Özdemir et al., 2012).

Gümüşköy–Ortaklar geothermal field has been managed by a company. There are three wells known. The reservoir temperatures are about 130 ^{o}C and 170 ^{o}C. The depths of the wells are over the 2000 meters (Çağlayan & Dünya, 2012).

Davutlar–Kuşadası geothermal field has still been under consideration and research still continues. There are two wells known. The reservoir temperatures are about 50 ^{o}C (Keskin, 1972; Tarcan et al., 2000; Uysal, 2002; Karaca & Destur, 2012).

CHAPTER 4

INPUT DATA AND ANALYSES

In this Chapter, the data acquired according to parameters which will be studied will be analyzed. General assessment of the Büyük Menderes Graben geothermal system will be performed based on the main parameters, like well depth, temperature, fault cut, ion and mineral concentration, geothermal water type and water origin.

As mentinoned in the previous Chapters, geothermal fields occur all along the Büyük Menderes Graben. MTA have studied long years in Aydın and Denizli provinces. Especially, the explorations and workings have accelerated in recent years. Prognosticatively, so many wells have been drilled. Mineral Research and Exploration Institute of Turkey defines eighteen geothermal fields and anomalies along the Büyük Menderes graben (Serpen et al, 2000). In this thesis, the study area is examined in 17 distinct fields according to their locations and explicit similarities. During the data collection, more than 100 wells drilled in the fields have been counted. The geothermal fields and the well names are shown in Table 4-1.

The data used in this thesis, well depth, well temperature, geochemical compounds, etc., are given in the appendices.

Table 4-1: Geothermal fields and well names attained in the Büyük Menderes Graben.

Field no	Geothermal Field Name	Well Names
1	Pamukkale–Karahayıt	KH1, KH2, KH3
2	Gölemezli	DG1, DG2, DG3, DG4, DG5, G1
3	Yenice	Yenice 1, Yenice 2, Yenice 3
4	Gerali	MDO1, DSG4
5	Kızıldere	KD1**, KD1A**, KD2**, KD3, KD4, KD6, KD7**, KD8, KD9**, KD111, KD12, KD13, KD14, KD15, KD16, KD17,KD20, KD21, KD22, R1, R2*, R3
6	Tekkehamam	TH1, TH2, TH3, TH4, TH6, TH7, KB1(private company), KB2, KB3, KB4, KB5, Tekke 1, DST19
7	Buharkent–Ortakçı	AO1, KB1(MTA)
8	Pamukören	AP1, AP2, AP3
9	Nazilli–Bozyurt–Güzelköy	NK1, NG1, NB1
10	Atça–İsabeyli	AT1, AT2, İS1
11	Salavatlı–Sultanhisar	AS1, AS2*, AS3, AS4, ASR1, ASR2, ASR3, ASR4*, ASR5*, SH1, SH2, ASMM5
12	Umurlu	AU1, AU2, ASK1
13	İmamköy–Yılmazköy–Ilıcabaşı–Kalfaköy	AY1, AY2, AMK12, İmamköy, Yılmazköy, Ayter 1, Ayter 2, DSİ1, DSİ2
14	Ömerbeyli–Alangüllü	ÖB1, ÖB2, ÖB3, ÖB4, ÖB5, ÖB6, ÖB7, ÖB8, ÖB9, ÖB10, ÖB11, ÖB14, ÖB17, ÖB19, A1, A2, AG20, AG22*, AG24*, AG25*, AG26*, AG2
15	Hıdırbeyli–Bozköy	HB1, HB2, HB3, HB4, HB5, HB6, HB7, HB8, HBR1, GM1, GM2, GM3, GD1, GD2
16	Ortaklar–Gümüşköy	GK5, GS1, GK3, KG4, R-GK1*, AOG1, AGG16, ORT4, GK1, GK3A
17	Söke–Davutlar	Davutlar, AKD2

4.1 Data Analyses Based on Lithology

Büyük Menderes geothermal field lithologies are Paleozoic, Tertiary and Quaternary rocks and sediments. Paleozoic mainly consists of metamorphic rocks of the Menderes Massif which are the basement rocks such as gneisses, types of schists and marbles. Tertiary rocks are commonly composed of Miocene and Pliocene lacustrine and marine sediments like limestone, sandstone, siltstone, claystone and marn. The youngest lithologies are Quaternary deposits such as terrace deposits, slope debris, uncemented sediments and alluviums.

In this part of the thesis, the lithologies of the defined 17 geothermal fields in the study area are examined, explained, compared and contrasted.

** : observation well
* : reinjection well

4.1.1 Lithologies of Denizli Geothermal Fields

Büyük Menderes Graben consists of six geothermal fields in the Denizli province. They, from east to west, are Pamukkale–Karahayıt, Gölömezli, Yenice, Gerali, Tekkehamam and Kızıldere (Figure 3-1). These fields were examined separately.

Generally, the geothermal fields' stratification in Denizli province is similar to each others. Paleozoic Menderes metamorphics such as gneiss, marble, schist; and limestones, marbles and ophiolitic mélange of Lycian nappes form the basement rocks. Above the metamorphics, a sequence of Kızılburun formation, Sazak formation, Kolonkaya formation and Tosunlar formation occur. These sedimentary rocks have fluvial and lacustrine character. The youngest units are Quaternary deposits which are alluvium, alluvial fan, terrace deposits, slope debris and travertines occur at the top (Figure 4-1).

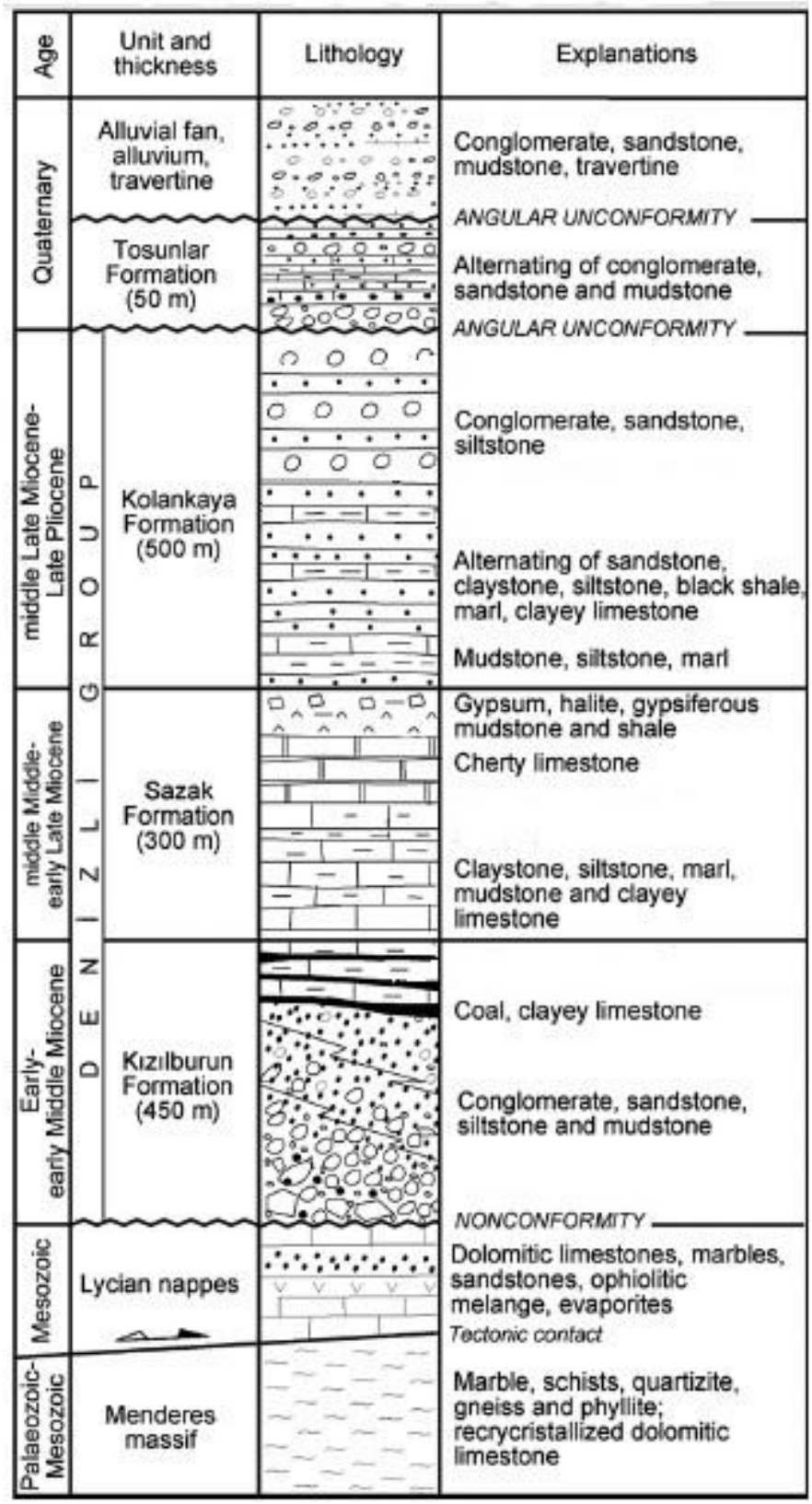

Figure 4-1: Generalized columnar sequence of Denizli basin-fill succession (Alçiçek et al., 2007 and references there in).

4.1.1.1. Lithology of Pamukkale-Karahayıt Geothermal Field

Pamukkale–Karahayıt lithological units consist of sedimentary and metamorphic rocks. Their ages range from Paleozoic to Quaternary. The Paleozoic basement rocks are gneiss, schist, marble, limestone, Menteşe ophiolites and Bozkaya mélange (Özler, 2000). Tertiary sediments are continental and lacustrine deposits. They are Dağdere formation, block gravel, graveled mudstone, graveled sandstone and sandstone; Kızıldere formation, alternation of conglomerate, sandstone, claystone and lignite strata; Sazak formation, limestone, marl, siltstone and travertine; Acıdere formation, marl, clayey limestone, mudstone, sandstone and travertine; Gökpınar formation, alternating units of conglomerate, sandstone and mudstone (Özler, 2000). The Quaternary is composed of terrace deposits, alluvium, slope debris, alluvial fans and travertine.

4.1.1.2. Lithology of Gölömezli Geothermal Field

Gölömezli geothermal field is composed of Paleozoic Menderes Massif rocks, such as gneiss, quartzite, calcschist, micaschist and marble; Upper Miocene and Pliocene Kızılburun, Sazak, Kolonkaya ve Tosunlar formations and Quaternary units, which contains terrace deposits, alluvium, slope debris, alluvial fans and travertines (Tamgaç, 2010). Kızılburun, Sazak, Kolonkaya ve Tosunlar formations generally consist of claystone, siltstone, sandstone, conglomerate, marl, clayey limestone, sandy limestone and limestone.

4.1.1.3. Lithology of Gerali Geothermal Field

Gerali geothermal field is also composed of Paleozoic to Quaternary rocks. Paleozoic basement rocks consist of schist of Menderes Massif metamorphics. Above Menderes Massives, marbles of İğdecik formation, limestone, sandstone, conglomerate and siltstone of Kızılburun formation, limestone of Sazak formation and clay strata occur from bottom to top (Karamanderesi & Ölçenoğlu, 2005). Quaternary sediments are uncemented old terrace deposits, slope debris, and alluvium.

4.1.1.4. Lithology of Tekkehamam Geothermal Field

Tekkehamam geothermal field stratification is very similar to Kızıldere geothermal field. Basement rock is Paleozoic Menderes Massif. The Massif are comprised, from bottom to top, of gneisses, quartzite-gneiss-schist alternations, schists, and alternation of quartzites, micaschists and marbles known as the İğdecik formation (Şimşek, 1984). The Neogene sedimentary rocks are represented, from bottom to top, by the Kızılburun formation consisting of conglomerate and sandstone; the Sazak formation, which consists of limestone and marl; and the Kolonkaya formation, consisting of marl and sandstone (Şimşek, 1984). The Upper Pliocene Tosunlar formation is represented by poorly consolidated conglomerates, sandstone and mudstone. The Quaternary deposits are alluvium, terrace deposits, slope debris and travertine.

4.1.1.5. Lithology of Kızıldere Geothermal Field

In the Kızıldere geothermal field, the basement is made up of Paleozoic metamorphic rocks that consist of gneiss, schist, and the İğdecik formation, which is represented by alternating with quartzites, mica schists, and marbles (Şimşek, 1984). The basement rocks are overlain by Pliocene sediments of fluvial and lacustrine character, which consist of Kızılburun formation, Sazak formation, Kolonkaya formation and Tosunlar formation (Şimşek, 1984). The Kızılburun formation is an alternation of red and brown conglomerates, sandstones, shales, and lignites. The Sazak formation is composed of intercalated gray limestones, marls, and siltstones. The Kolonkaya formation contains yellowish green marls, siltstones, and sandstones. The Tosunlar formation is composed of alternating conglomerates, sandstones, and mudstones with fossiliferous clayey units. Quaternary unit is alluvium which overlies all of the units

4.1.2 Lithologies of Aydın Geothermal Fields

Aydın province has the most geothermal fields in Turkey. The geothermal fields are divided into eleven seperate geothermal fields. They are Buharkent–Ortakçı, Pamukören, Nazilli–Bozyurt–Güzelköy, Atça–İsabeyli, Salavatlı–Sultanhisar, Umurlu, İmamköy–Yılmazköy–Ilıcabaşı–Kalfaköy, Ömerbeyli–Alangüllü,

Hıdırbeyli–Bozköy, Ortaklar–Gümüşköy and Söke–Davutlar geothermal fields from east to west (Figure 3-1).

Broadly speaking the region between Buharkent–Ortakçı and Söke–Davutlar geothermal fields has similar stratigraphy with Denizli geothermal fields. Basement rocks are Menderes metamorphics. Neogene sedimentary units occur above metamorphics. Söke–Davutlar geothermal field has Davutlar volcanics which can be considered as a difference (Figure 4-2).

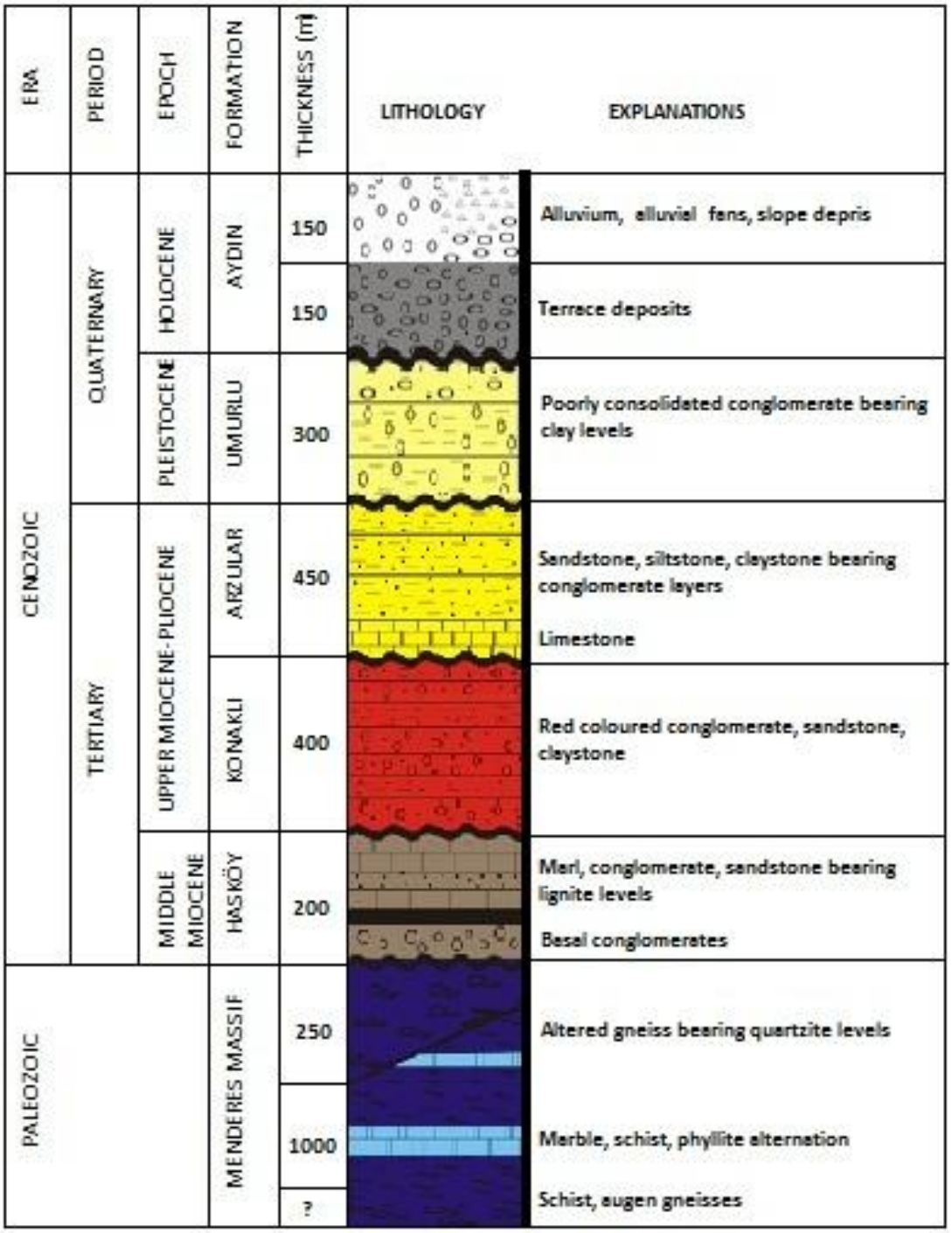

Figure 4-2: Generalized columnar sequence of Aydın basin-fill succession (Karahan & Bülbül, 2007)

4.1.2.1 Lithology of Buharkent-Ortakçı Geothermal Field

Buharkent–Ortakçı geothermal field has Paleozoic augen gneisses, schists, quartzites, and amphibolites as basement rock. Sedimentary deposits of Pliocene age overlie the basement rock. They are claystone, clayey limestone and sandstone of Kolonkaya

formation and conglomerate, sandstone, siltstone and mudstone of Asartepe formation (Kaya & Gökgöz, 2005). Alluvium and alluvial fans of Quaternary period overlie all of the formations.

4.1.2.2 Lithology of Pamukören Geothermal Field

Pamukören geothermal field has Paleozoic rocks and Tertiary to Quaternary sedimentary formations. The basement units are represented by Menderes massif metamorphics and are composed of gneisses, chloride-schist, mica-schist, quartz-schist, quartzite, phyllites and intercalating marble layers (Atmaca, 2010). Tertiary sediments belong to Miocene and Pliocene. Miocene sedimentary deposits are conglomerate, sandstone, claystone, siltstone and marl. Pliocene sedimentary rocks are sandstone, claystone, and siltstone. The Quaternary deposits are alluvium, terrace deposits, slope debris and travertine.

4.1.2.3 Lithology of Nazilli–Bozyurt–Güzelköy Geothermal Field

Nazilli–Bozyurt–Güzelköy geothermal field stratification is very similar to Pamukören geothermal field. Menderes Massif metamorphics represent the Paleozoic as a basement rock. The metamorphics are gneisses, schists and marbles. Tertiary units are conglomerate, sandstone, claystone, siltstone and marl which are Miocene in age. Moreover, Pliocene sedimentary rocks are sandstone, claystone, and siltstone. The Quaternary deposits are alluvium, terrace deposits, slope debris and travertine (Karahan, 2010a; Purtul, 2010).

4.1.2.4 Lithology of Atça–İsabeyli Geothermal Field

Atça–İsabeyli geothermal field has also Menderes massif metamorphics as the basement rock which are augen gneisses, chloride-schist, mica-schist, quartz-schist, calc-schist, phyllites and intercalating marble layers. Tertiary sediments are represented by conglomerate, sandstone, claystone, siltstone and marl. The Quaternary units are Pleistocene and Holocene pebbly, clayey series and alluvium, terrace deposits, alluvial fans and travertine (Karahan & Güdücü, 2008; Turalı & Karahan, 2009; Karahan, 2010).

4.1.2.5 Lithology of Salavatlı–Sultanhisar Geothermal Field

Salavatlı–Sultanhisar geothermal field has the basement rocks comprising orthogneiss, paragneiss, fine-grained schists, coarse-grained augen gneiss, mica schist, quartz schist, metaquartzite and marble. Neogene sedimentary rocks include coarse- and fine-grained sandstones, siltstones, and well-cemented conglomerates, and are a thin lignite layer at the base of the sequence. The Quaternary deposits are alluvium and slope debris (Karamanderesi, 1987; Demirel & Beker, 2005; Karahan, 2007; Bülbül, 2008; Serpen & Aksoy, 2010).

4.1.2.6 Lithology of Umurlu Geothermal Field

Umurlu geothermal field has Paleozoic basement and Neogene sedimentary deposits. Gneiss units are represented by alternation of quartzite, quartz-schist and phyllite. In addition to quartz-schist, mica-schists are present above the marble units which are massive and alternate with phyllite. Neogene sediments are conglomerate, claystone, siltstone and sandstone which belong to Miocene and Pliocene. Uncemented gravelly, sandy, clayey units which represent Pleistocene overlie the Neogene sediments. Alluvial fans of Holocene age reserve large areas in Umurlu geothermal field (Karahan & Güdücü, 2008; Karahan & Dönmez, 2009; Karahan et al., 2009).

4.1.2.7 Lithology of İmamköy–Yılmazköy–Ilıcabaşı–Kalfaköy Geothermal Field

İmamköy–Yılmazköy–Ilıcabaşı–Kalfaköy geothermal field has the augen gneisses, schists, metaquartzites and marble units of Paleozoic basement rocks. Upper Miocene units are reddish sandy, clayey units while Pliocene layers are yellowish pebbly conglomerates and sandstones. The Quaternary units are terrace deposits, slope debris and alluviums (Candaş, 2002; Toksoy & Aksoy, 2003; Yolal & Karahan, 2010).

4.1.2.8 Lithology of Ömerbeyli–Alangüllü Geothermal Field

Ömerbeyli–Alangüllü geothermal field has Paleozoic Menderes Massif metamorphics as the oldest units. These units, from bottom to top, are gneiss, mica-schist, dolomitic marble, quartz-schist and again marble. Miocene aged units are

sandstone, conglomerate and clayey limestone. Early Pliocene units are, from bottom to top, conglomerate, sandstone, clayey limestone, siltstone, shale and marl. The Quaternary deposits are young alluviums (Filiz et al., 2000; Karakuş, 2010 and references there in).

4.1.2.9 Lithology of Hıdırbeyli–Bozköy Geothermal Field

Hıdırbeyli–Bozköy geothermal field, Menderes metamorphics occur as basement rocks. Augen gneiss, migmatitic gneiss and granitic gneiss are common. Gneiss units alternate with quartzite, quartz-schist and phyllite. Moreover, quartz-schist, phyllite, mica-schist and muscovite-schist, marble above gneisses and schists represent the Menderes metamorphics. Marble and phyllite alternation is exposed in the geothermal field. Above Menderes metamorphics, Lower Miocene units overlie. They are reddish conglomerate, sandstone and claystone. Pliocene units above Miocene deposits are sandstone, claystone, siltstone and clayey units.The youngest units are Pliocene loose conglomerate and sandstone, Holocene alluvium, alluvial fan, talus and terraces (Karahan, 2008; Söğüt, 2011).

4.1.2.10 Lithology of Söke–Davutlar Geothermal Field

Paleozoic rocks of Söke–Davutlar geothermal field are schists and marbles which form the basement. Schists are mica-schist, quartz-schist and calc-schist. Neogene Kuşadası formation has conglomerate, sandstone, claystone, marl and clayey limestone which overlie the metamorphics. Another Neogene deposits are Davutlar Volcanics which have a thin layer of tufite at the bottom and are basaltic lawa flows. The youngest units are Quaternary alluviums (Tarcan et al., 2000; Uysal, 2002).

4.2 Data Analyses Based on Reservoir Characteristics

The geothermal fields in the study area are generally being fed by meteoric waters. Meteoric waters recharge the reservoir rock and are heated at depth and move up to the surface through the active faults by convection currents. Büyük Menderes Graben system has mainly Paleozoic metamorphics and Neogene sedimentary rocks as reservoir rocks while the cap rocks are impermeable units of sedimentary deposits.

In this part of the thesis, the reservoir features, aquifer and cap rock, age of the reservoir units, tectonic components and fault cuttings in the wellbores, of the defined 17 geothermal fields in the study area are examined, explained, compared and contrasted.

Pamukkale–Karahayıt and Gölömezli geothermal fields have a primary reservoir rocks which are quartzite, and marble with secondary permeability represented by a network of joints, fractures, faults and karstic features (Özler, 2000; Tamgaç, 2010). These rocks represent Paleozoic basement rocks. Moreover a second reservoir unit, Sazak formation, is Miocene and Pliocene limestone and travertine. Cap rock of the primary reservoir is Kızılburun formation composed of clay, silt, marl, sandstone and gravel (Özler, 2000).

The main reservoir of Gerali geothermal field is sandstone and limestone of Kızılburun formation and Menderes Massif marbles with a temperature measured at 125 ^{o}C degrees maximum. In the second reservoir, limestone of Sazak formation, the temperature was measured as 96-100 ^{o}C degrees. Cap rocks of the Gerali geothermal field are schist of Menderes Massif metamorphics, clay levels of Kızılburun formation and clay strata of Pleistocene age from bottom to top. The main fault lines are in the direction of E-W; secondary fault lines are in the direction of N-S, and NE-SW. Fault lines cut with drilling MDO-1, are E-W directed (Karamanderesi & Ölçenoğlu, 2005).

Tekkehamam and Kızıldere geothermal fields have three productive zones according to drilling studies until now. The upper reservoir rock is composed of limestones of the Pliocene Sazak formation, which are intensely faulted and fractured. Sazak formation shows both lateral and vertical gradations to marl and sandstone. The lateral facies changes of Sazak formation limit the continuity of the reservoir, and therefore reduce its reservoir rock characteristics (Şimşek, 1984). This reservoir is water dominated. The second reservoir below the upper one is the metamorphic basement of İğdecik formation, and composed of alternations of marble-quartzite-schist, which has high fracture permeability. The second reservoir exhibits a lateral continuity over a large area, has relatively high secondary porosity and permeability,

and higher temperatures (Şimşek et al., 2005). The third reservoir is the deepest one which constitutes the Paleozoic gneisses and quartzites. This reservoir is associated with the main graben boundary fault line at depth. The first cap rocks are siltstone and sandstone alternations of the Tosunlar formation, and alternations of sandstone, marl and siltstone of Kolankaya formation which is the upper one. The second one is the well-consolidated conglomerates, sandstone and claystone alternations of the Kızılburun formation which act as the second cap rock. The marl and claystone alternations of the Sazak formation act also as a second cap rock. The micashists act as cap rock for the third deep reservoir.

The Kızıldere geothermal field is located on the northern boundary fault of the graben, and is roughly bounded by the geothermally inactive listric-type Gökdere fault from the north and by the geothermally active, nearly E-W trending, Kızıldere fault from the south (Eşder et al., 1994). The Tekkehamam geothermal field, on the other hand, is located on the southern boundary fault of the Büyük Menderes Graben. The young tectonism in the field is the major source for the occurrence of geothermal resources. Due to the intense tectonic activities in the field, the hard and fragile lithologies in the stratigraphy gained secondary permeability, which resulted in the occurrence of reservoir rocks for the geothermal fluids (Şimşek, 1984).

In Pamukören geothermal field, the East-West trending Graben was formed by step-like normal fault systems as a result of uplifting of Menderes Massif in a north-south direction extensional tectonics (Atmaca, 2010). In the region, the deeper reservoir rocks are gneisses and marbles of Menderes Massif which have secondary permeability due to tectonic activities. Sandy and pebbly levels of Neogene rocks form the shallow geothermal reservoir. The clayey and silty levels of Tertiary units and schist of the Menderes Massif have cap rock properties (Yolal, 2010).

Nazilli–Bozyurt–Güzelköy, Atça–İsabeyli and Umurlu geothermal fields have reservoir and cap rocks same with Pamukören geothermal field. Gneisses and marbles of the Menderes Massif and Neogene sedimentary units, sandstones, and huge sized sedimentary deposits form the reservoir rocks while clayey and silty parts of Tertiary sediments and schists of the Menderes Massif compose the cap rocks

(Karahan & Güdücü, 2008; Karahan & Dönmez, 2009; Karahan et al., 2009, Karahan, 2010a; Purtul, 2010). Intersection areas of the East–West trending graben faults and North–South strike slip faults are the weakness points of all these regions. This weakness zones are the most active geothermal regions in the fields.

Salavatlı–Sultanhisar geothermal field has Menderes metamorphic units as reservoir rock composed of gneisses, several types of schists and marbles. Neogene rocks form the shallow geothermal reservoir. Sedimentary units consist of clayey sediments, silts and gravels which serve as cap rock for the geothermal reservoir. Tectonically, SWW-NEE oriented two major faults that can be related to the formation of graben in the north of the field and an older major inferred fault with NWW-SEE orientation crossing through the center of the field control geothermal system (Serpen et al., 2006).

İmamköy–Yılmazköy–Ilıcabaşı–Kalfaköy geothermal field has reservoir rock composed of gneiss and marble. Neogene units, sandy and pebbly sediments, also form the shallow reservoir. Metamorphic schists and clayey units of Neogene age constitute the cap rocks of geothermal field (Yurttaş, 2008).

Ömerbeyli–Alangüllü geothermal field consists of two reservoirs and generally the deepest reservoir is composed of Paleozoic fractured gneiss, quartz schist, and karstic marbles of the Menderes Massif metamorphics, whereas the shallow reservoir is composed of Miocene to Pliocene sandstones and conglomerates.The cap rocks are Neogene impermeable claystone and mudstone (Filiz et al., 2000). The Germencik geothermal fields are controlled by E-W-trending faults.

The suitable reservoir rocks of Hıdırbeyli–Bozköy geothermal field are altered gneisses and marbles of the Menderes metamorphics. In addition to this, sandy and pebble bearing Neogene formations can account for shallow geothermal reservoirs. The clay and silty sediments of Neogene units and schists of the Menderes Massif are the main cap rocks in the region (Söğüt, 2011). Geothermal system is effective in the formation of faults in the north-south direction, extending to east-west-trending

graben-bounding normal faults, depending on the geothermal sites which also form geological boundaries (Söğüt, 2011).

Söke–Davutlar geothermal field has impermeable schists of metamorphics as basement. Karstic marbles are the deeper reservoir rocks of the geothermal fluid. Basaltic volcanics which are fractured have also aquifer characteristics. Kuşadası Formation constituting clayey levels forms the cap rock of the geothermal feld. Active faults in the region trend in west–east and north east–south west directions and west–east-trending Davutlar fault controls the geothermal activity in Söke–Davutlar geothermal field (Tarcan et al., 2000).

In this thesis, the stratigraphies of geothermal wells were studied in detail. According accessed well datais expressed in Table 4-2. The table shows the main reservoir units which produce geothermal liquid with highest temperature for each field. The main reservoir units of the studied geothermal fields are Paleozoic metamorphic units. These units are generally karstic marbles, fractured gneisses and rarely some types of schists. In addition to main reservoir units, most of the geothermal fields have shallower and cooler reservoir units. These secondary reservoir rocks are younger Neogene sedimentary deposits like largely limestone and sandstone, conglomerate and sandy, pebbly units.

The reservoir units which compose highest temperature geothermal fluid are shown in the table below. There are 61 wells with fault existence data. Moreover, the numbers “1” and “0” represent the fault cut and absence of the fault cut in the wellbore, respectively. The average temperature of the wells cut by a fault is about 162 ^{o}C while the average temperature of the wells without a fault cut is about 125 ^{o}C. So, higher temperatures were obtained from the wells which a fault is cut. Most geothermal fields are controlled by extension of graben-bounding normal faults. There are mainly two faults type trending in North–South and East–West directions. The junction points of these faults are the weakness zones where the high temperature fluid can be reached. Moreover, East–West trending faults control the Büyük Menderes Graben geothermal system.

Table 4-2: Main reservoir units of the fields and fault cut relations.

Well Name	Depths (m)	T (°C)	Dist. to sea (km)	Fault	Reservoir units
KH 1	452,00	58,00	165,00	0,00•	marble–limestone
KH 2	468,00	58,50	164,33	1,00*	marble–limestone
KH 3	570,00	61,50	163,67	1,00	marble–limestone
DG 1	1289,00	95,48	156,67	0,00	quartzite–marble, limestone
DG 3	549,00	66,00	157,80	1,00	quartzite–marble, limestone
DG 4	750,00	70,00	157,83	0,00	quartzite–marble, limestone
DG 5	750,00	62,00	157,77	1,00	quartzite–marble, limestone
MDO-1	814,00	96,00	148,33	1,00	limestone
MDO-1a	1143,00	125,00	148,33	1,00	sandstone–limestone–marble
DSG 4	2171,00	117,98	146,67		marble–quartzite–calcschist
TH1	615,50	116,00	136,67	1,00	limestone
TH2	2001,00	170,00	137,00	1,00	
KD-1	540,00	203,00	137,18	1,00	limestone
KD-2	706,50	175,00	136,87	1,00	limestone
KD-3	370,00	158,00	136,83	1,00	limestone
KD-4	486,00	166,00	138,19	1,00	limestone
KD-111	504,85	164,00	137,19	1,00	marble–quartzite–schists
KD-6	851,00	196,00	137,20	1,00	marble–quartzite–schists
KD-7	667,00	204,00	137,20	1,00	marble–quartzite–schists
KD-8	576,50	193,00	137,22	1,00	limestone
KD-9	1241,00	170,00	137,17	1,00	marble–quartzite–schists
KD-12	404,70	160,00	138,17	0,00	limestone
KD-13	763,00	195,00	137,20	1,00	marble–quartzite–schists
KD-14	597,00	207,00	137,21	1,00	marble–quartzite–schists
KD-15	510,00	205,00	137,22	1,00	marble–quartzite–schists
KD-16	666,00	207,00	137,21	1,00	marble–quartzite–schists
KD-21	898,00	202,00	137,21	1,00	marble–schist
R1	2260,00	242,00	137,00	1,00	gneiss–quartzite
R-2	1371,89	204,00	137,20		gneiss–quartzite
R3	2250,00	241,00	137,20	0,00	marble–schist–gneiss

• : absence of fault cut

* : fault cut

Table 4-2: Continued.

Well Name	Depths (m)	T (^{o}C)	Dist. to sea (km)	Fault	Reservoir units
AP 2	1090,00	182,41	112,60	1,00	gneiss–marble
AP 3	925,00	182,79	112,67	1,00	gneiss–marble
NG 1	2152,00	127,36	102,67	1,00	gneiss–marble
NB 1	1829,00	140,31	99,33	1,00	gneiss–marble–schist–phillite
AT 1	1186,00	123,64	88,33	1,00	marble–phillite–micaschist
AT 2	700,00	122,90	88,33	0,00	marble–phillite–micaschist–gneiss
İS 1	1150,00	88,30	88,67	0,00	gneiss–schist–phillite
SH 1	988,00	145,00	80,00	1,00	gneiss–micaschists–quartzschist–marble
SH 2	986,00	146,00	81,33	1,00	gneiss–micaschists–quartzschist–marble
ASR 1	1430,00	150,00	71,67	1,00	gneiss–schist
ASR 2	900,00	165,00	71,33	0,00	marble
ASR 3	900,00	169,42	73,67	1,00	gneiss–schist–marble
AS 1	850,00	169,77	73,00	1,00	marble
AS 2	962,00	175,50	70,33	1,00	marble
AU 1	1211,00	154,39	66,17	1,00	marble–phillite
AU 2	1582,00	149,58	66,33	0,00	marble–phillite
ASK 1	2000,00	154,48	66,00	1,00	marble–phillite
İmamköy	1300,00	160,00	61,67	1,00	
Yılmazköy	1100,00	160,00	60,00	1,00	marble–schist
AY 1	1501,00	142,00	60,67	1,00	marble–schist
AY 2	2500,00	190,00	61,00		
Ayter 1	471,00	84,50	60,00	1,00	conglomerate
Ayter 2	355,00	101,50	60,33	1,00	conglomerate

Table 4-2: Continued.

Well Name	Depths (m)	T (^{o}C)	Dist. to sea (km)	Fault	Reservoir units
A 2	480,00	102,80	38,33	0,00	marble–calcschist
OB2	975,50	231,00	37,00	1,00	gneiss–schists–metaquartzite–marbles
OB3	1196,70	230,00	36,33	1,00	gneiss–schists–metaquartzite–marbles
OB4	285,00	213,00	37,33	1,00	gneiss–schists–metaquartzite–marbles
OB5	1302,00	221,00	37,67	1,00	gneiss–schists–metaquartzite–marbles
OB6	1100,00	221,00	36,60	1,00	gneiss–schists–metaquartzite–marbles
OB7	2398,00	232,00	36,20	1,00	gneiss–schists–metaquartzite–marbles
HB 1	873,00	120,54	27,00	1,00	gneiss–schist
HB 2	280,00	141,78	26,67	1,00	gneiss–marble–schist
AGG 16	1180,00	66, 15	8,33	0,00	marble, gneiss
Davutlar	203,00	43,00	6,67		marble
AKD 2	785,00	58,00	6,67		

4.3 Data Analyses Based on Temperature

Büyük Menderes Graben geothermal fields have the highest reservoir temperature measurements in Turkey. The temperature values are acquired from 102 wells in 17 fields. The minimum, maximum and average temperatures of the fields are shown in Table 4-3 (see also Appendix A). The three highest average temperature values were gathered from Kızıldere, Ömerbeyli–Alangüllü and Pamukören fields. Söke–Davutlar, Yenice and Pamukkale–Karahayıt fields have the lowest average temperatures in the Büyük Menderes Graben. Moreover, it was recognized that there is not any gradual increase or decrease of average temperature values according to distance to sea which is assumed as a constant point to analyse the fields according to their locations in the graben.

Table 4-3: Minimum, maximum and average temperature values of the 17 fields.

Fields	**Well Number**	**Max. T (^oC)**	**Min. T (^oC)**	**Ave. T (^oC)**
Pamukkale–Karahayıt	3	61,50	58,00	59,00
Gölemezli	5	95,48	62,00	73,30
Yenice	3	63,00	38,00	51,00
Gerali	2	125,00	114,00	119,50
Kızıldere	22	242,00	157,00	193,14
Tekkehamam	8	170,00	100,00	123,25
Buharkent–Ortakçı	2	147,00	56,70	101,85
Pamukören	2	182,79	182,41	182,60
Nazilli–Bozyurt–Güzelköy	2	140,31	127,36	133,84
Atça–İsabeyli	3	123,64	88,3	111,61
Salavatlı–Sultanhisar	8	175,50	128,00	156,09
Umurlu	3	154,48	149,58	152,82
Yılmazköy–İmamköy–Ilıcabaşı–Kalfaköy	9	190,00	84,50	132,17
Ömerbeyli–Alangüllü	19	232,00	102,80	210,60
Hıdırbeyli–Bozköy	5	174,00	120,54	154,63
Ortaklar–Gümüşköy	4	178,00	66,15	155,33
Sökes–Davutlar	2	58,00	43,00	50,50

The temperature values of 98 wells analyzed according to well depths and the distance of well locations to the sea. The change of temperature with depth is shown below in Figure 4-3. Moreover the change of temperature with well distance to sea is shown in Figure 4-4.

According to analysis of temperature change with well depth, the temperature increases as the well depth increases. Moreover, there is no relationship between the location of a geothermal field and temperature according to analysis.

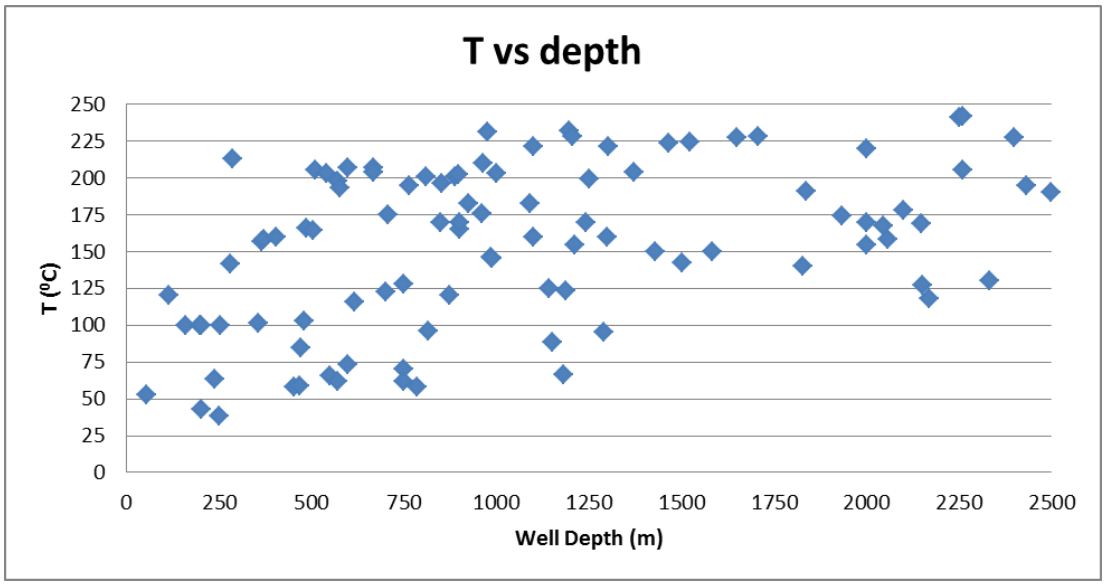

Figure 4-3: The change of temperature with depth in the Büyük Menderes Graben.

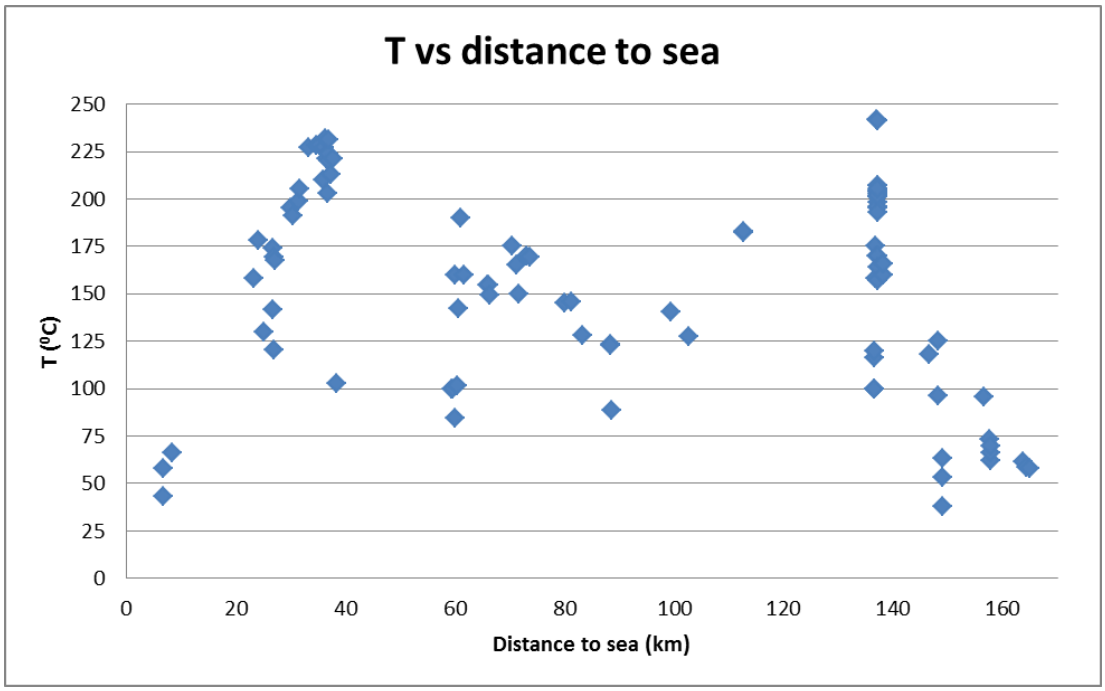

Figure 4-4: The change of temperature with distance of the well locations to the sea.

4.4 Data Analyses Based on Geochemistry

The chemical studies done in the fields were researched. The ion contents, mineral contents, SiO_2 (Silisium dioxide) and trace element B (Boron), TDS (Total Dissolved Solids), water type, water origin, pH and electrical conductivity (EC) of 60 wells in

the graben were examined. The major cations, Na^+ (Sodium), Ca^{2+} (Calcium), K^+ (Potassium), NH_4^+ (Ammonium), Mg^{2+} (Magnesium) and major anions, Cl^- (Chloride), HCO_3^- (Bicarbonate), SO_4^{2-} (Sulfate) were the analyzed ion types.

The chemical parameters studied were analyzed based on temperature, well depths and well distance to sea. In addition to diffuculty of chemical data acquisition, the ion and mineral contents and TDS values of water samples taken from different well depths and different temperatures had been used due to lack of data. 60 wells have been examined based on studied chemical parameters. Moreover, geothermal water types of geothermal fields have been examined.

4.4.1 Analyses Based on Chemical Compounds

4.4.1.1 Analyses Based on Some Major Cation Compounds

The major cations, Na^+, Ca^{2+}, K^+, NH_4^+, Mg^{2+}, were analyzed at first. The change of cation values with temperature is shown in Figure 4.5 to Figure 4.9. It is seen that Na^+ and K^+ amounts increase while Ca^{2+} and Mg^{2+} amounts decrese as the temperature rises.

As a known fact, Na^+ concentration increases as the temperature rises. There is a slight increase in Na^+ concentrations as the temperature rises according to the result of analysis. Moreover, AGG 16 (Ortaklar–Gümüşköy) and Davutlar wells which are close to sea have very high Na^+ values, although their temperatures are low about 60 ^oC. Besides, GK 1 well in Gümüşköy has low Na^+ concentration unexpectedly with high temperature (Figure 4-5.).

In general, the solubility of Ca^{2+} decreases with increasing temperature. The analysis shows an expected result. However, Ca^+ values in AGG 16 well are very low although it is expected to be high in concentration due its lower temperature. GK 1 well in Gümüşköy is close to sea and has unexpectedly high Ca^+ concentration with a very high temperature (Figure 4-7.).

Mg^{2+} concentration is generally low in geothermal water while its concentration is high in cold water (Gunnlaugsson, 2008). So, as the temperature increases, the decrease of Mg^{2+} amount is an expected result. Furthermore, Mg^{2+} ions have some unexpected results in some wells. AY 1 and AY 2 wells in Aydın, Davutlar well close to sea and GK 1 well have very high Mg^{2+} concentrations though Mg^{2+} value is generally low in geothermal water (Figure 4-8.).

Increase in K^+ concentrations when the temperature rises is an ignorable result of K^+–temperature analyses because of the change of K^+ concentrations is not significant. K^+ concentrations in OB1 and OB8 wells in Ömerbeyli geothermal field are low contrary to general trend analyzed. Besides, K^+ concentration is very high incongruously in AGG 16 well which has low temperature (Figure 4-6.).

There is no relation between temperature and NH_4^+ ions. In other words, NH_4^+ concentrations are very unsteady in relation with temperature. In addition, NH_4^+ concentrations are very low in the wells with respect to other NH_4^+ ions except for the NH_4^+ concentration of OB 4 well in Ömerbeyli and Ayter 1 well in Aydın (Figure 4-9.).

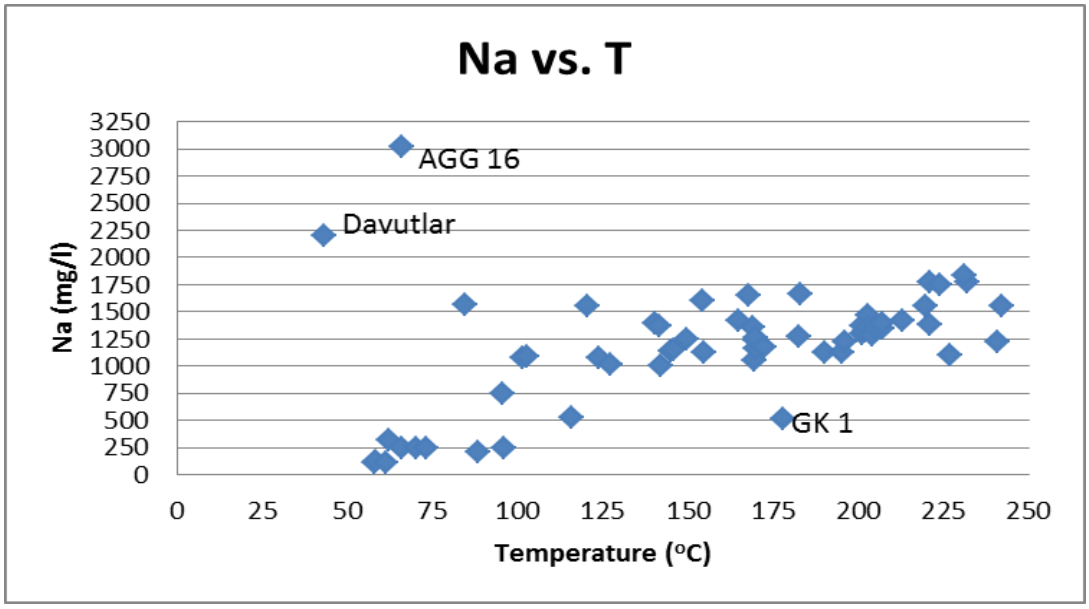

Figure 4-5: The change of Na values with temperature.

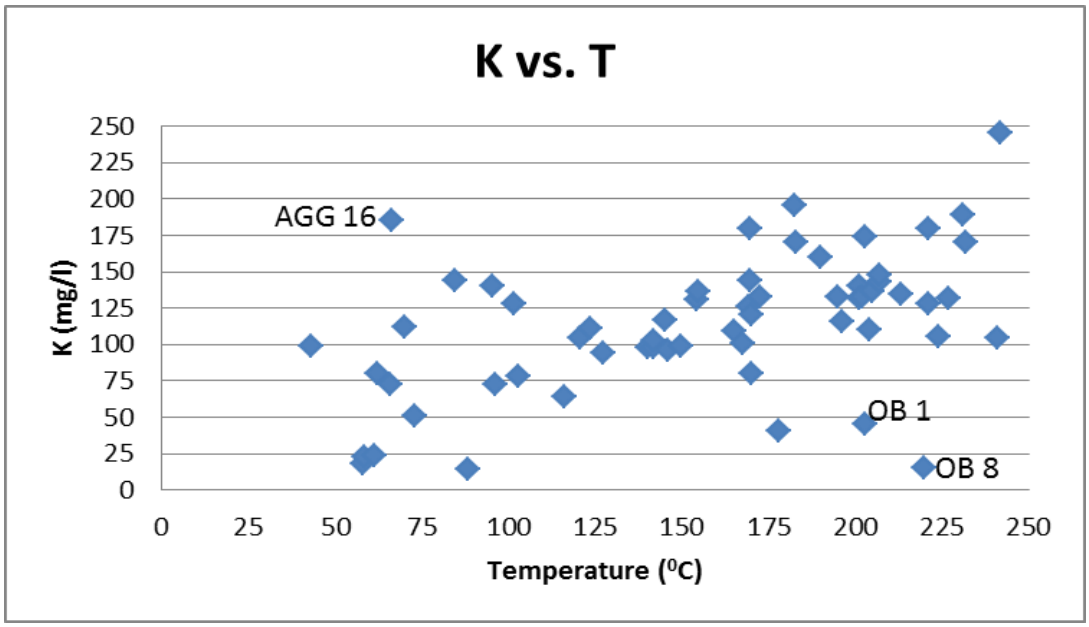

Figure 4-6: The change of K values with temperature.

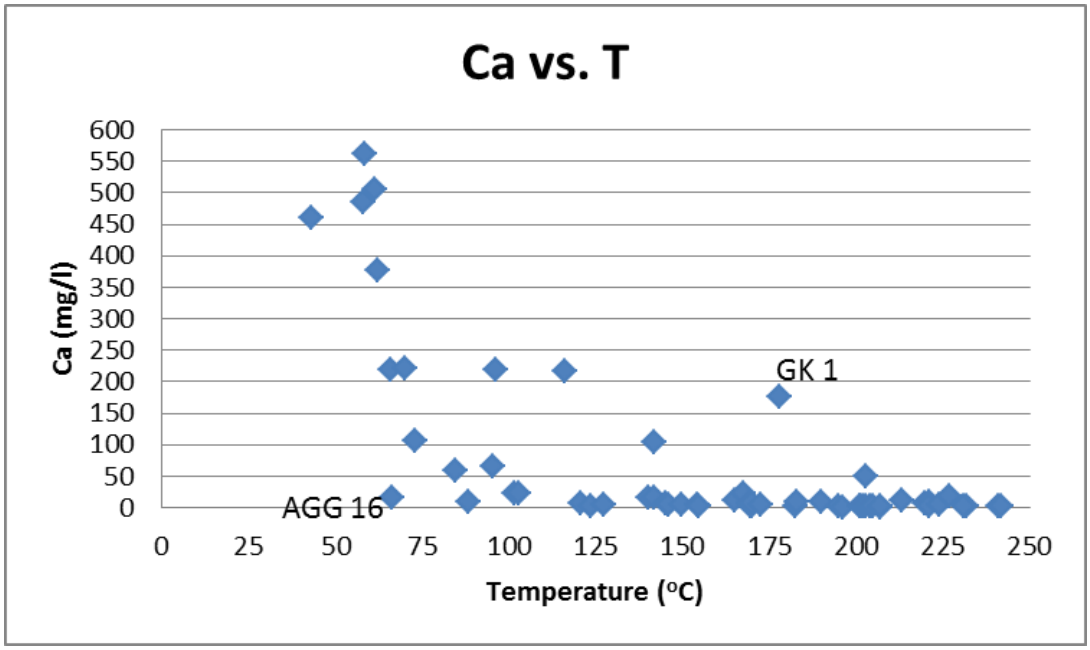

Figure 4-7: The change of Ca values with temperature.

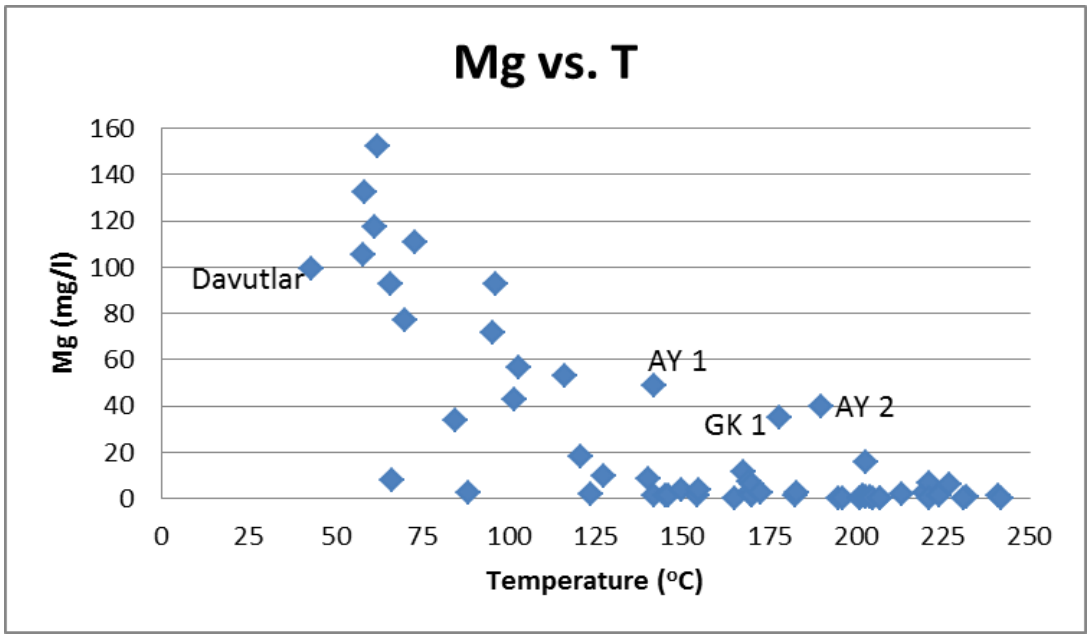

Figure 4-8: The change of Mg values with temperature.

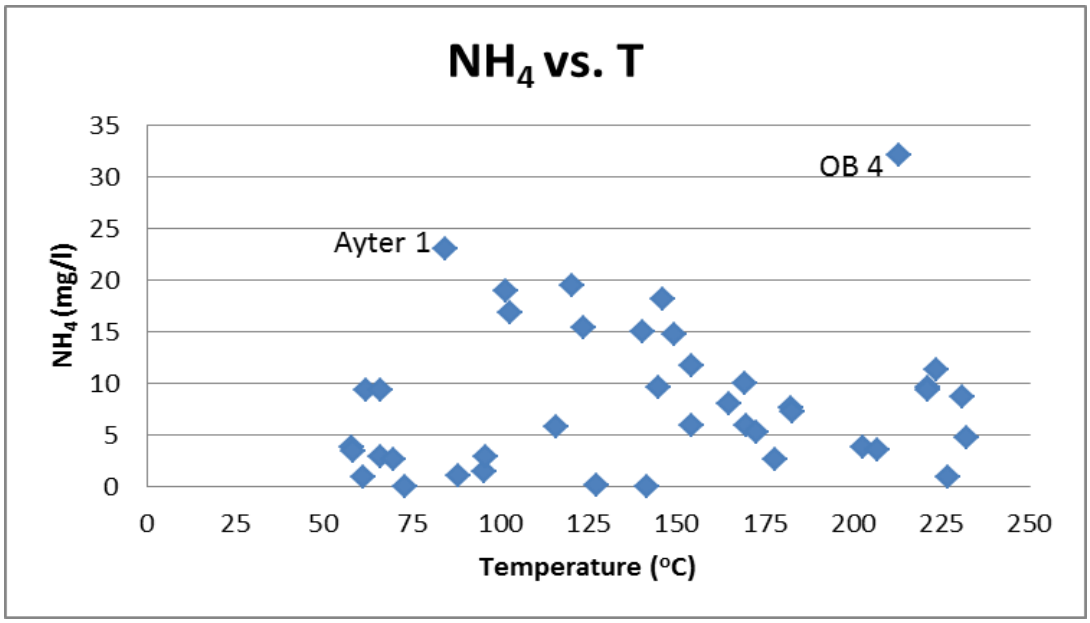

Figure 4-9: The change of NH_4 values with temperature.

The change of cation values with respect to well depths are shown in Figure 4.10 to Figure 4.14. The cation values examined are very changeable with respect to well depth. That means there is no good relation between cation amounts and well depth.

Na^+ ion variance analyses according to well depth shows that Na^+ concentration does not depend on well depth. The Na^+ concentrations have more or less relatively adjacent values to each other except AGG 16, GK 1, İS 1 and Davutlar wells (Figure 4-10.).

Moreover, K^+ values do not depent on well depth. The concentrations are scattered between about 50 mg/l and 200 mg/l. However, there are some exceptions such as wells, R 1, GK 1, OB 8 and İS 1 from Kızıldere, Ortaklar-Gümüşköy, Ömerbeyli-Alangüllü and Atça-İsabeyli geothermal fields respectively (Figure 4-11.).

Ca^+ concentrations are about 50 mg/l in the wells and there is no regular range according to well depth. Some concentrations are very high like in Davutlar well, differing from the general trend (Figure 4-12.).

Mg^+ and NH_4^+ ion analyses based on well depth are more or less similar. As seen in the Figure 4.13 and Figure 4.14, the concentrations are very scattered and indepently changing.

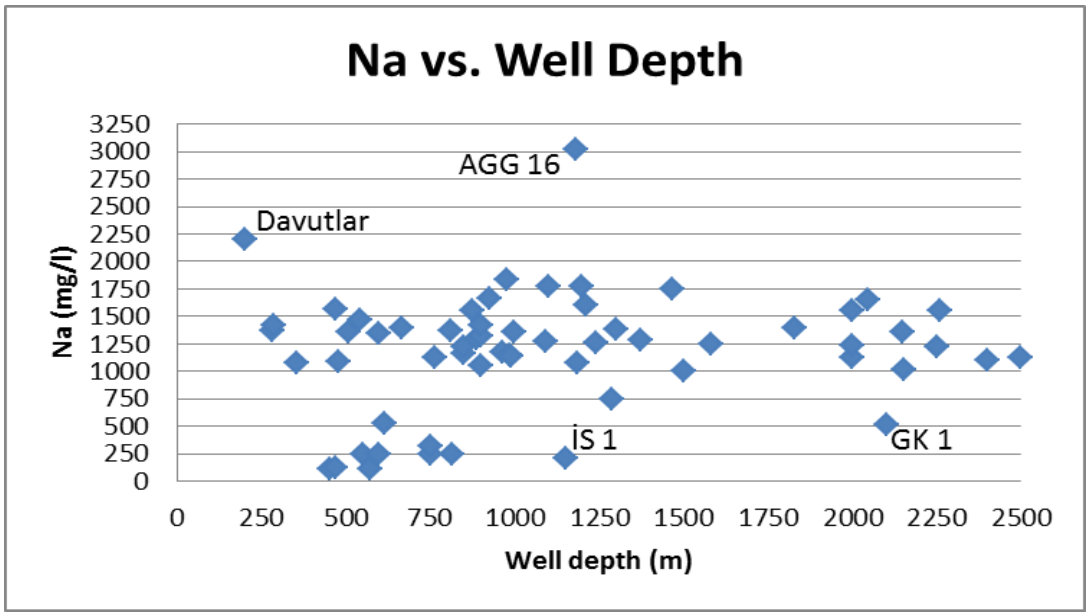

Figure 4-10: The change of Na values with well depth.

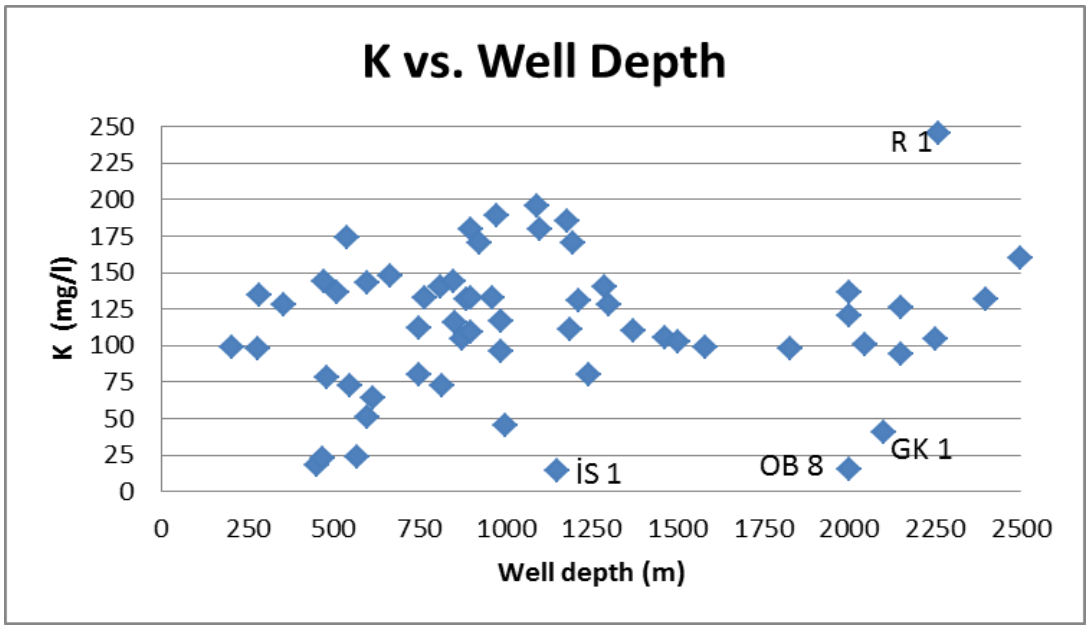

Figure 4-11: The change of K values with well depth.

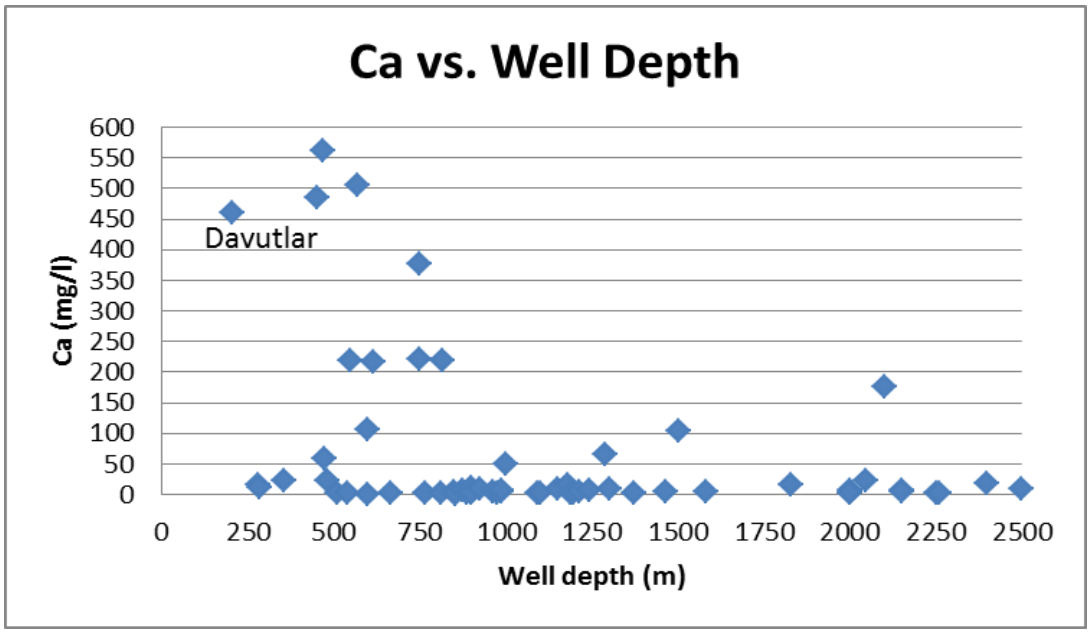

Figure 4-12: The change of Ca values with well depth.

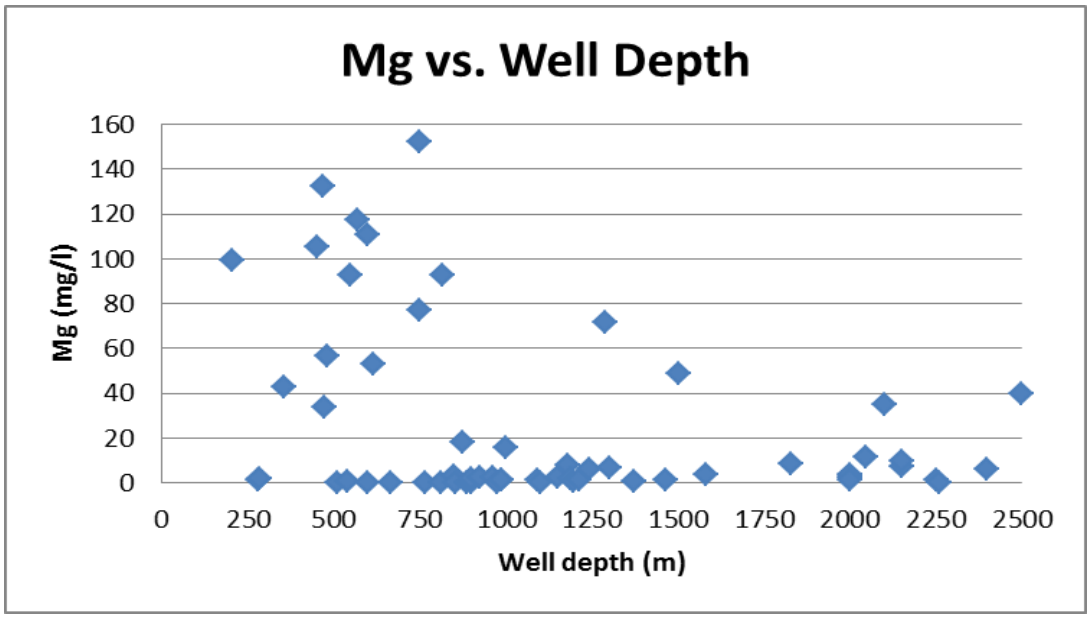

Figure 4-13: The change of Mg values with well depth.

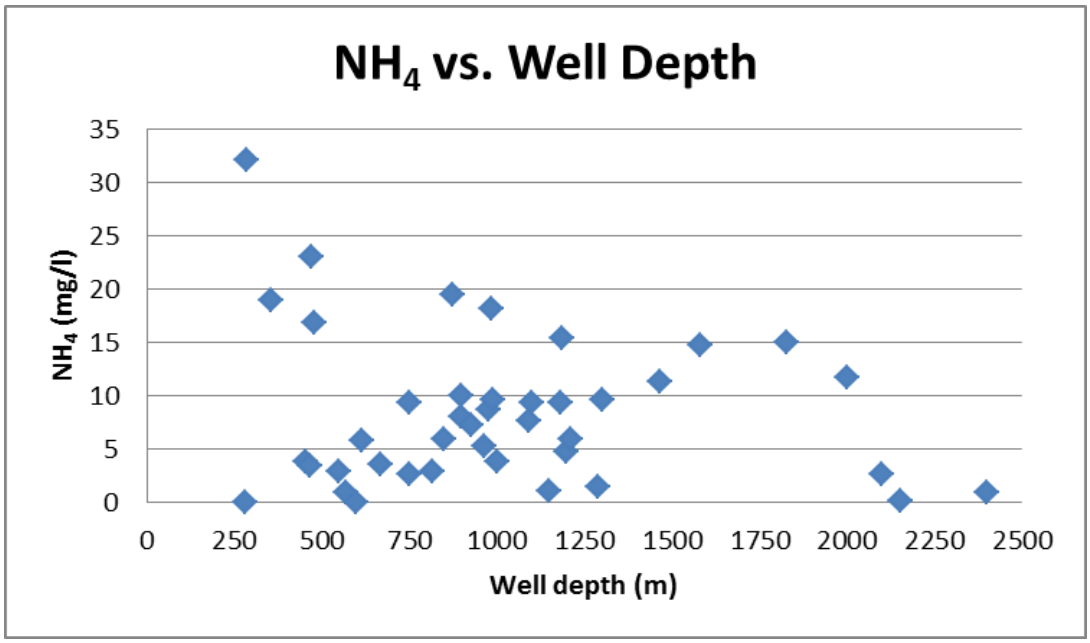

Figure 4-14: The change of NH_4 values with well depth.

The relation between cation values and well distance to sea is more or less parallel to well depth–cation relation. The relations between cations and well distances to sea are shown in Figure 4.15 to Figure 4.19.

Na^+ concentrations slightly increase in the wells close to sea as the well locations get closer to sea. This slight increase in the well close to sea can be due to mixing of sea water and meteoric water. Apart from this, Davutlar and AGG 16 wells have very high Na^+ concentrations. Furthermore, Na^+ concentrations of GK1 and İS 1 wells are very low differing from the general trend (Figure 4-15.).

K^+ concentrations are distributed in a wide range undepently based on well distance to sea. Ca^+ and Mg^+ concentration distributions according to well distance to sea are similar to each other. The results of the Ca^+ and Mg^+ analyses show that there is no relationship between Ca^+ and Mg^+ concentrations and well distance to sea. In addition, Davutlar well has high Ca^+ and Mg^+ concentrations different from the general trend.

Additionaly, NH_4^+ ion analysis based on the well distance to sea does not present good results. NH_4^+ ions change indepently of well locations with respect to sea. Besides, ÖB 4 well in Ömerbeyli geothermal field has very high NH_4^+ concentration (Figure 4-19.).

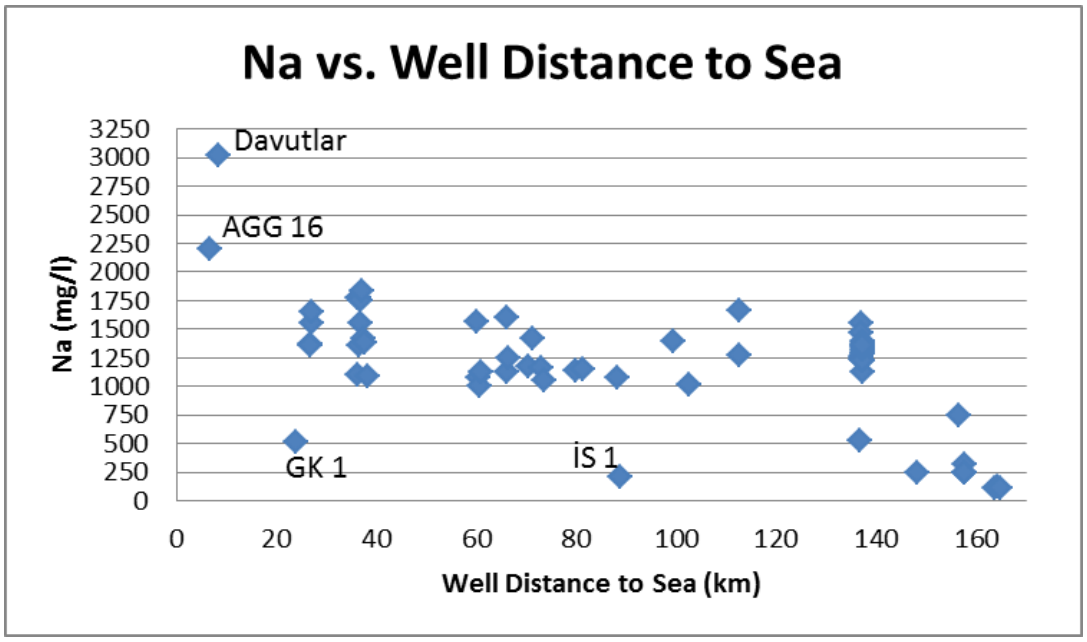

Figure 4-15: The change of Na values with well distance to sea.

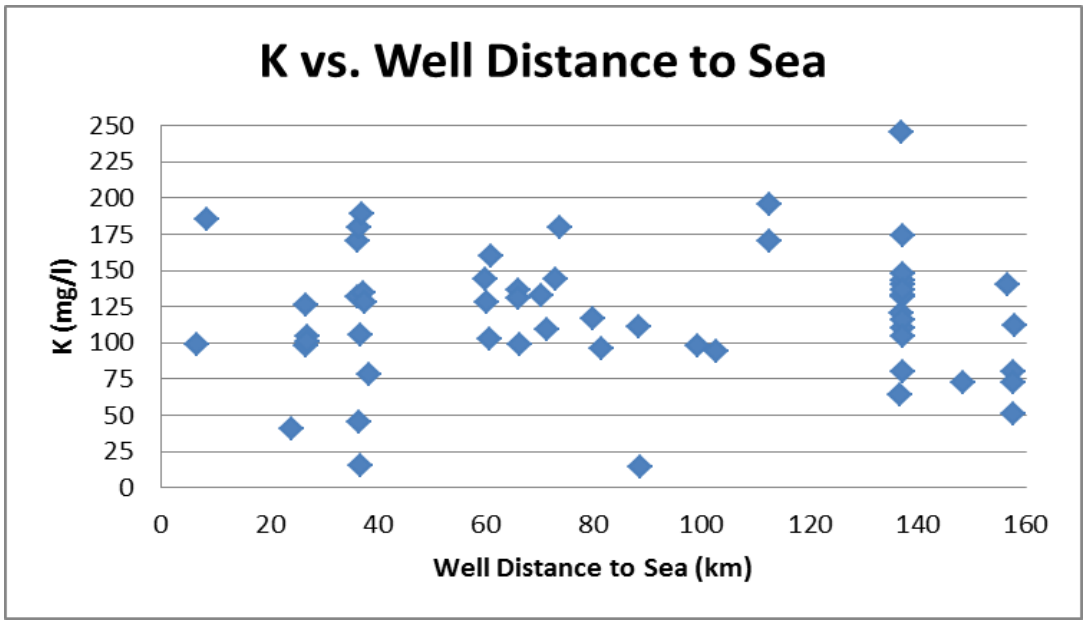

Figure 4-16: The change of K values with well distance to sea.

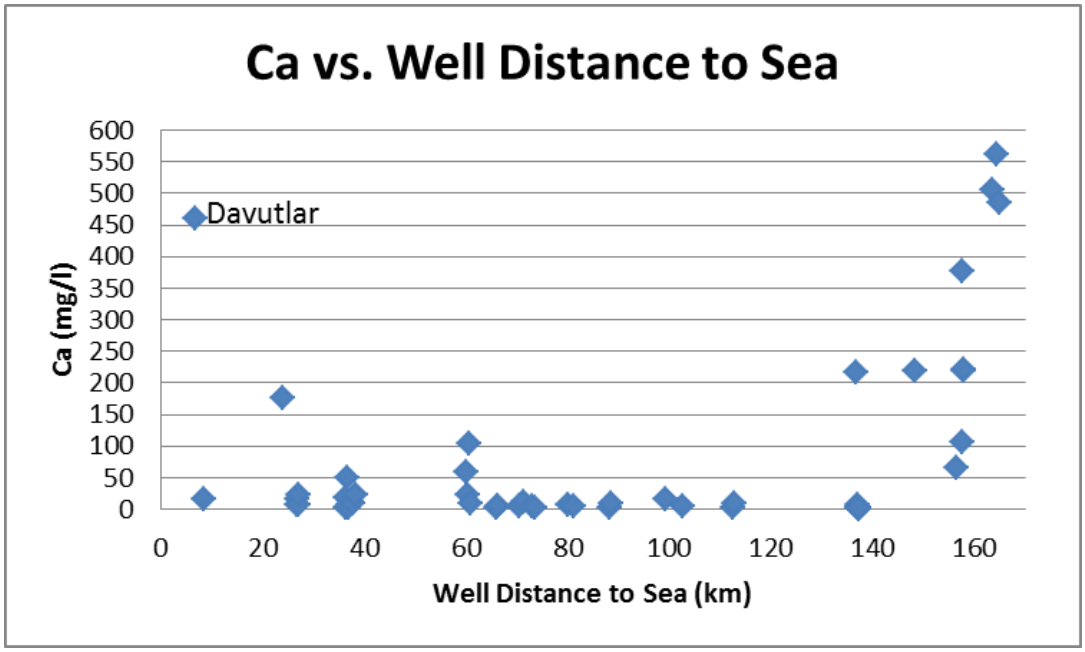

Figure 4-17: The change of Ca values with well distance to sea.

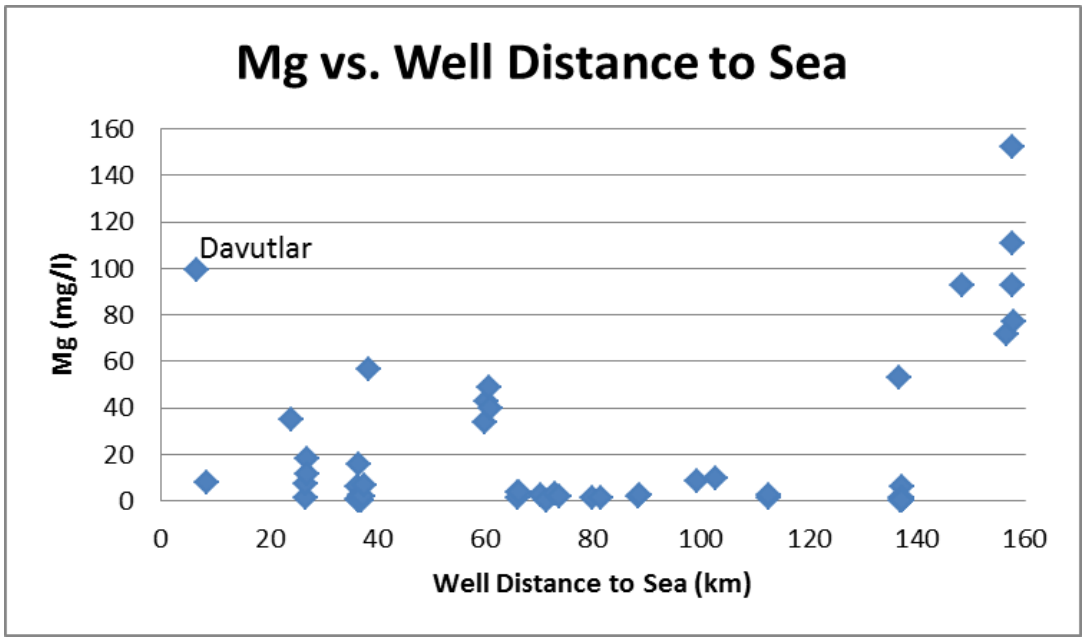

Figure 4-18: The change of Mg values with well distance to sea.

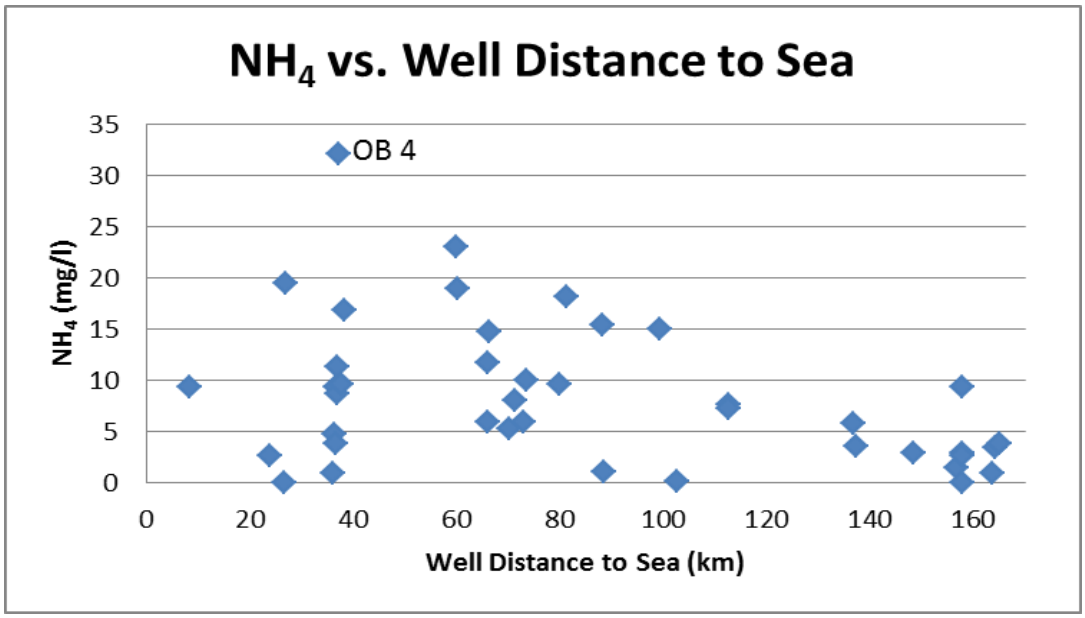

Figure 4-19: The change of NH_4 values with well distance to sea.

4.4.1.2 Analyses Based on Some Major Anion Compounds

The major anions, Cl^-, HCO_3^- and SO_4^{2-} were the other analyzed ion types. The change of anion values with temperature is shown in Figure 4.20 to Figure 4.22. It is seen from the analyses that there is no correlation between temperature and anions. All examined anion values are variable independently.

The relation inbetween Cl^- and temperature is not a significant relation that the values are scattered indepently. Moreover, it seen that Davutlar and GM 2, Hıdırbeyli, wells have very high Cl^- concentrations. This can be due to closeness of these two wells to the sea and mixing of sea water (Figure 4-20.).

The relation between HCO_3^- and temperature is also similar to Cl^-–temperature relation with having no dependency. AGG 16, Ortaklar–Gümüşköy, well has high HCO_3^- concentration (Figure 4-21.).

Furthermore, SO_4^{2-}–temperature relation has not good results with having no dependency on temperature. It can be remarkable that TH1, Tekkehamam, and KD 9, Kızıldere, wells have high SO_4^{2-} concentration while AGG 16, Ortaklar–Gümüşköy, well has low SO_4^{2-} concentration (Figure 4-22.).

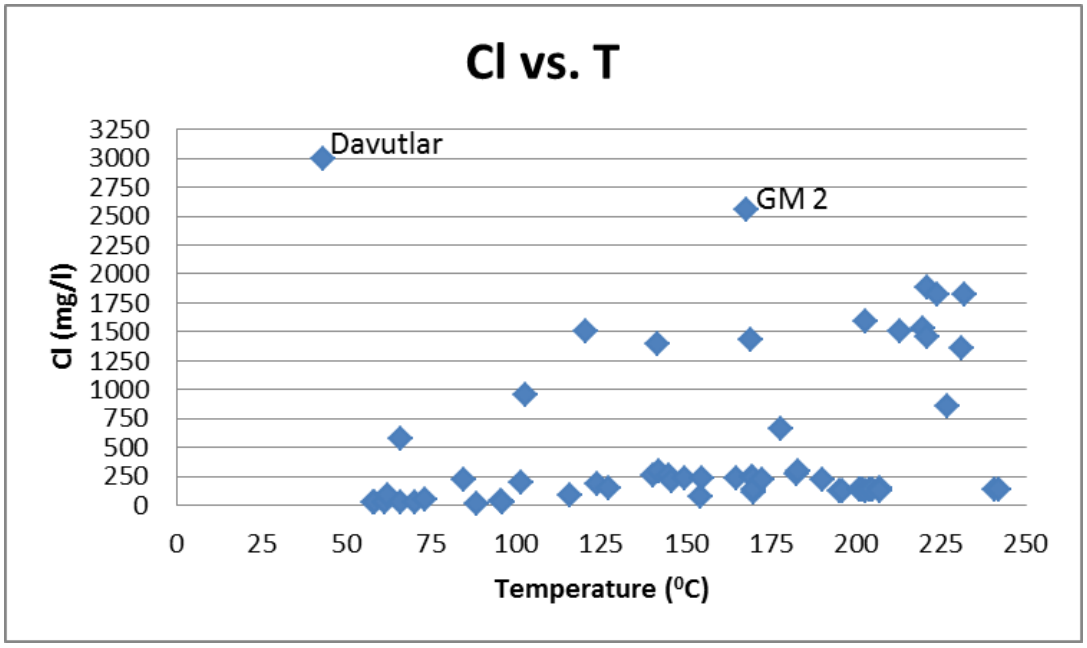

Figure 4-20: The change of Cl values with temperature.

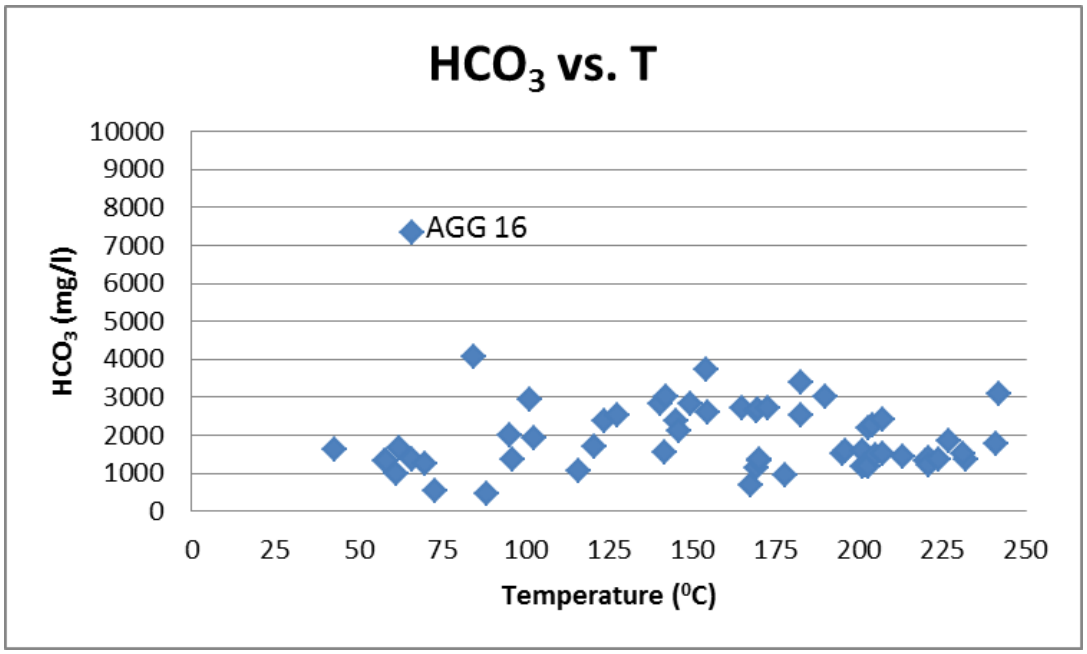

Figure 4-21: The change of HCO_3 values with temperature.

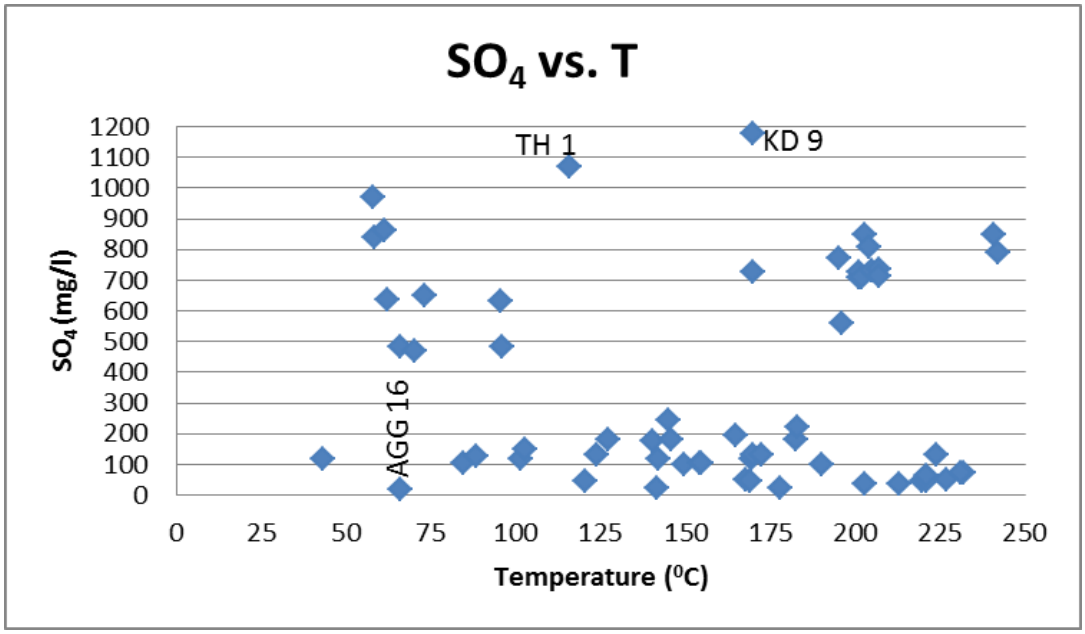

Figure 4-22: The change of SO_4 values with temperature.

Figure 4.23 to Figure 4.25 show the distribution of anions with well depth. It is clearly seen that the relation inbetween well depth and anions is very changeable. The anion values have scattered in a wide range for Cl^- and SO_4^{2-} analyses. HCO_3^- analysis has relatively in a narrow range based on well depth. However, AGG 16 well has very high HCO_3^- concentration. Moreover, Davutlar and GM 2 wells have

high Cl^- concentrations while, TH 1, Tekkehamam field, and KD 9, Kızıldere field, have very high SO_4^{2-} concentrations.

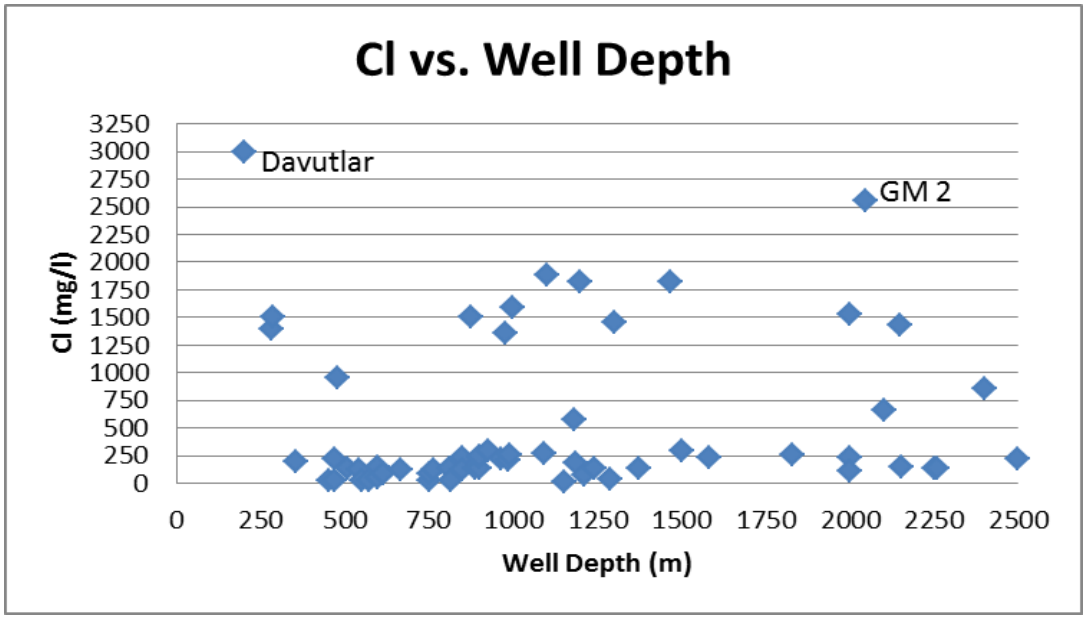

Figure 4-23: The change of Cl values with well depth.

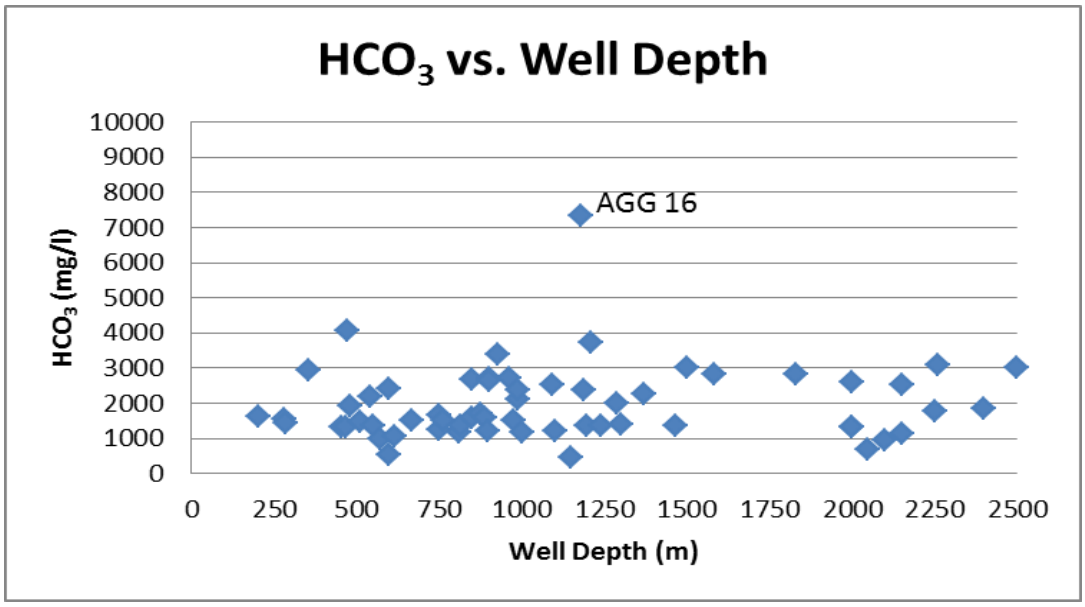

Figure 4-24: The change of HCO_3 values with well depth.

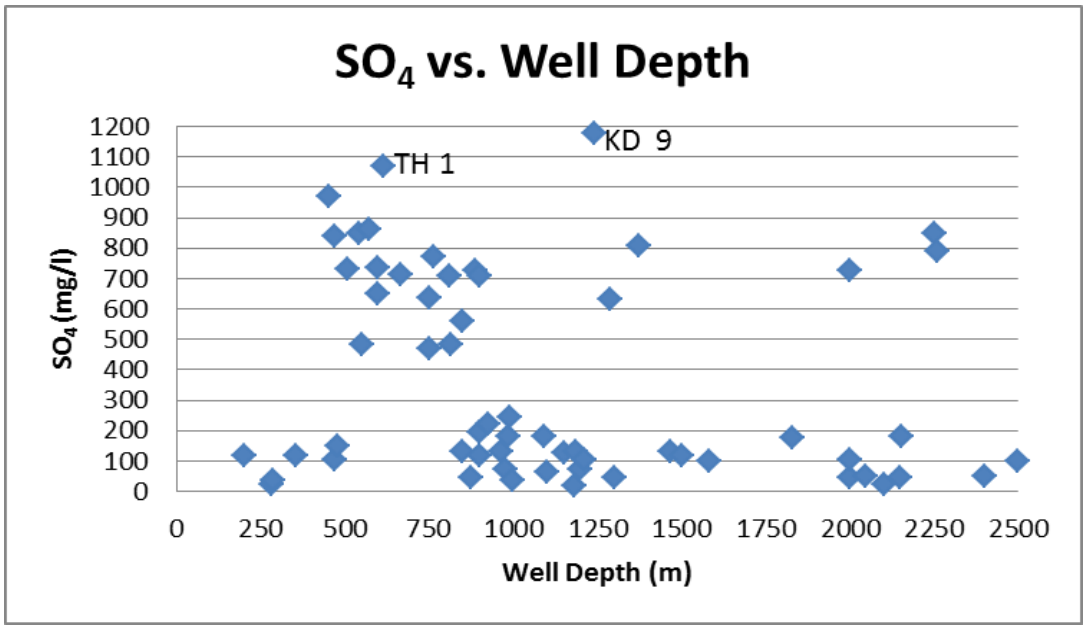

Figure 4-25: The change of SO_4 values with well depth.

Moreover, the relations between well distance to sea and anions are analyzed and shown in Figure 4.26 to Figure 4.28. Cl^- and SO_4^{2-} values change with well distance to sea significantly. Cl^- amounts increase and SO_4^{2-} amounts decrease as the well distance to sea decreases. However, HCO_3^- does not change in a regular range. Besides, although Cl^- amounts change regularly, some values show differencies. Davutlar and GM 2 wells have high Cl^- concentrations, while GK 1 and AGG 16 wells have very low Cl^- concentrations with respect to Cl^- concentrations of other wells which are close to sea. SO_4^{2-} concentrations decrease as the distance of well locations to sea decrease. TH 1, Tekkehamam field, and KD 9, Kızıldere field, have very high SO_4^{2-} concentrations. Moreover, HCO_3^- amounts change between about 500 mg/l and 4000 mg/l. But, AGG 16 well has the value of 7320 mg/l of HCO_3^- ions.

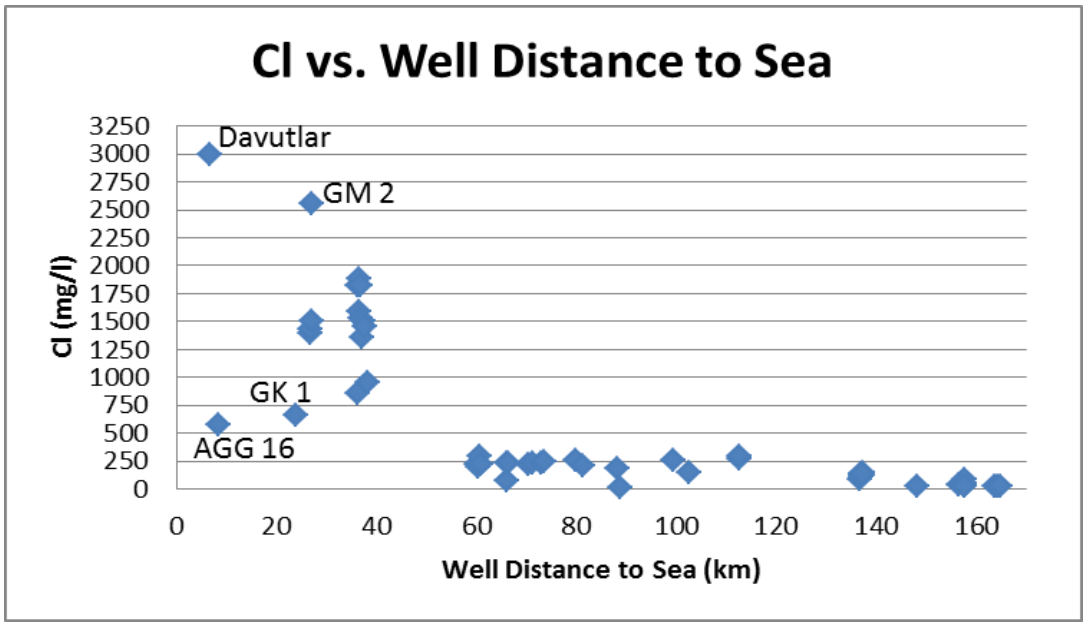

Figure 4-26: The change of Cl values with well distance to sea.

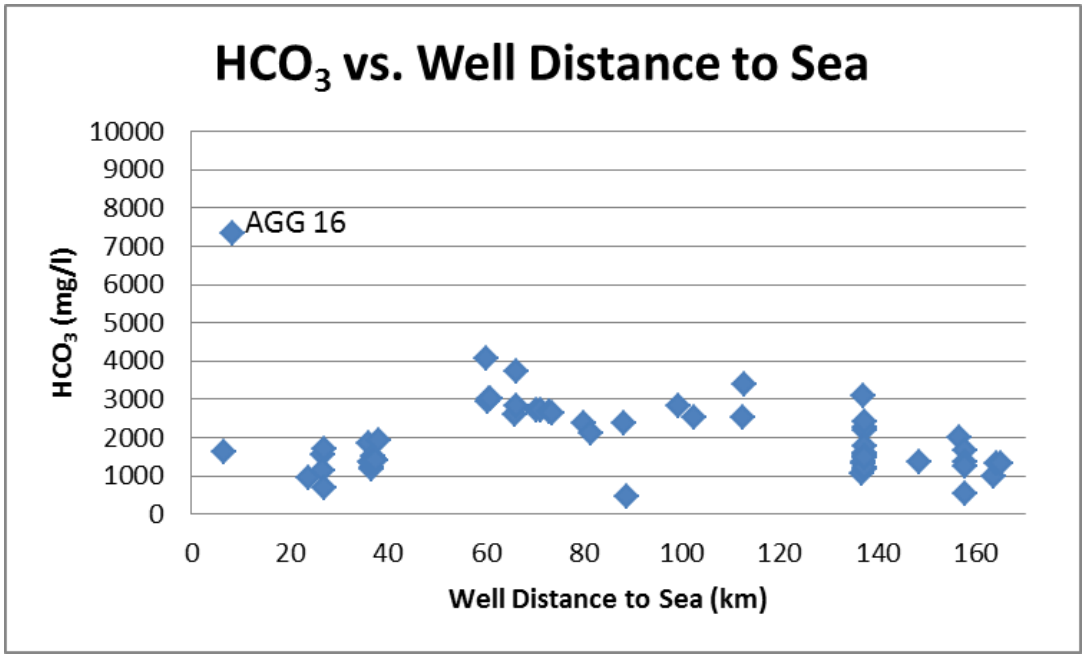

Figure 4-27: The change of HCO_3 values with well distance to sea.

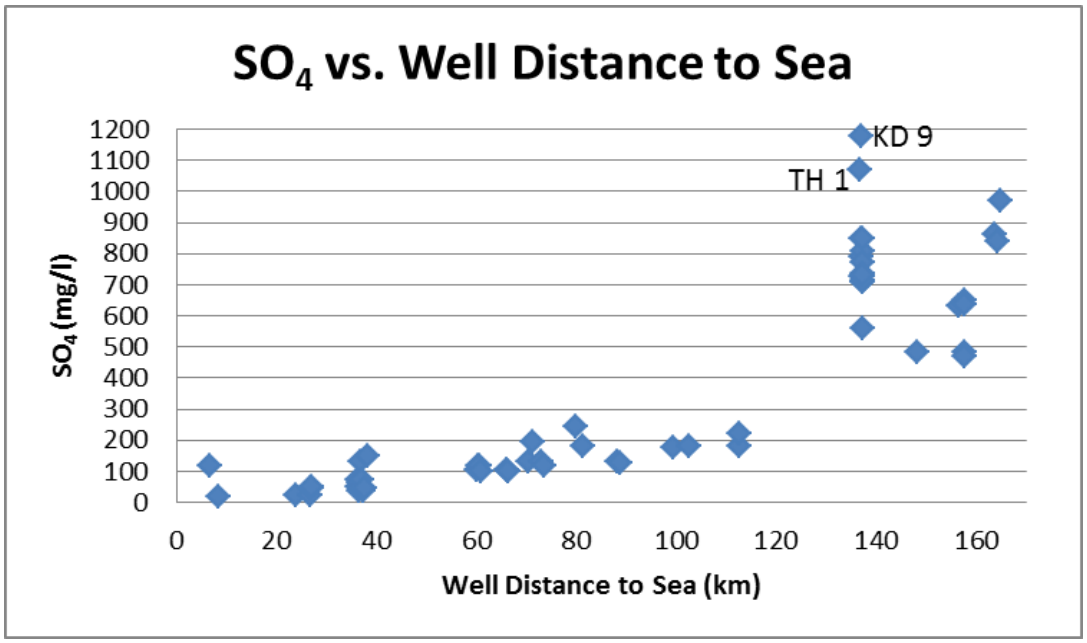

Figure 4-28: The change of SO_4 values with well distance to sea.

4.4.1.3 Analyses Based on SiO_2, B, TDS, EC and pH Values

The results of SiO_2, TDS, B, pH and EC and temperature correlations are shown in Figure 4.29 to 4.33. SiO_2 and pH values show good relation with temperature values. SiO_2 concentrations increase as the temperature of the water increases. DG 4 and R1 wells have high SiO_2 values with respect to SiO_2 values of other wells. pH values also increases with temperature. Moreover, the other parameters, B and EC, show more or less linear correlation with temperature. AGG 16 and Davutlar wells have very high EC values with respect to othwer wells'. This can be related to sea water mixing and salinity. TDS amounts slightly increase with temperature although most of the ion solubilities increase with increasing temperature. KH 3, AGG 16 and Davutlar wells have very high TDS amounts.

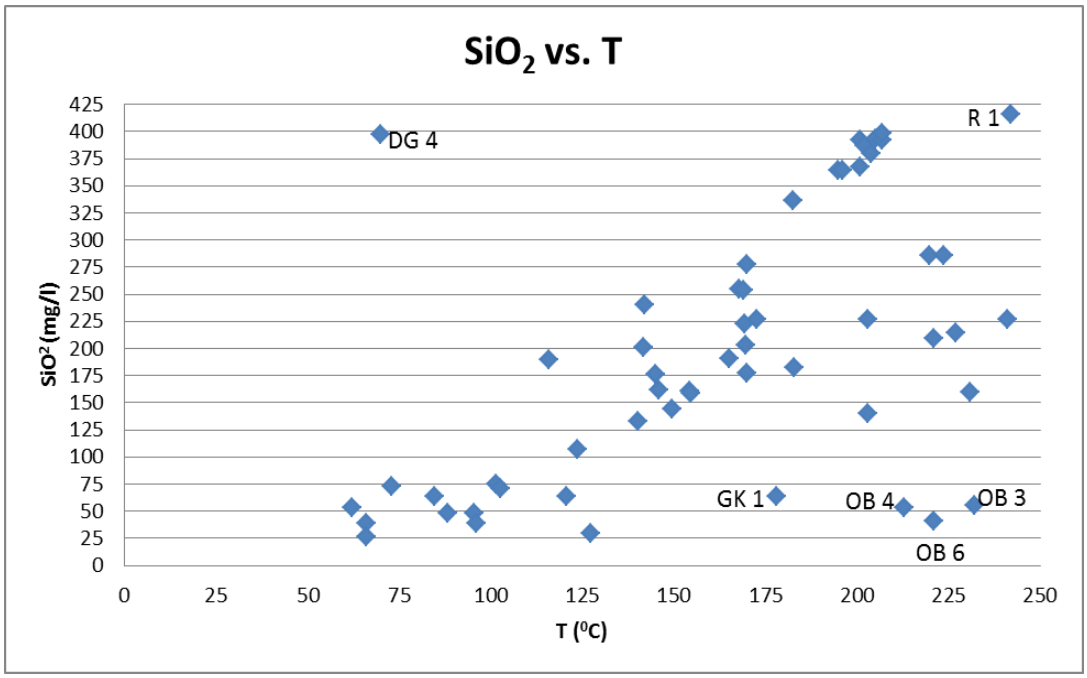

Figure 4-29: The change of SiO_2 values with temperature.

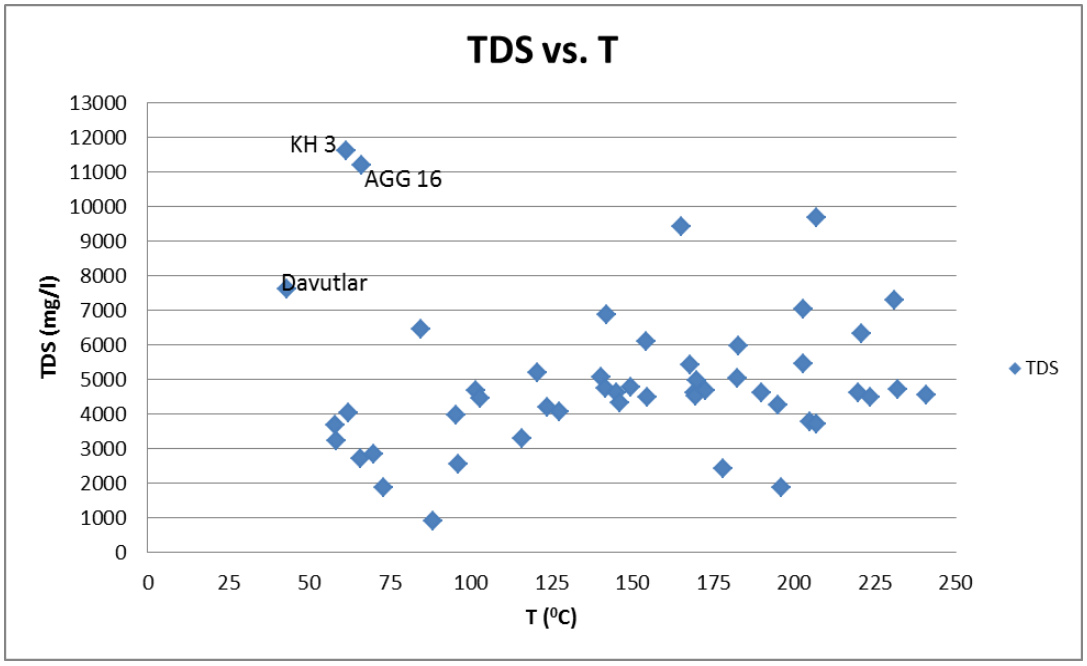

Figure 4-30: The change of TDS values with temperature.

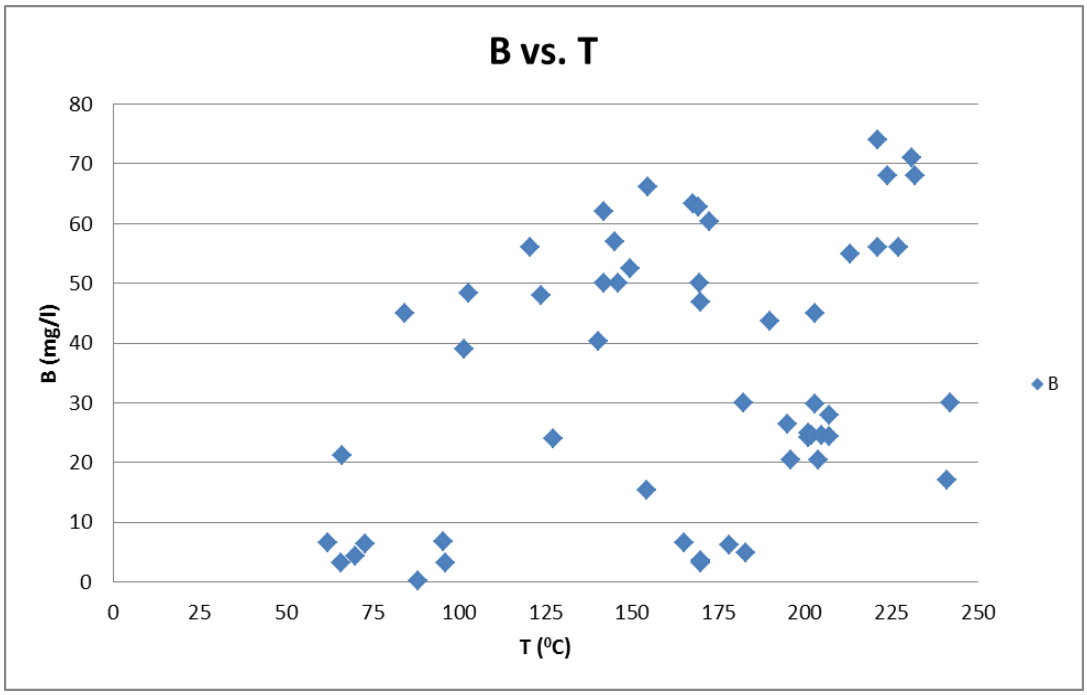

Figure 4-31: The change of Boron values with temperature.

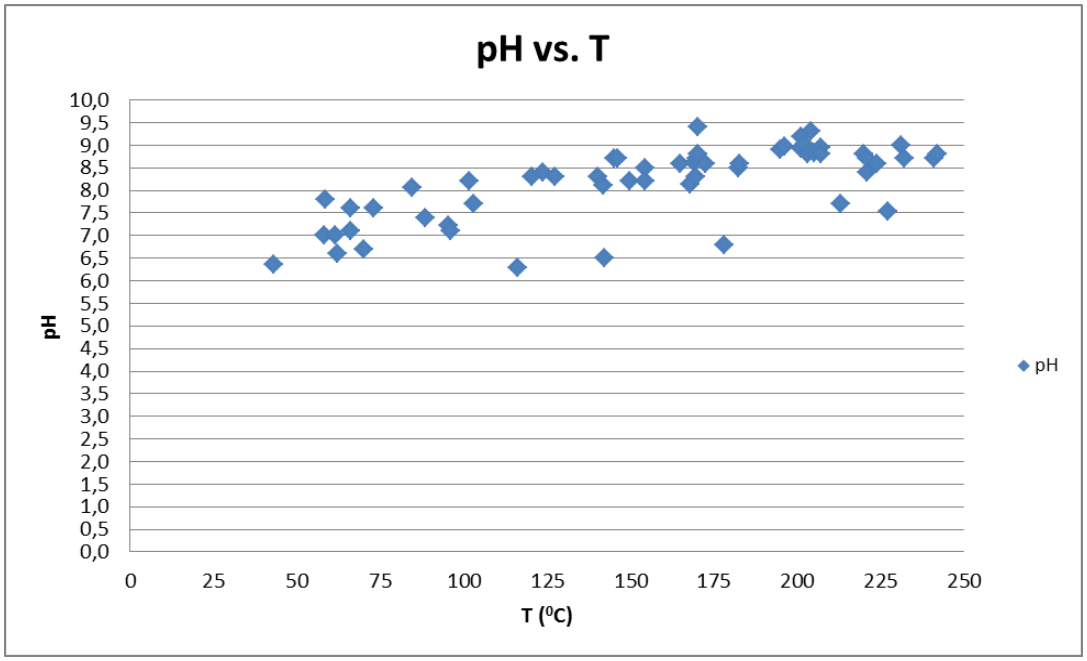

Figure 4-32: The change of pH values with temperature.

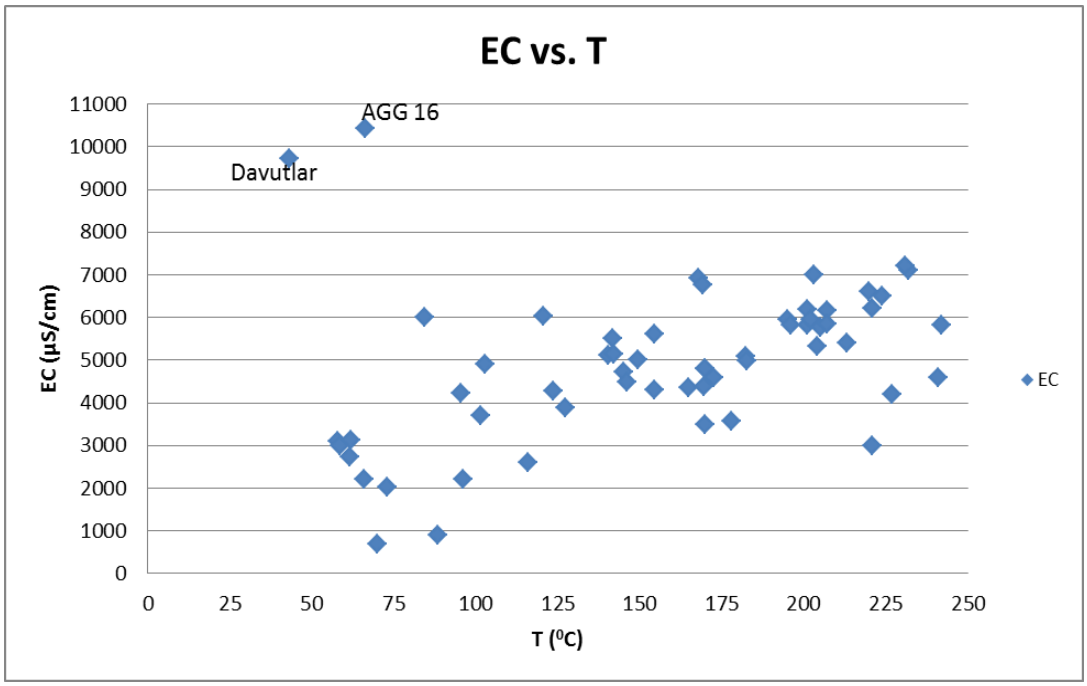

Figure 4-33: The change of EC values with temperature.

Moreover, the other analyses are the variance of SiO_2, TDS, B, pH and EC studied according to well depth. The results of analyses do not have a linear correlation. The results are shown in Figure 4.34 to 4.38. SiO_2, TDS and EC amounts do virtually not change with well depth. Additionally, B and pH values negligently increase with well depth.

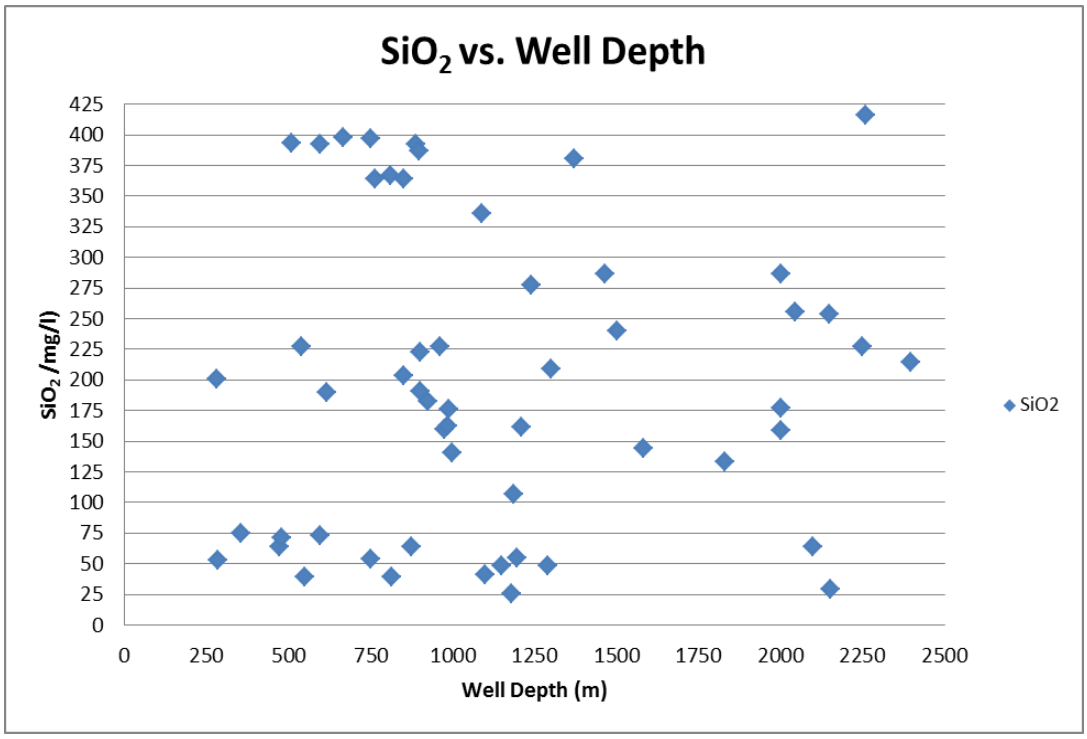

Figure 4-34: The change of SiO_2 values with well depth.

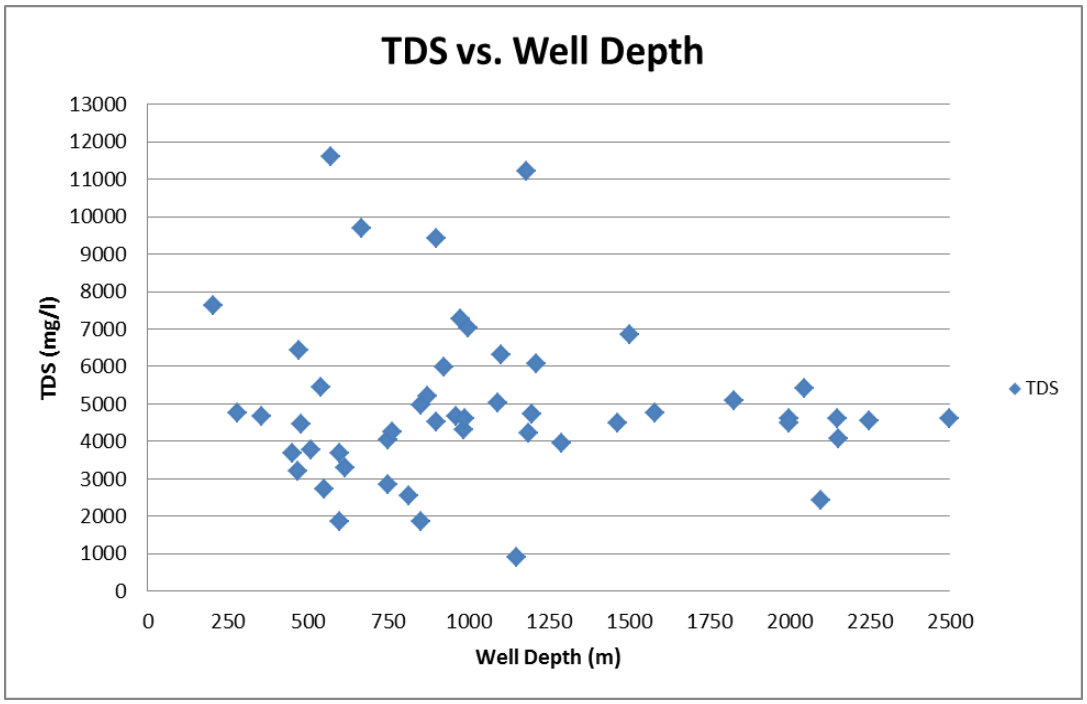

Figure 4-35: The change of TDS values with well depth.

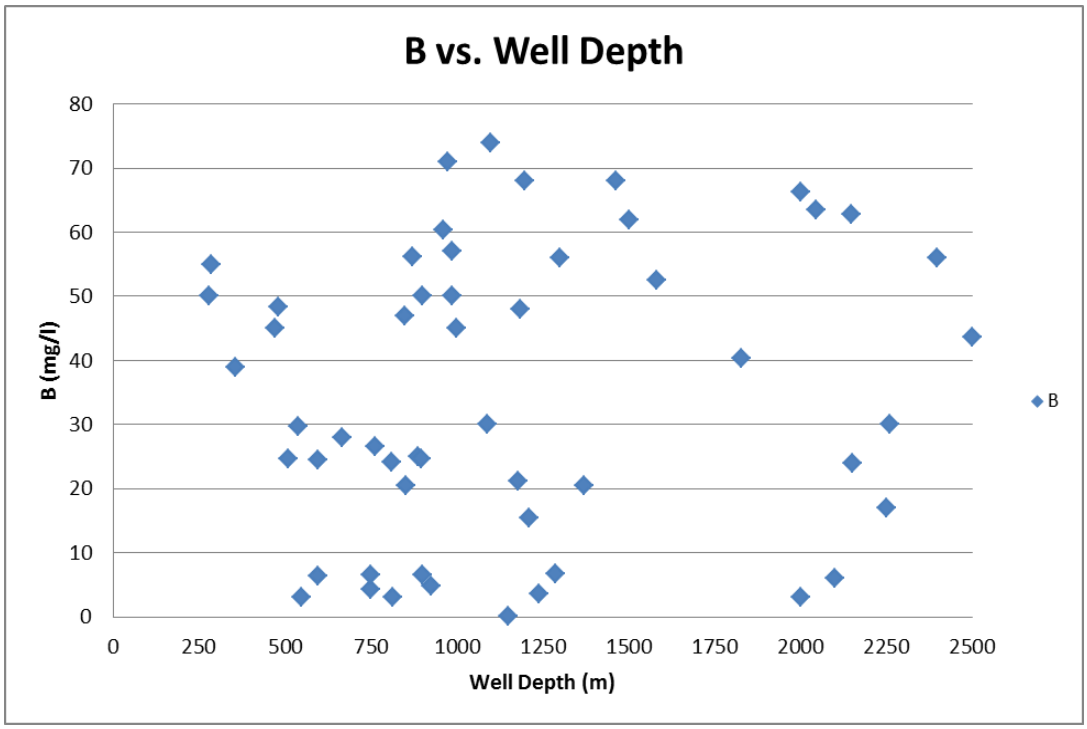

Figure 4-36: The change of B values with well depth.

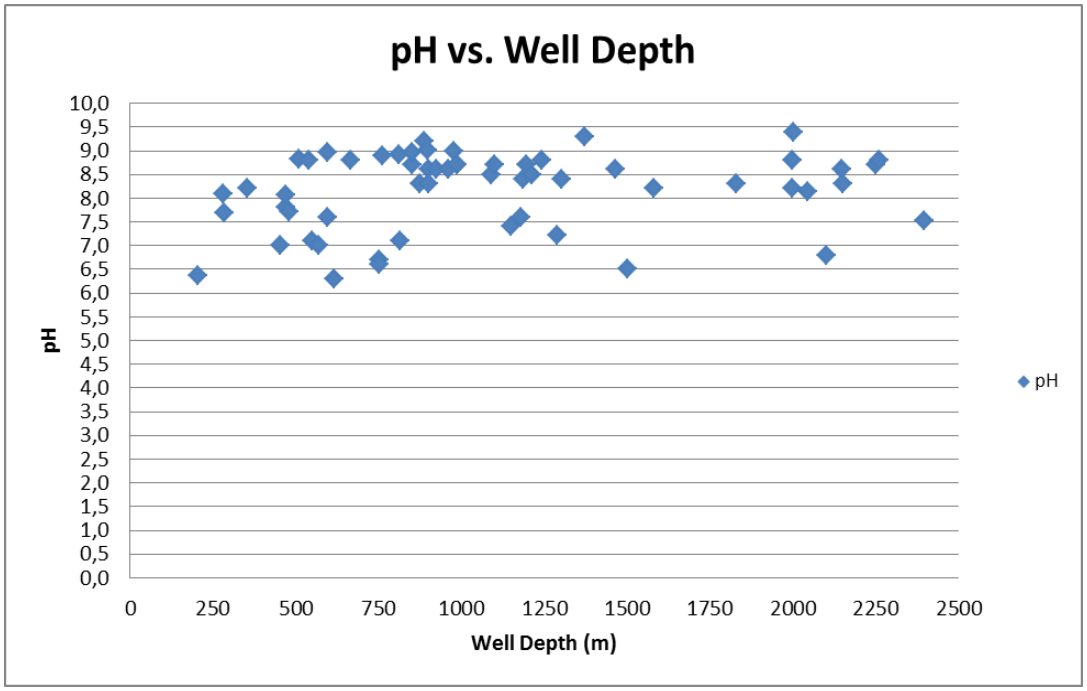

Figure 4-37: The change of pH values with well depth.

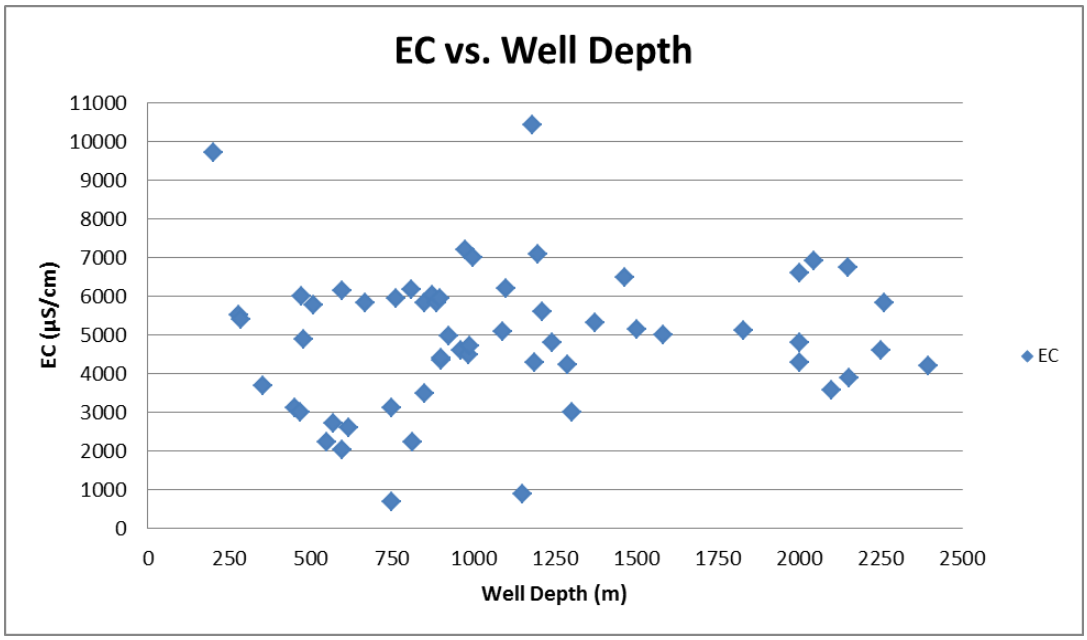

Figure 4-38: The change of EC values with well depth.

The change of SiO_2, TDS, B, pH and EC values with respect to well distance to sea is also examined. The outcomes can be observed in Figure 4.39 to 4.43. B values show good correlation with well distance to sea. B values increase as the distance decreases. EC values are higher in the wells close to sea with respect to others. High EC values can be related to salinity, in other words mixing of sea water. Others do not have any correlations with respect to well distance to sea as seen in the graphs.

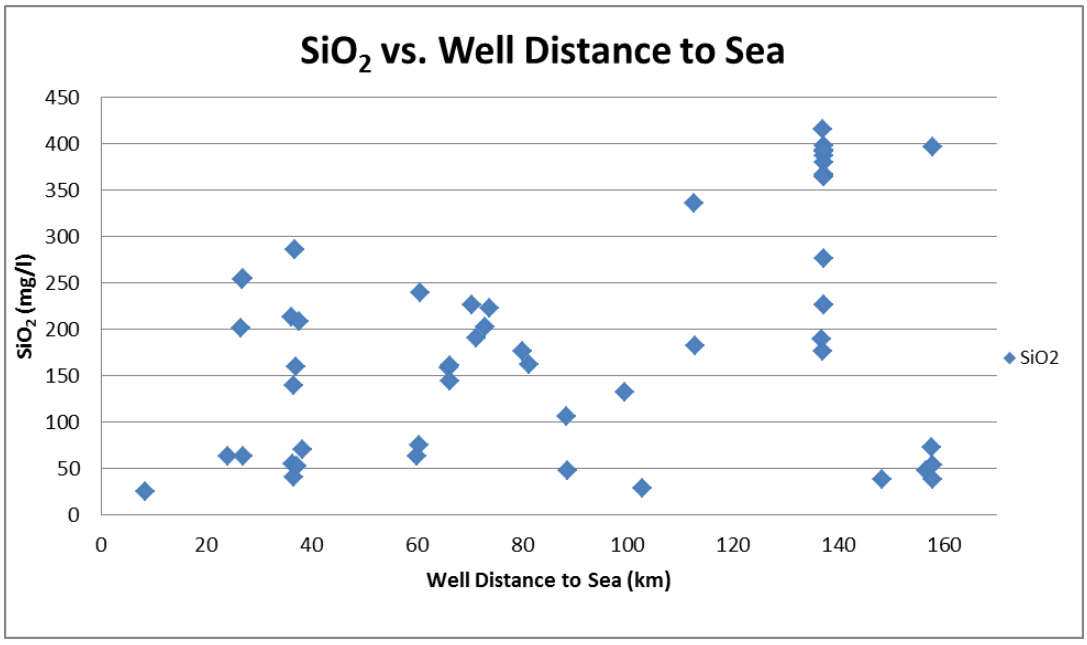

Figure 4-39: The change of SiO_2 values with well distance to sea.

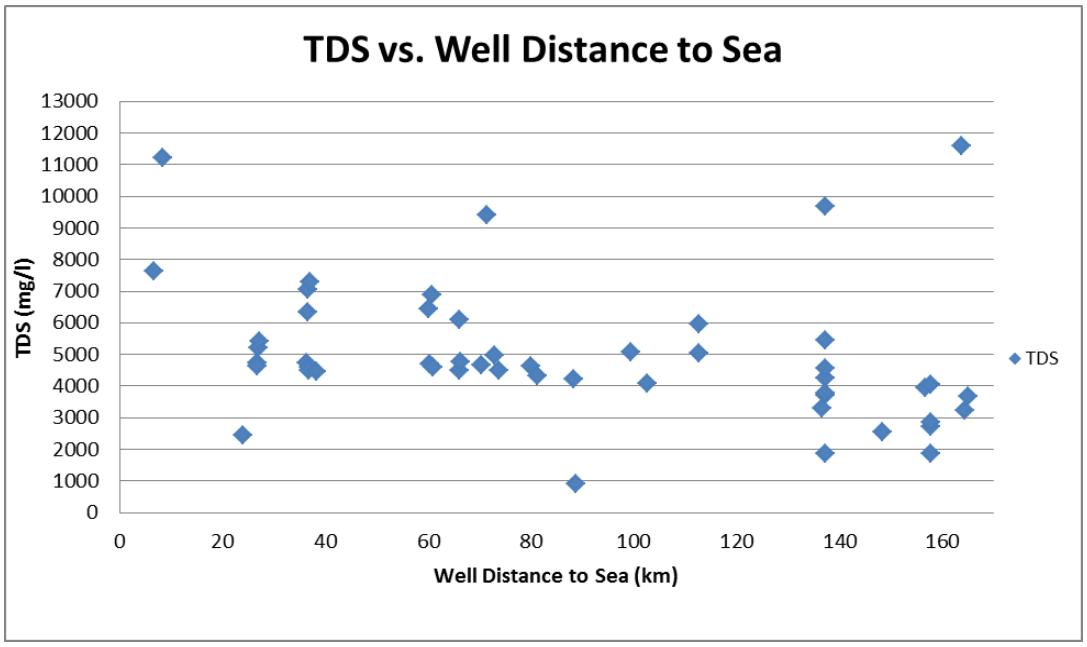

Figure 4-40: The change of TDS values with well distance to sea.

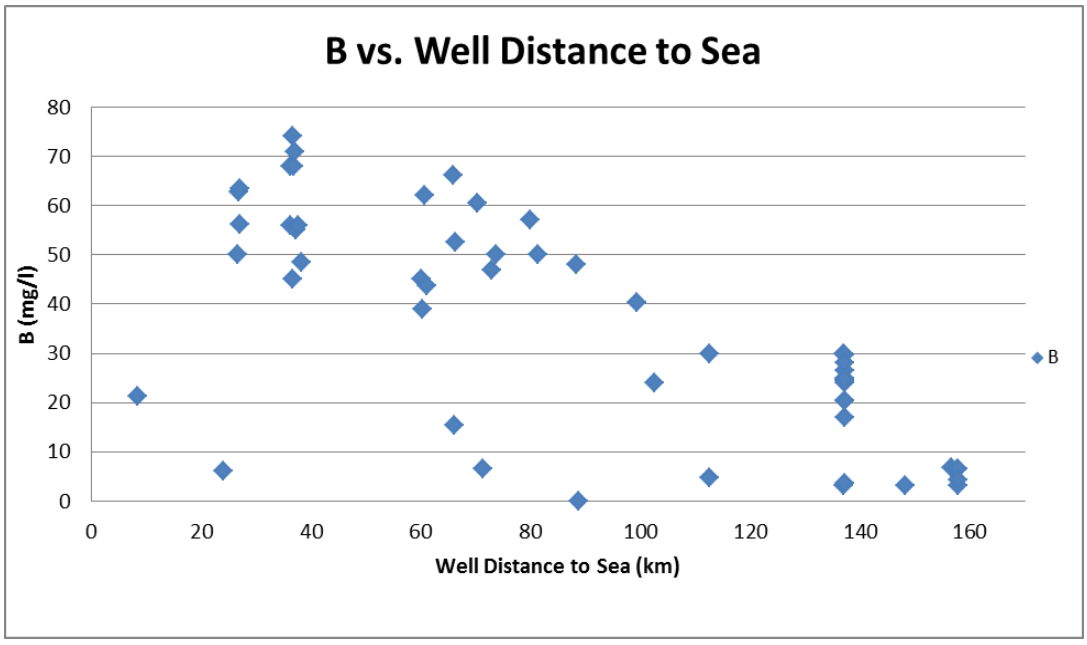

Figure 4-41: The change of B values with well distance to sea.

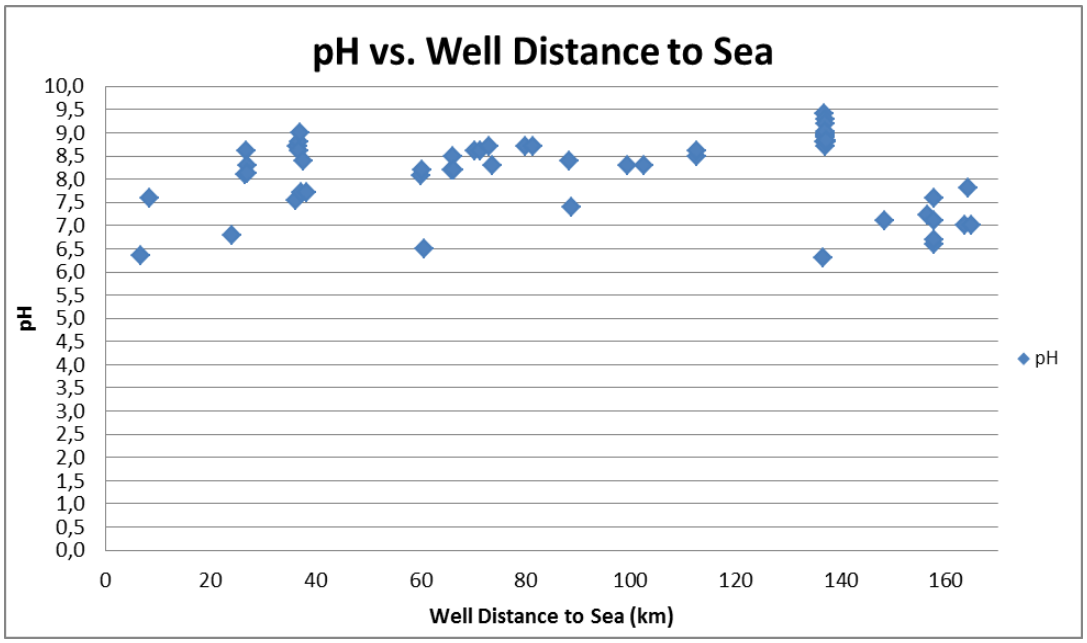

Figure 4-42: The change of pH values with well distance to sea.

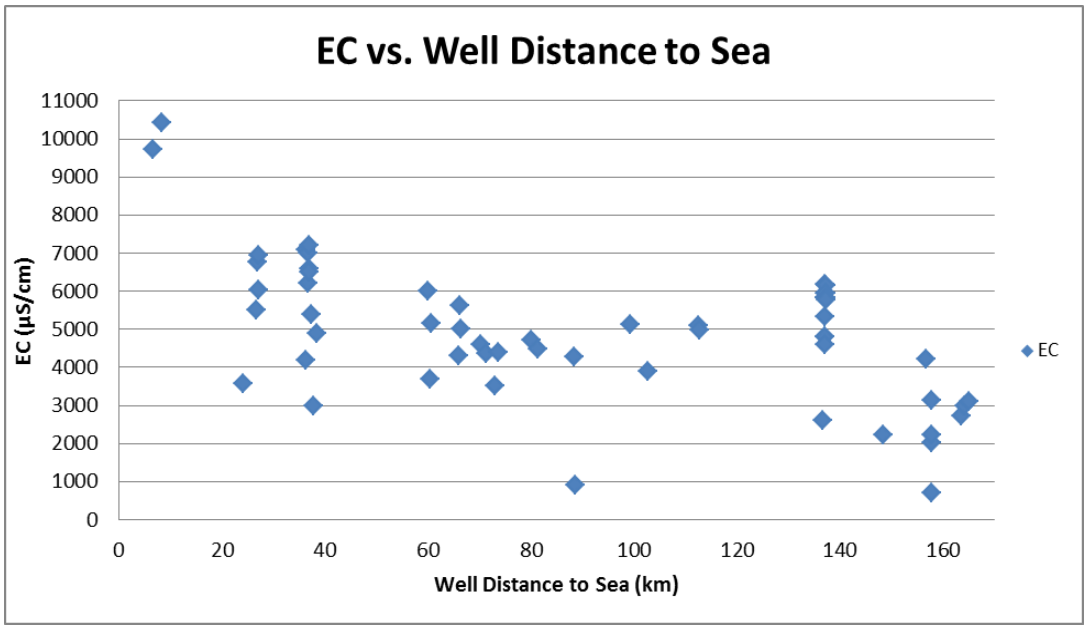

Figure 4-43: The change of EC values with well distance to sea.

4.4.2 Analyses of Average Chemical Compounds

The Büyük Menderes Graben System has identified 17 different geothermal fields. However, all of the data for these fields could not be reached. So, the average values of cations, anions, trace element, B and SiO_2, TDS, pH and EC were calculated for each attained at 15 geothermal fields. Each value was compared with temperature, well depth and distance of well location to sea.

The variation of the mean values (of the investigated parameters) with respect to average temperature of each field is observed to be more meaningful than those of the individual values. This was an expected result since we implicitly minimize the error in the data set by simply taking the average of the values. In addition, analyses of average values provided possibility of the examination on the basis of field instead of individual well.

4.4.2.1 Analyses of Average Chemical Compounds with Temperature

According to temperature analyses, Na^+ and K^+ average values increase as the average temperature rises. Although the fluid temperature of Söke-Davutlar geothermal field is low, average values of Na^+ ions are uxnexpectedly high. This high concentration of Na^+ can be related to sea water composition. Furthermore,

average of NH_4^+ ions does not show a clear change. It can be said that there is a slight increase in NH_4^+ values with respect to average temperature increase. Moreover, average Mg^+ and Ca^+ concentrations decrease clearly as the average temperature increases. The changes of average cations with respect to average temperature are shown in Figure 4.44 to 4.48.

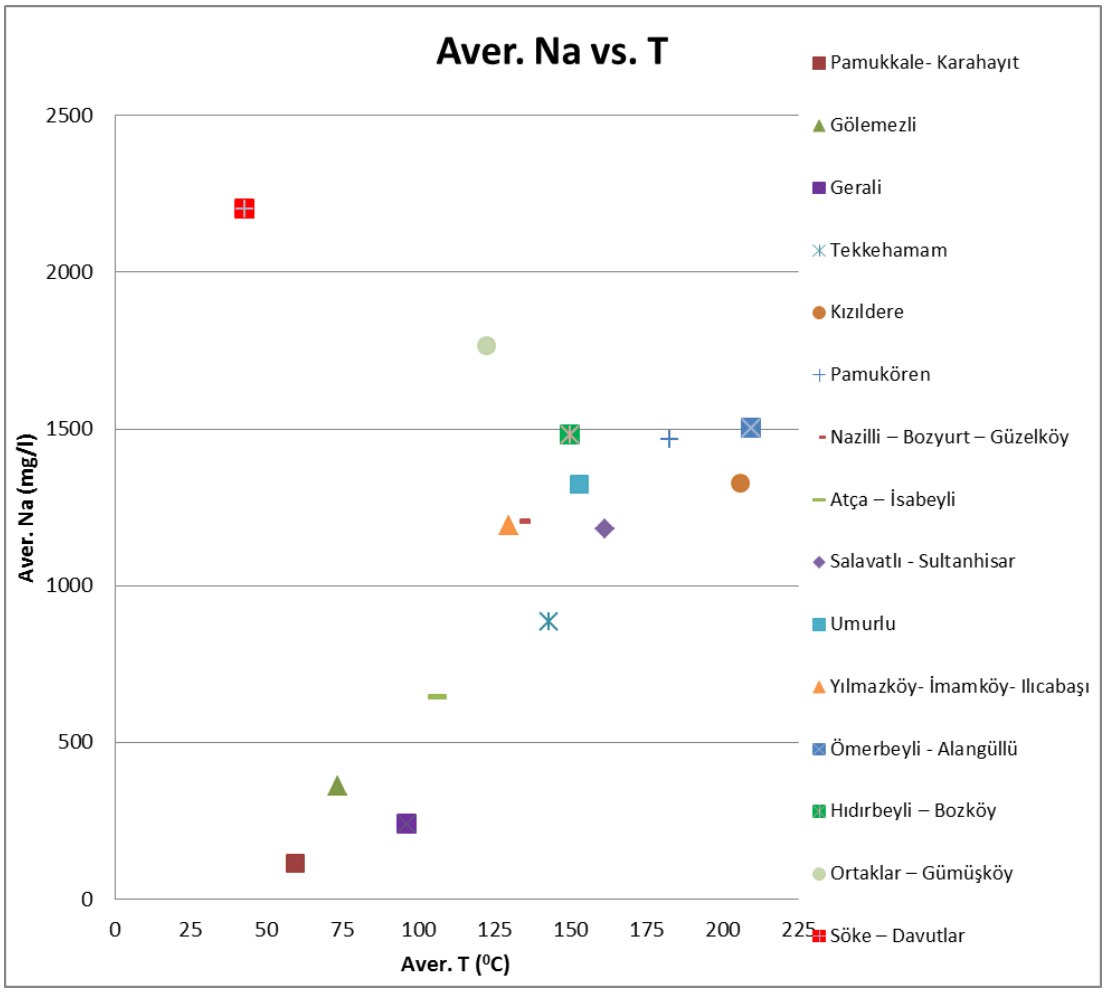

Figure 4-44: The change of average Na in geothermal fields with average temperature.

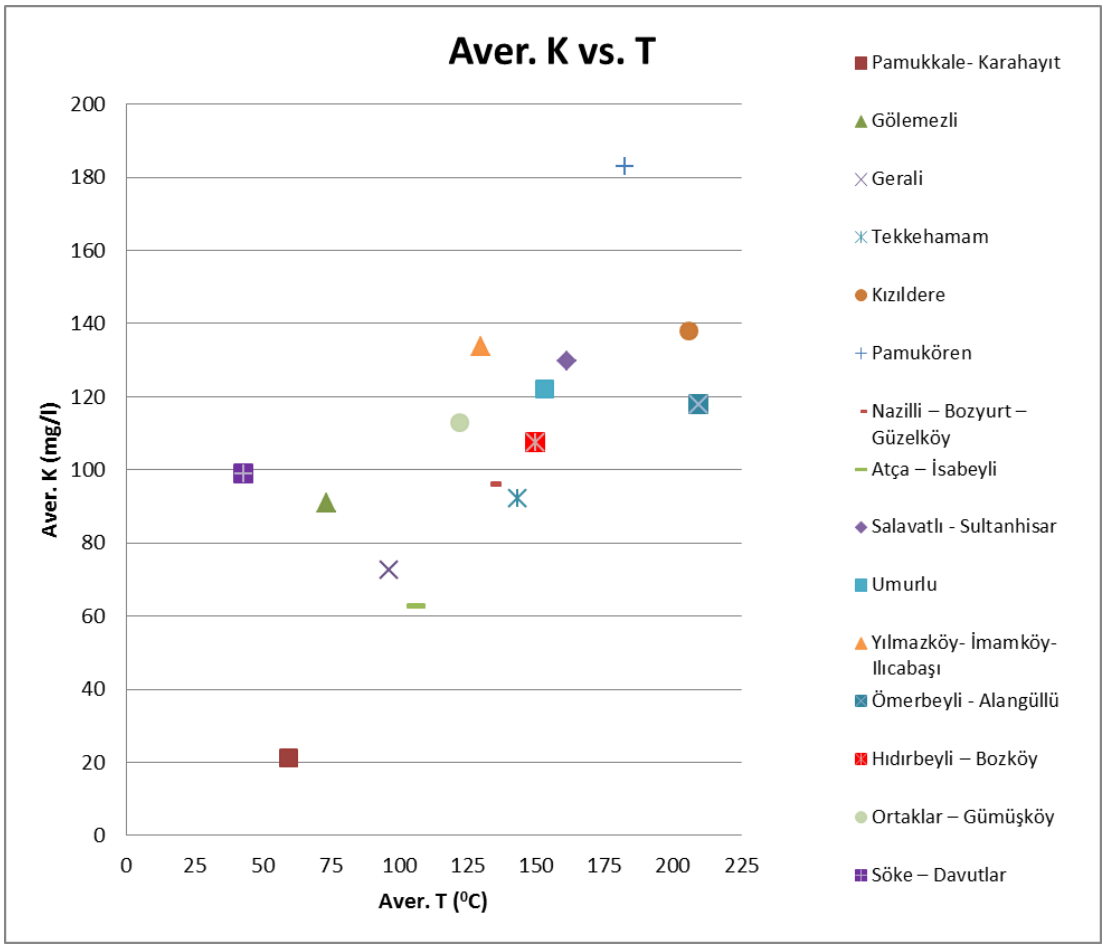

Figure 4-45: The change of average K in geothermal fields with average temperature.

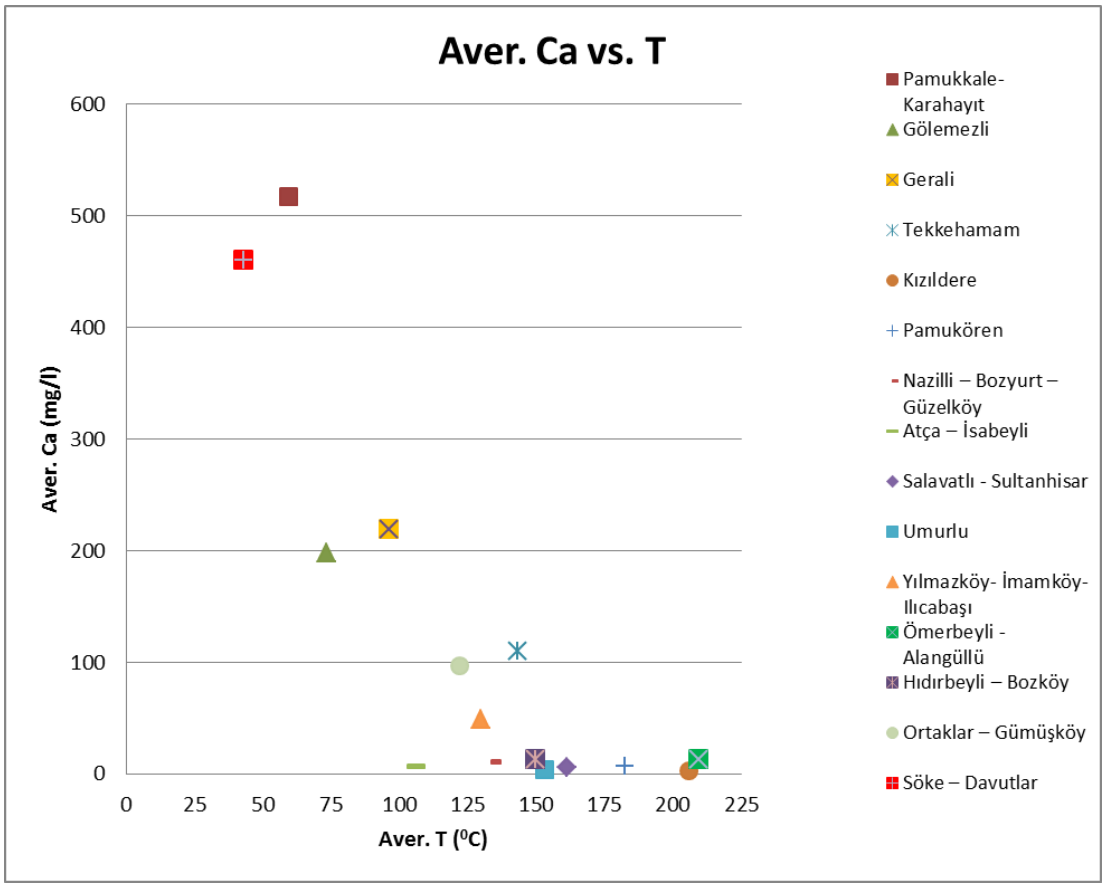

Figure 4-46: The change of average Ca in geothermal fields with average temperature.

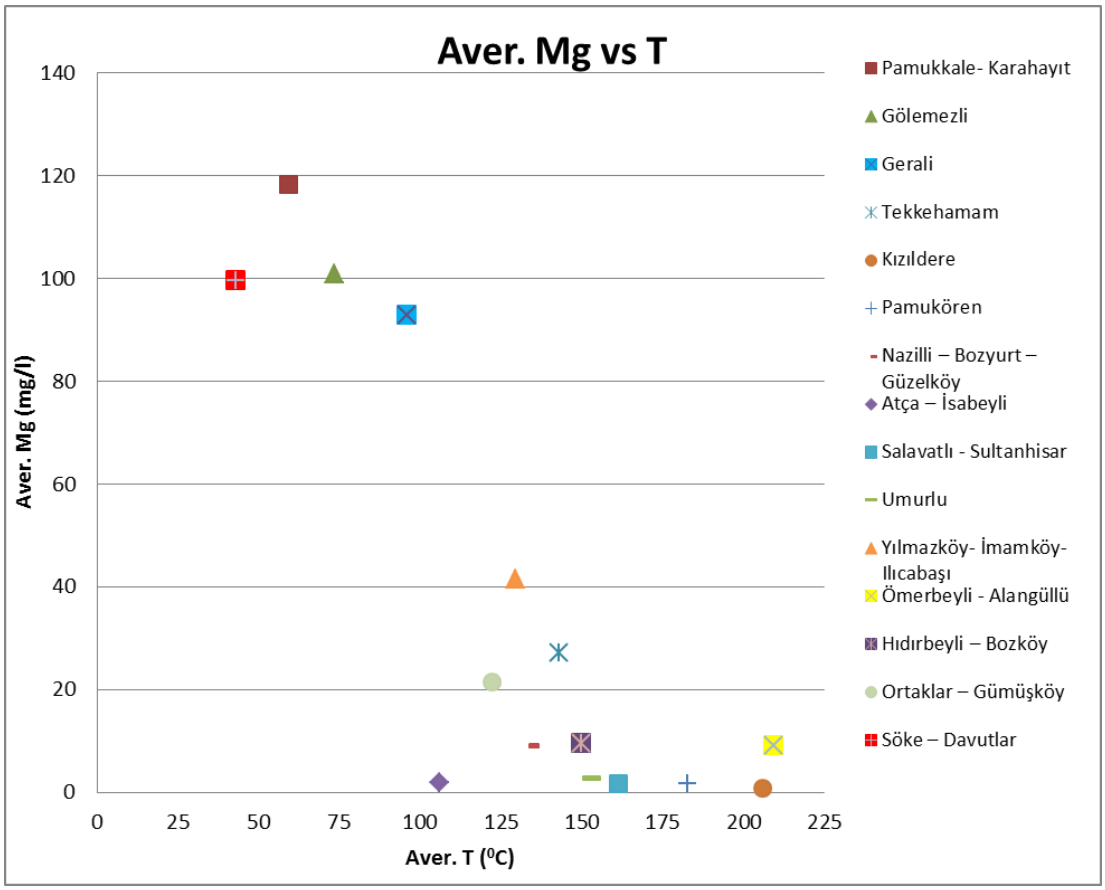

Figure 4-47: The change of average Mg in geothermal fields with average temperature.

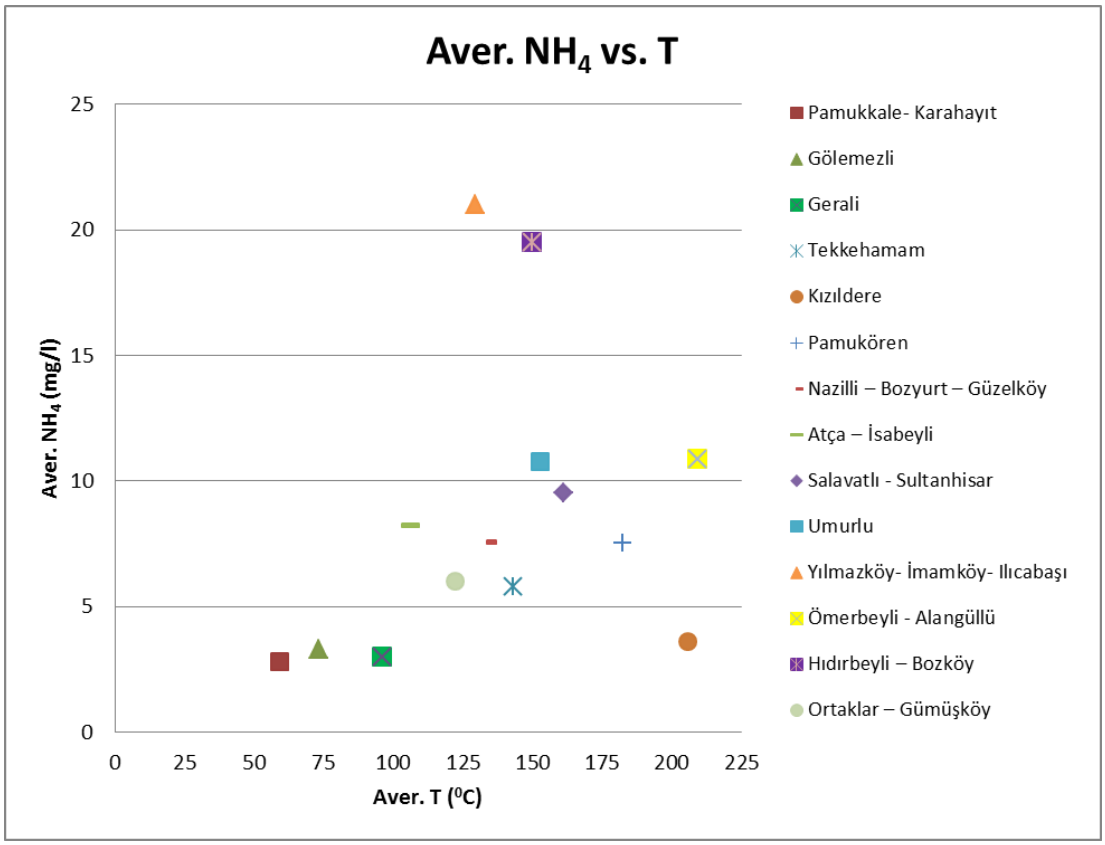

Figure 4-48: The change of average NH_4 in geothermal fields with average temperature.

Furthermore, the avarege concentrations of anions do not show significant variance with average temperature change. The change of average anion concentrations are shown in Figure 4.49 to Figure 4.51.

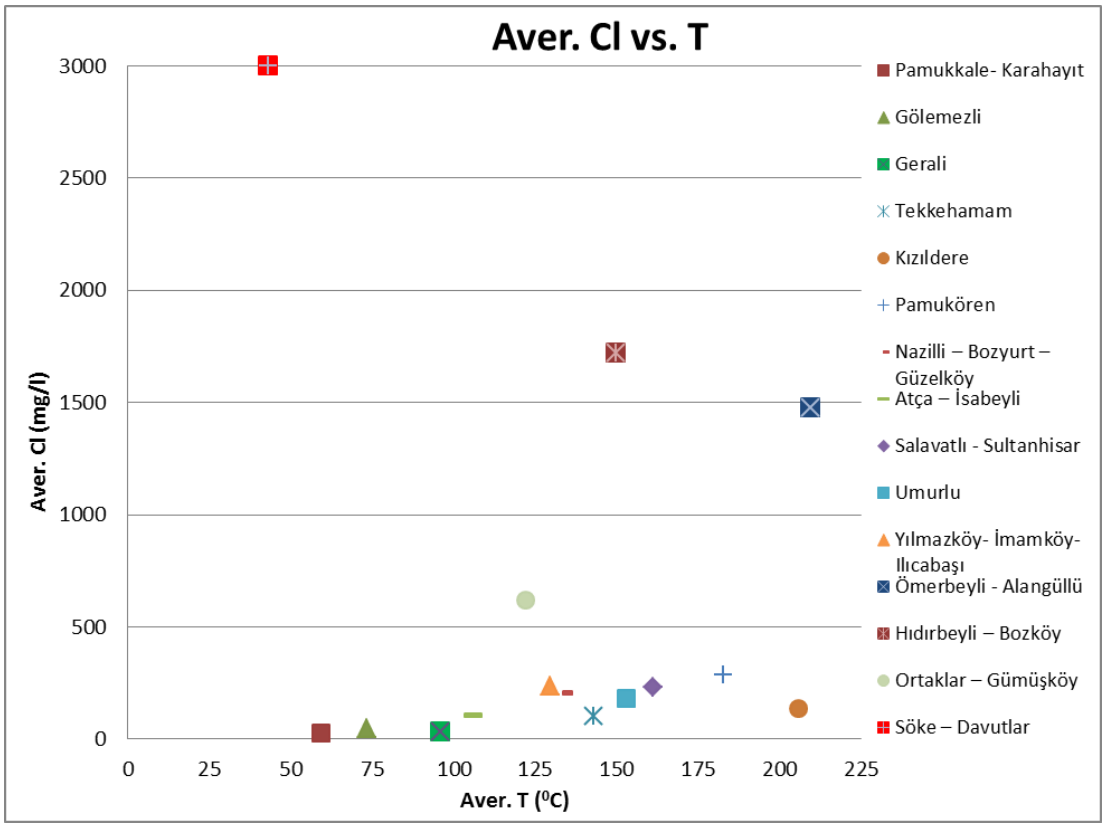

Figure 4-49: The change of average Cl in geothermal fields with average temperature.

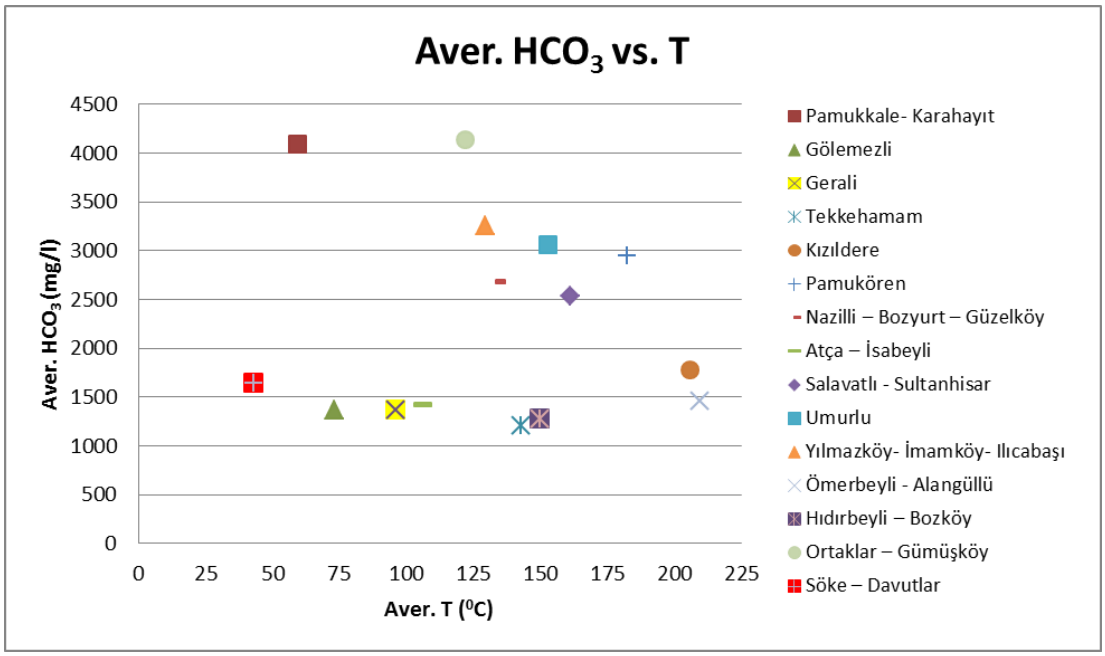

Figure 4-50: The change of average HCO_3 in geothermal fields with temperature.

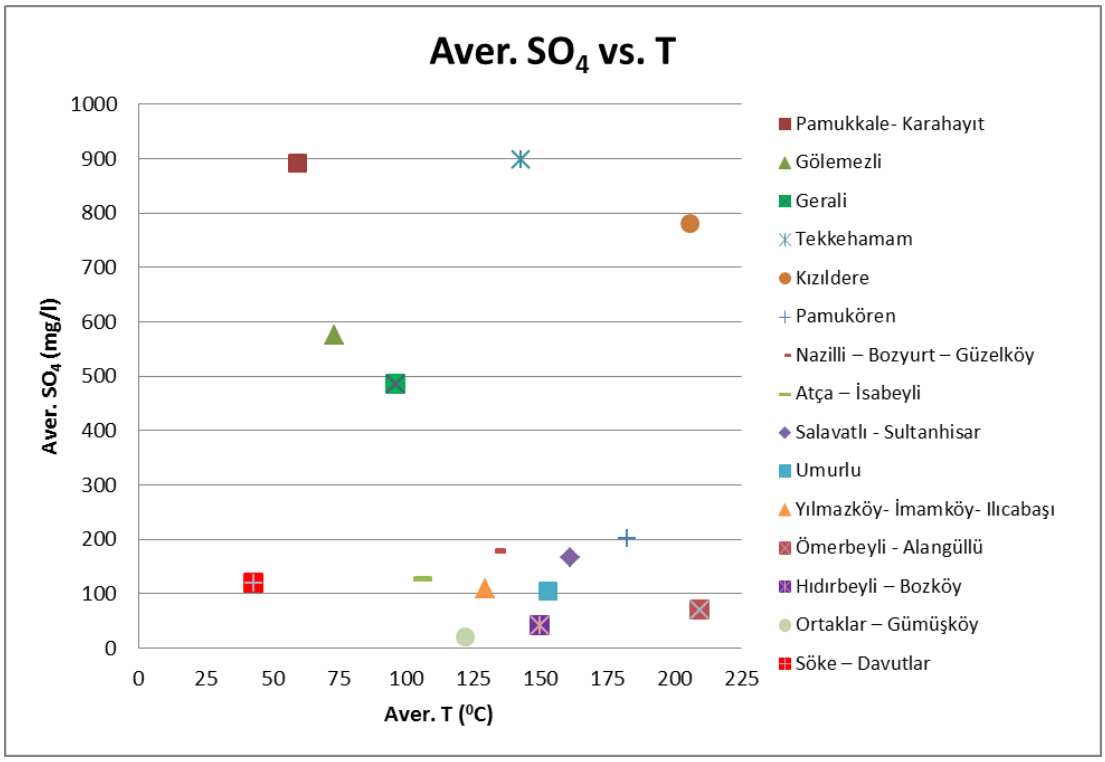

Figure 4-51: The change of average SO_4 in geothermal fields with temperature.

Average SiO_2 and pH values increase distinctively, as the temperature rises. Moreover, average Boron concentrations and EC values increase as the temperature rises. The results of SiO_2, EC pH and Boron values are expected. Although Söke-Davutlar field has low temperature values, average TDS and EC values are very high with respect to other wells with low temperature. This can be due to mixing of sea water and salinity. The changes of average SiO_2 and B concentrations and average pH, TDS and EC values with respect to average temperature change are presented in Figure 4.52 to Figure 4.56.

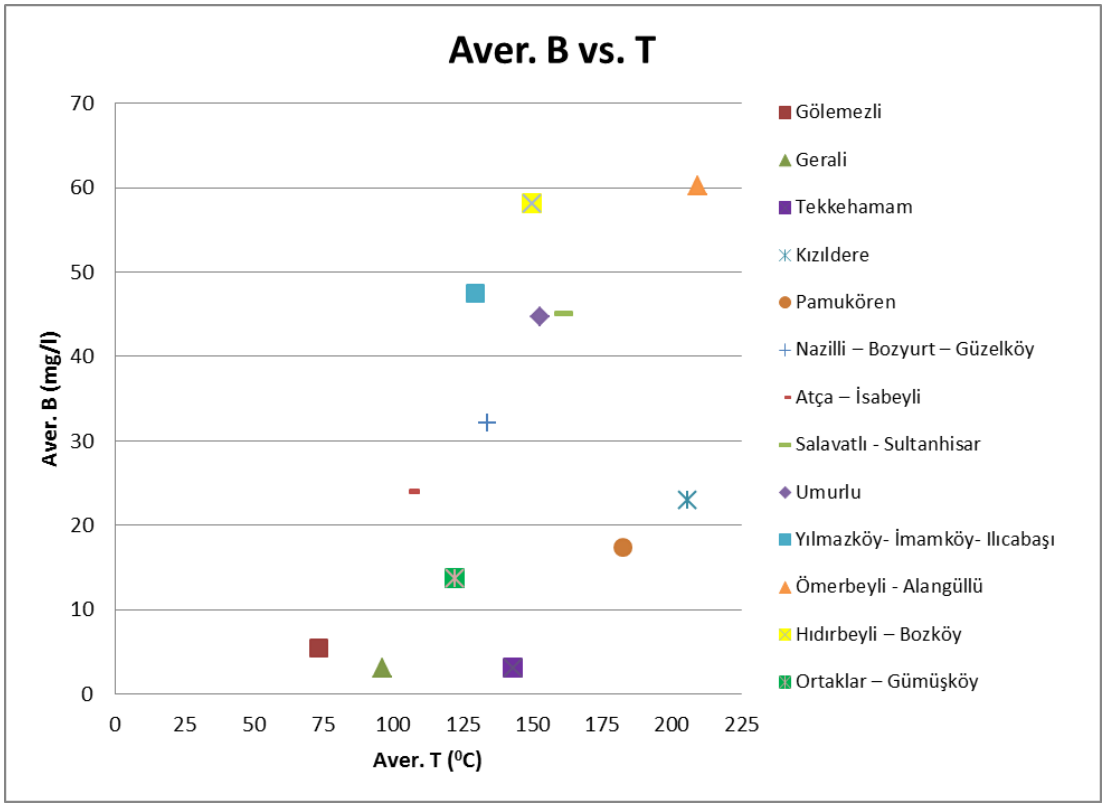

Figure 4-52: The change of average B in geothermal fields with average temperature.

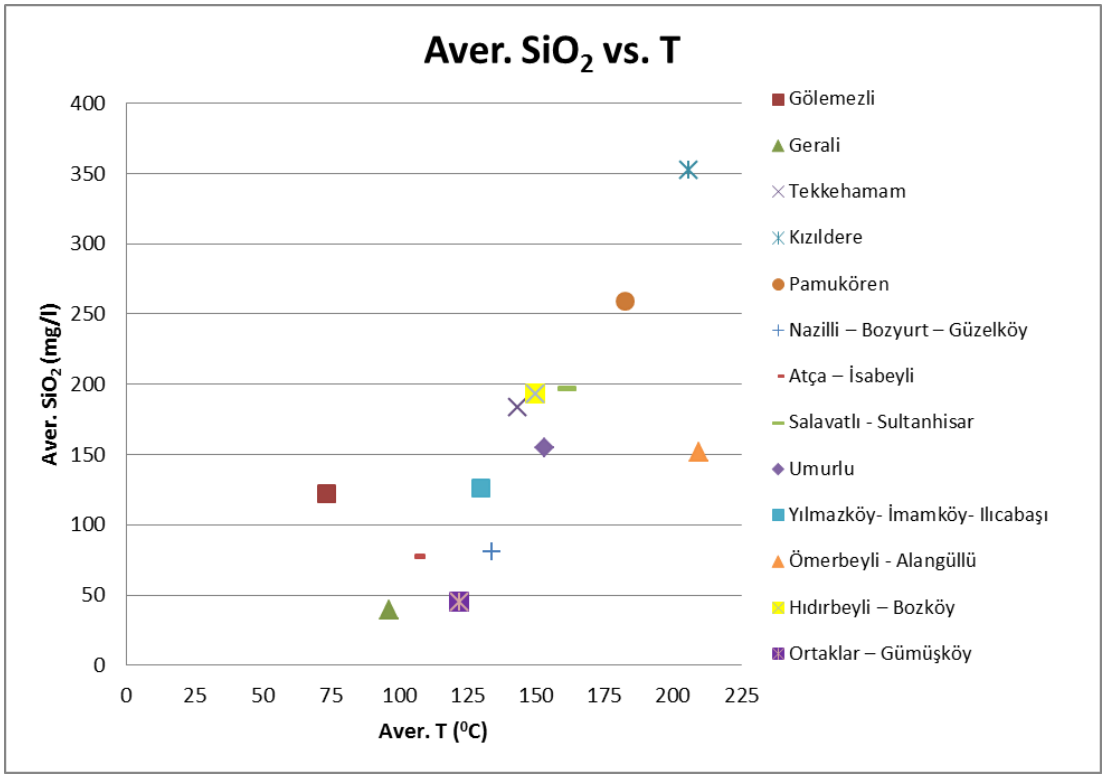

Figure 4-53: The change of average SiO_2 in geothermal fields with average temperature.

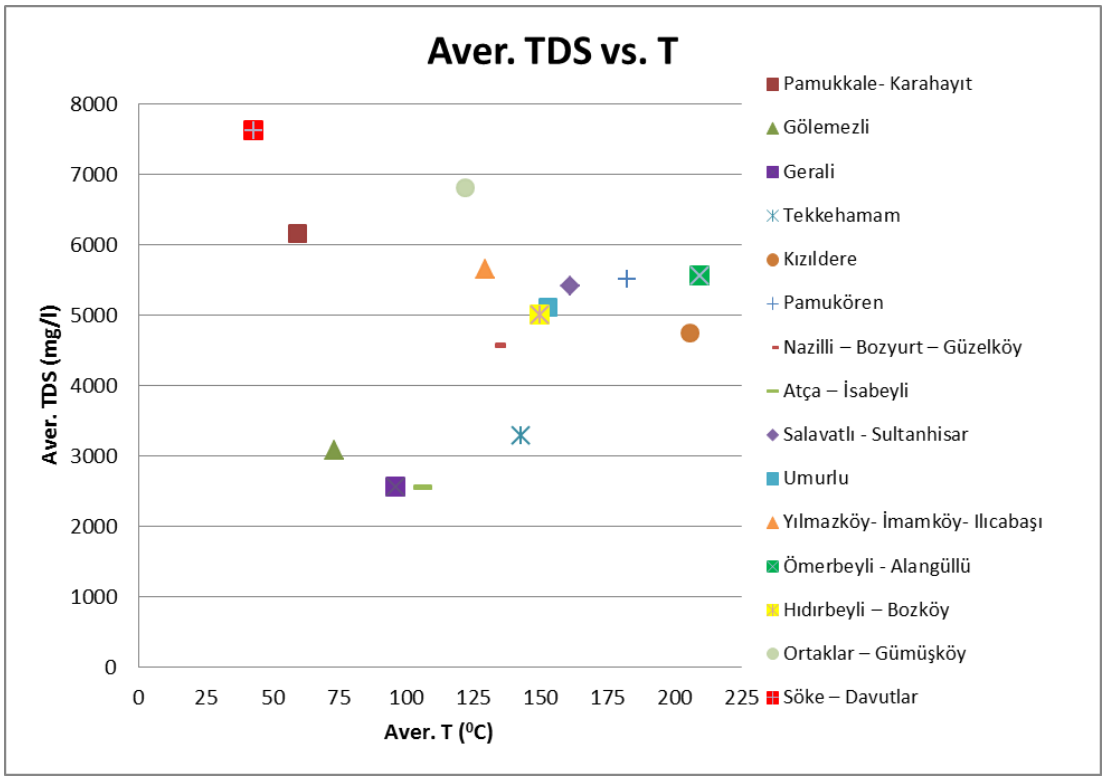

Figure 4-54: The change of average TDS in geothermal fields with average temperature.

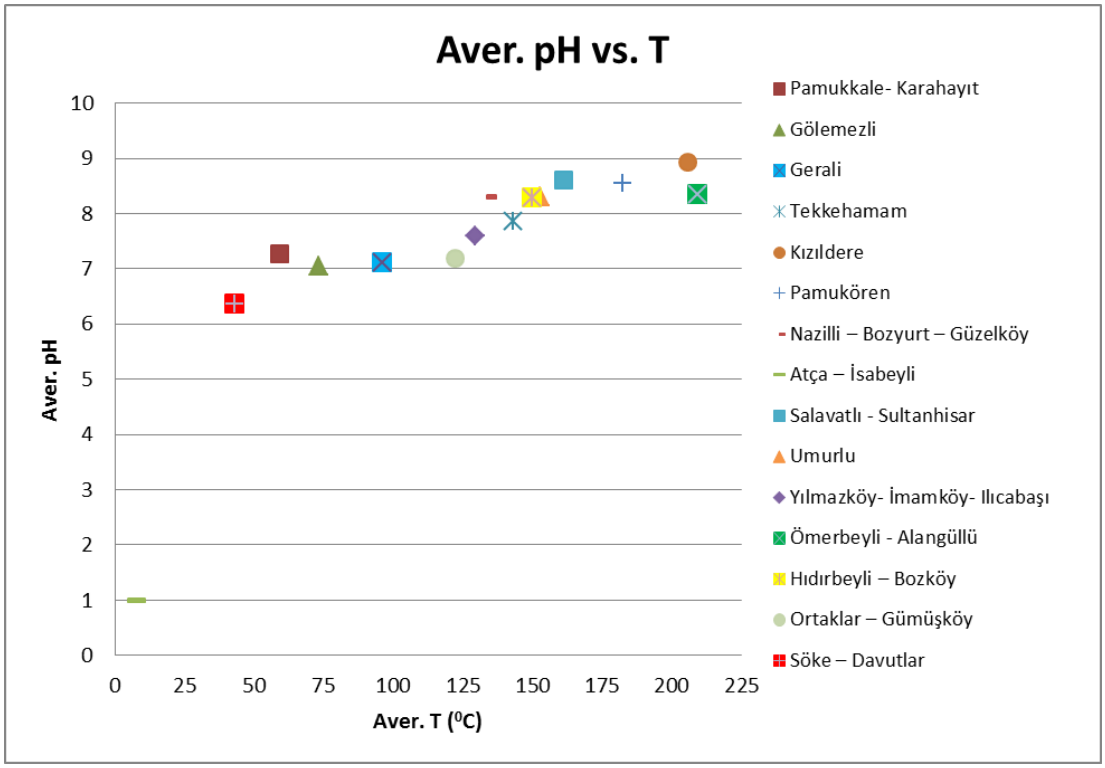

Figure 4-55: The change of average pH in geothermal fields with average temperature.

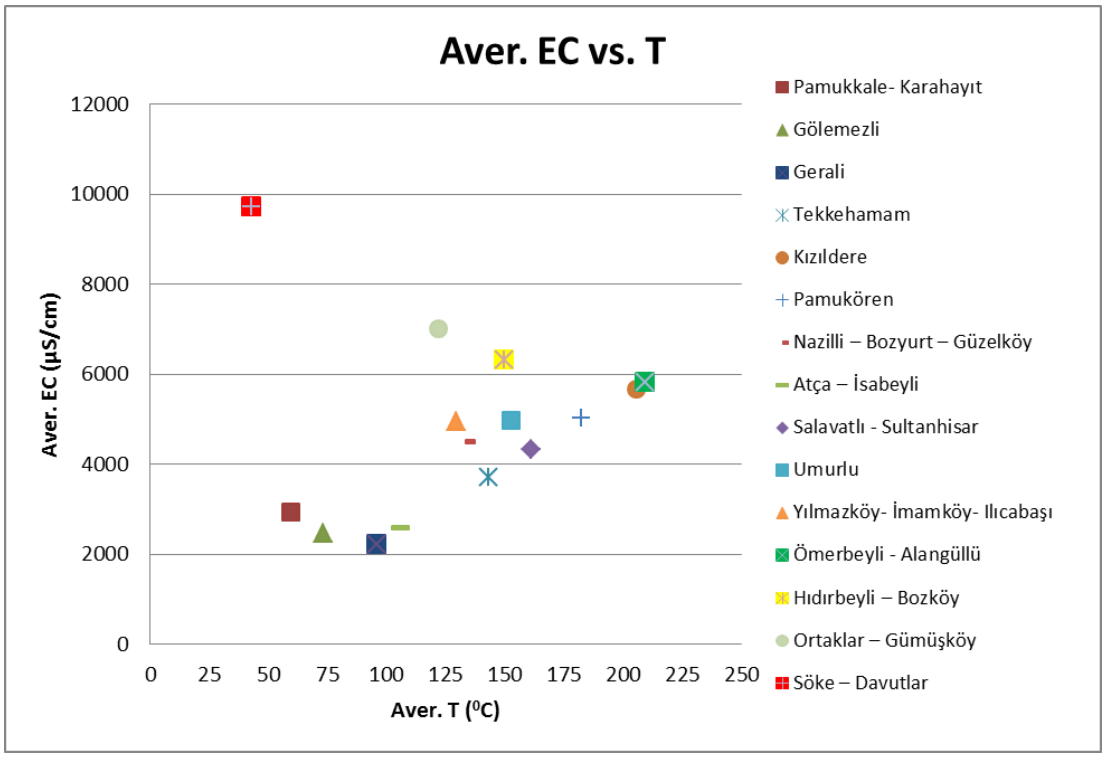

Figure 4-56: The change of average EC in geothermal fields with average temperature.

4.4.2.2 Analyses of Average Chemical Compounds with Well Depth

Average cation concentrations are analysed with respect to average well depth of each field. Average Ca^{2+} and Mg^{2+} concentrations decrease significantly as average well depth increases. Ca^{2+} and Mg^{2+} concentrations change are displayed in Figure 4.59 and Figure 4.60. Moreover, Na^{+} and K^{+} average concentrations increase with increasing well depth. As the well depth increases Menderes metamorphics form the reservoir rocks which contain Na^{+} and K^{+} ions in high amounts. Söke-Davutlar geothermal field also has high Na^{+} concentrations which can be the result of mixing of sea water. The change of other average value of anion, NH_4^{+} average concentration has no relation with average well depth.

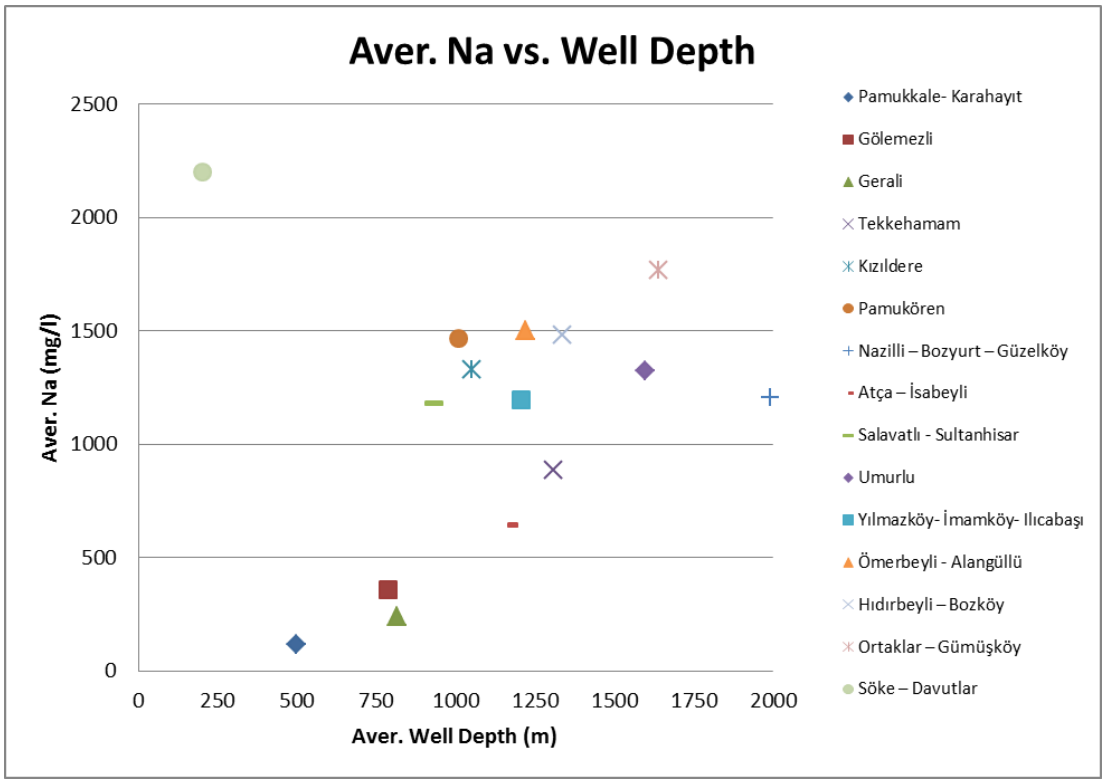

Figure 4-57: The change of average Na in geothermal fields with average well depth.

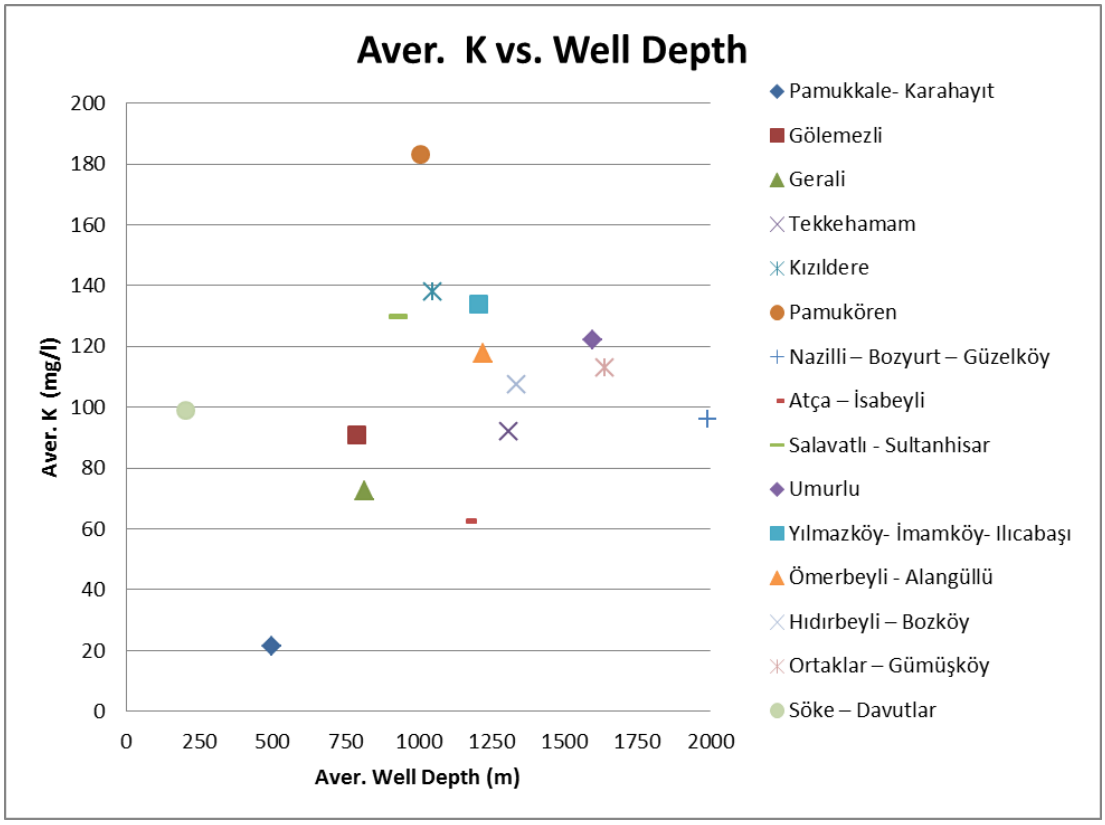

Figure 4-58: The change of average K in geothermal fields with average well depth.

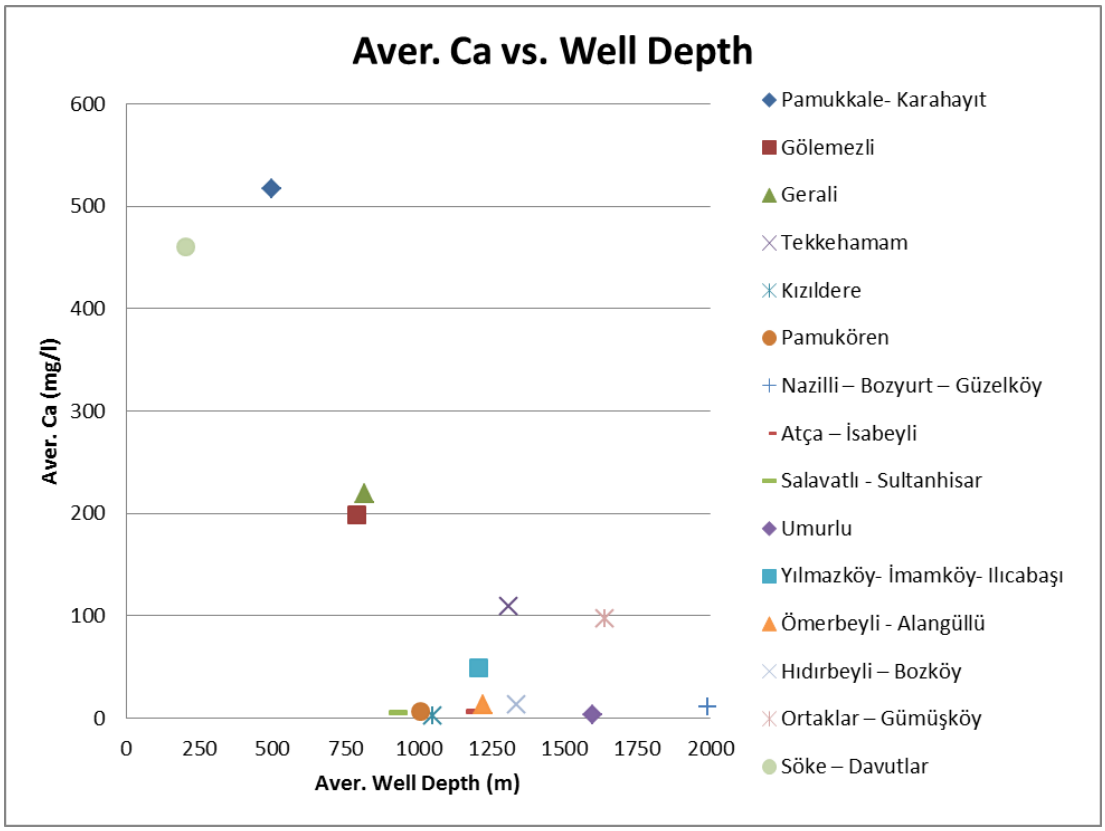

Figure 4-59: The change of average Ca in geothermal fields with average well depth.

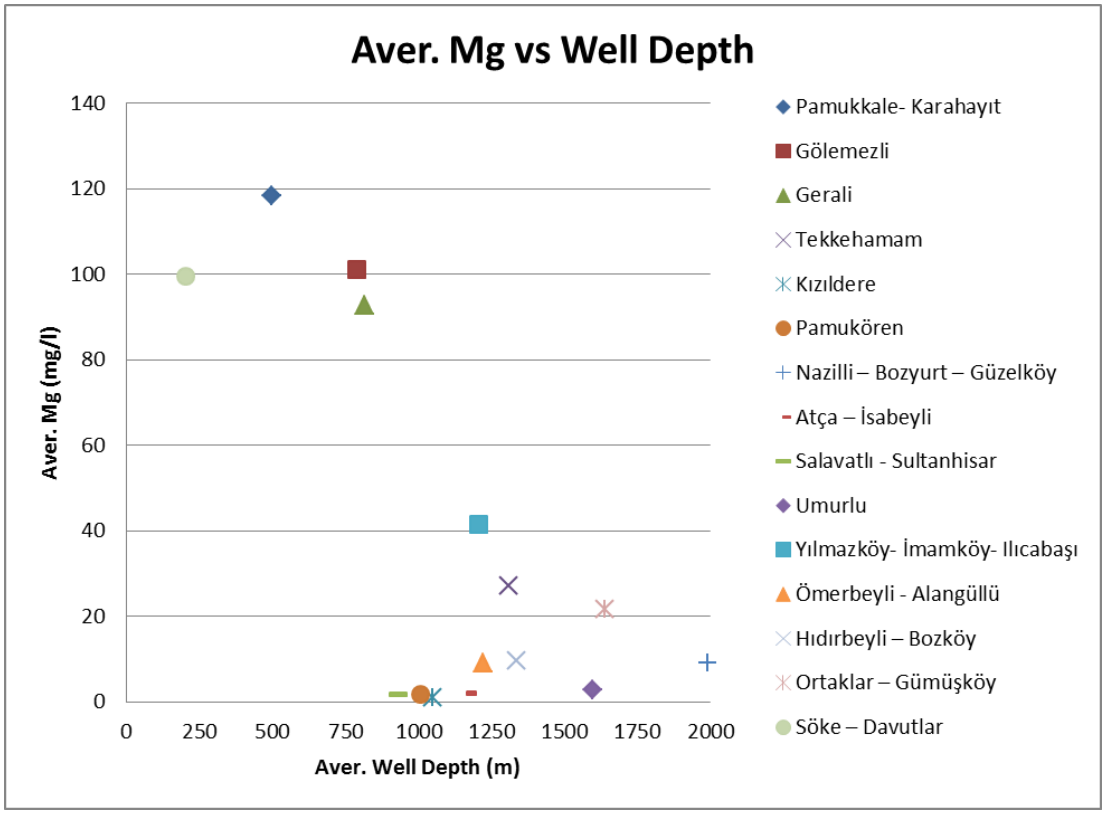

Figure 4-60: The change of average Mg in geothermal fields with average well depth.

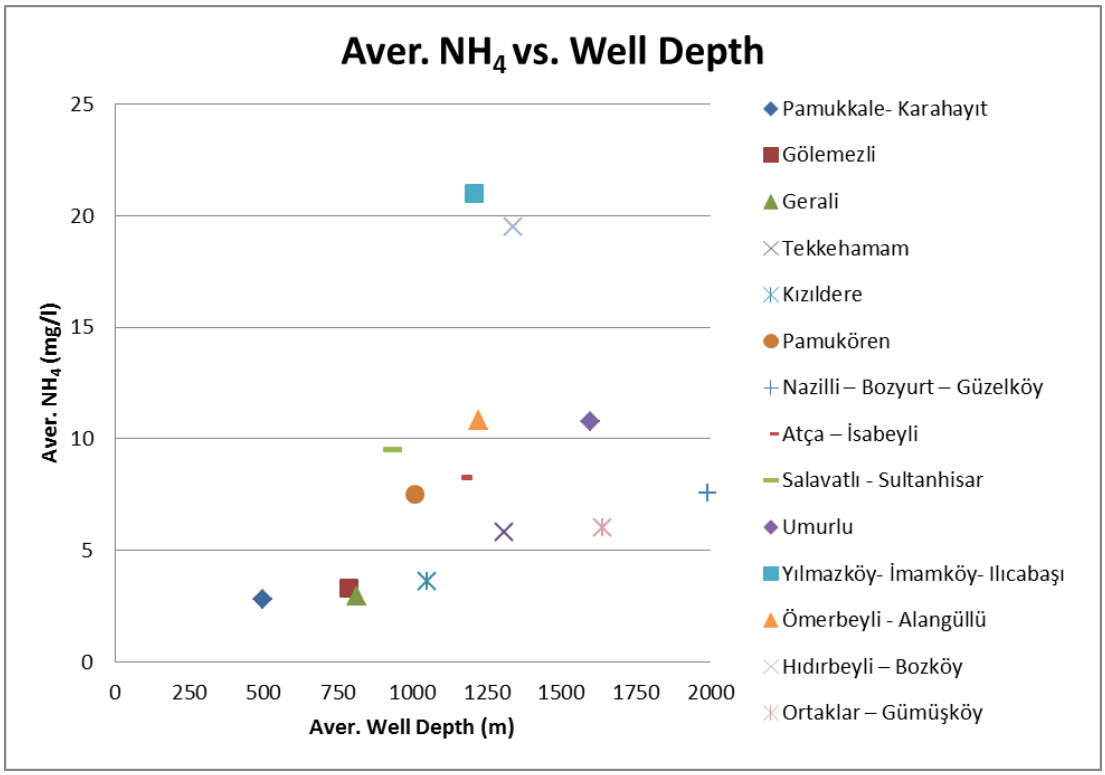

Figure 4-61: The change of average NH_4 in geothermal fields with average well depth.

The analyses of average anion concentrations with average well depth do not show significant variations. The average values of well depths do not affect on average anion concentrations. However, high Cl^- concentration of Söke-Davutlar geothermal field must be related to sea water mixing. The analyses of anions according to well depth are shown in Figure 4.62 to Figure 4.64.

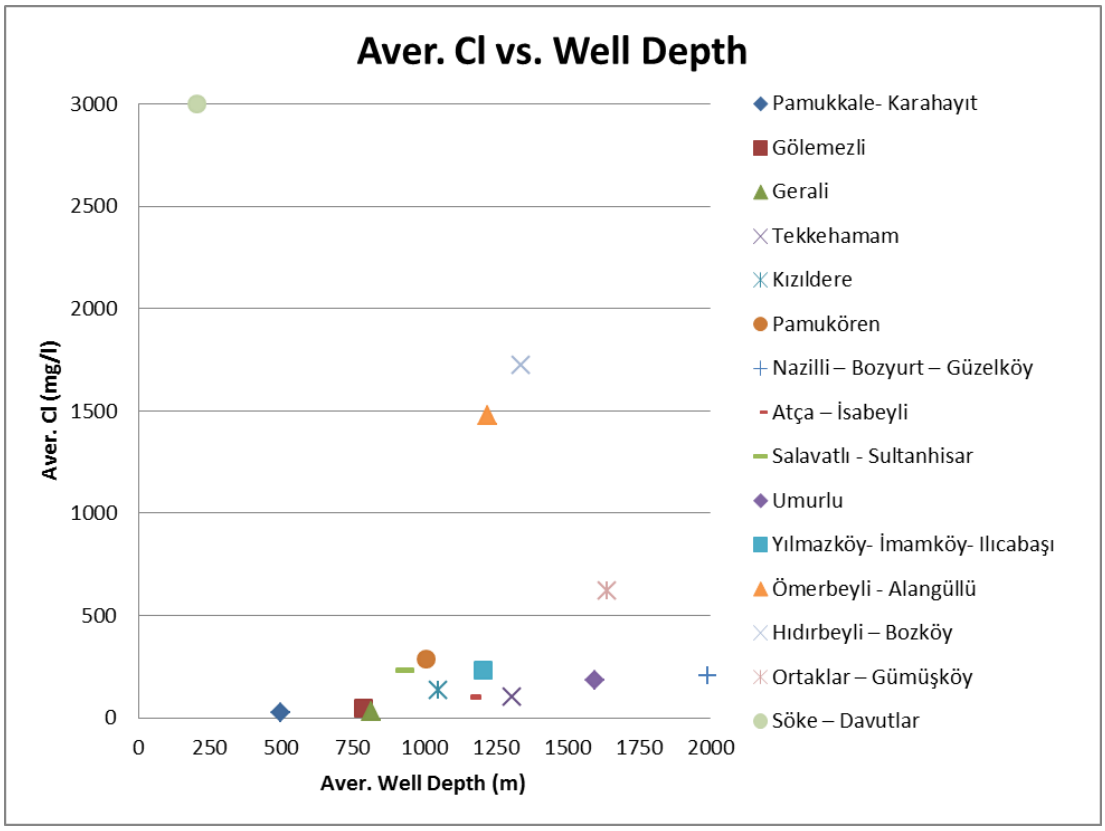

Figure 4-62: The change of average Cl in geothermal fields with average well depth.

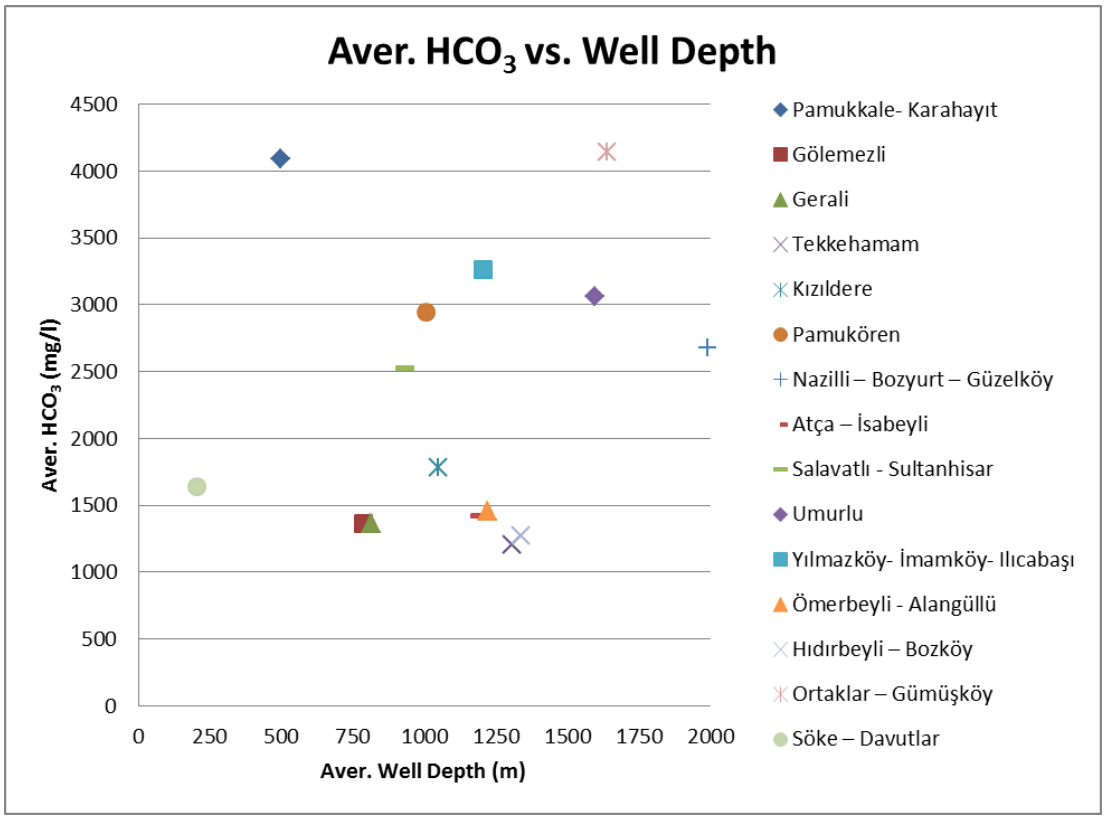

Figure 4-63: The change of average HCO_3 in geothermal fields with average well depth.

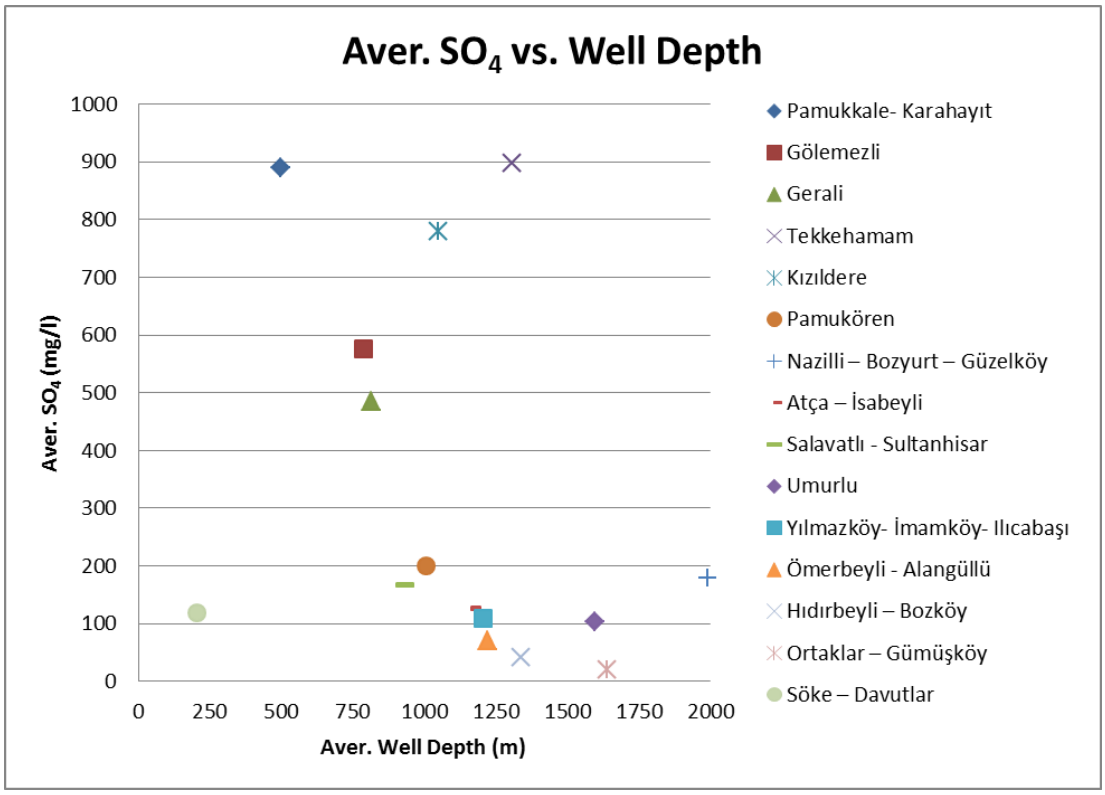

Figure 4-64: The change of average SO_4 in geothermal fields with average well depth.

Furthermore, average Boron and SiO_2 concentrations and TDS, EC and pH average values analyses do not show good correlation with average well depths. The changes of these values are shown in Figure 4.65 to Figure 4.69. They are very variable as the average well depth increases.

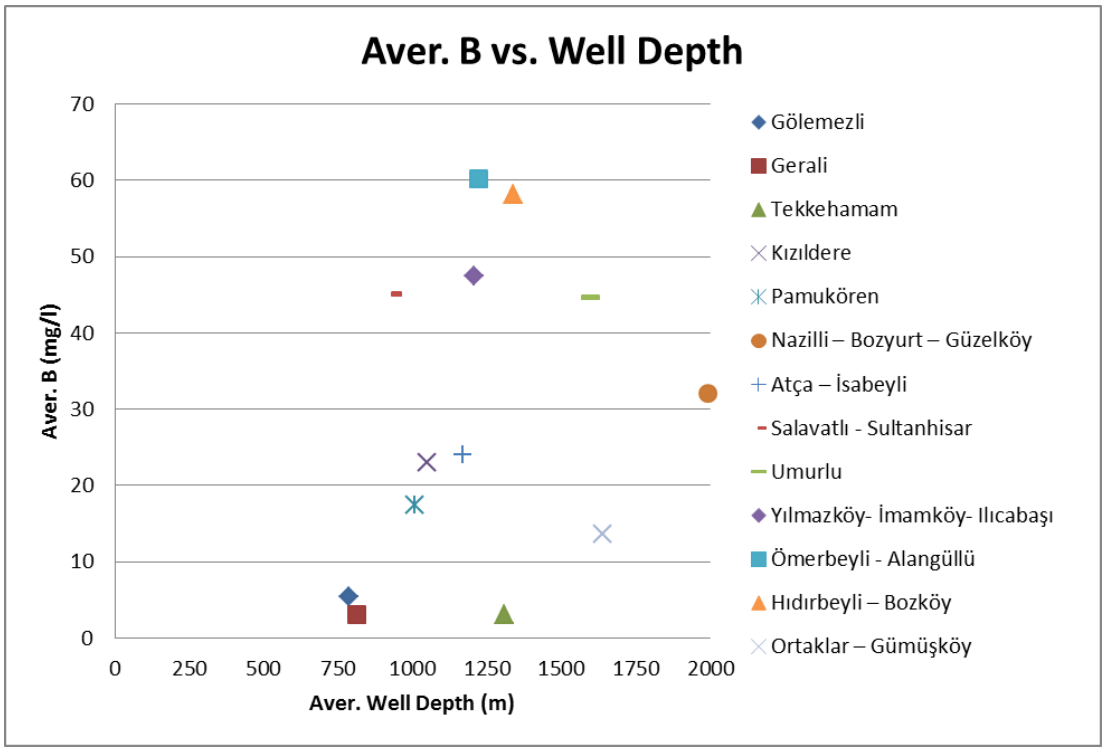

Figure 4-65: The change of average B geothermal fields with average well depth.

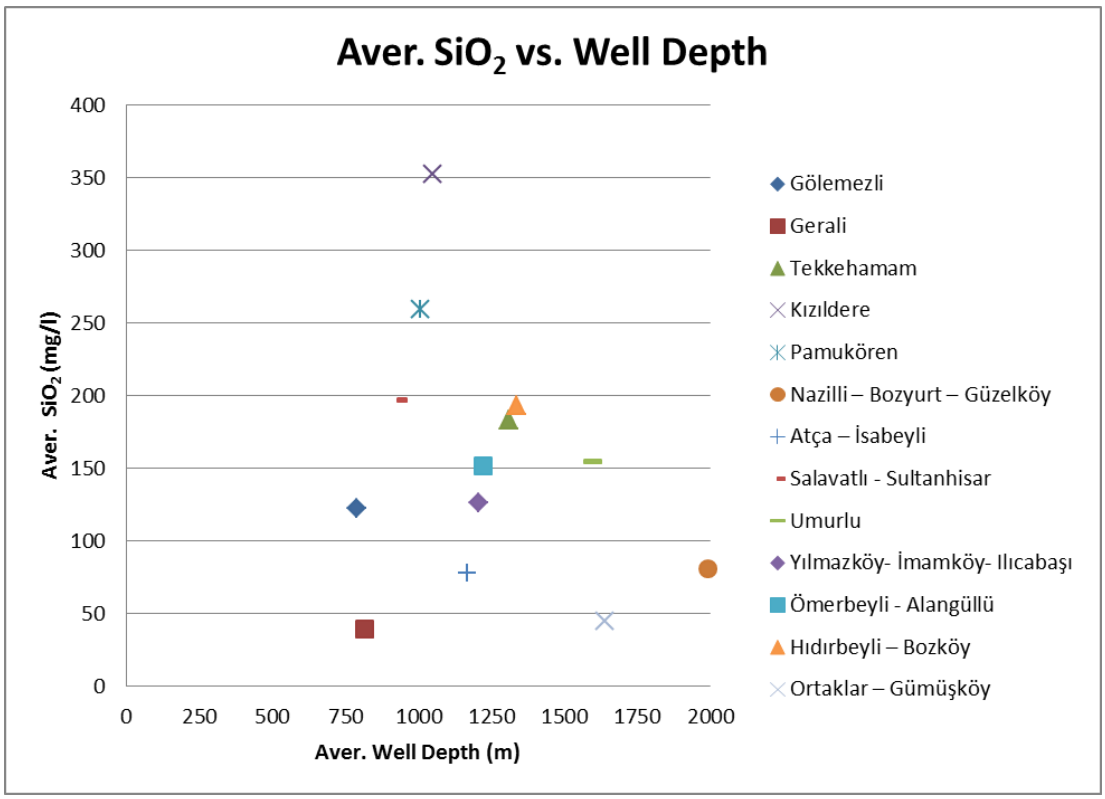

Figure 4-66: The change of average SiO_2 geothermal fields with average well depth.

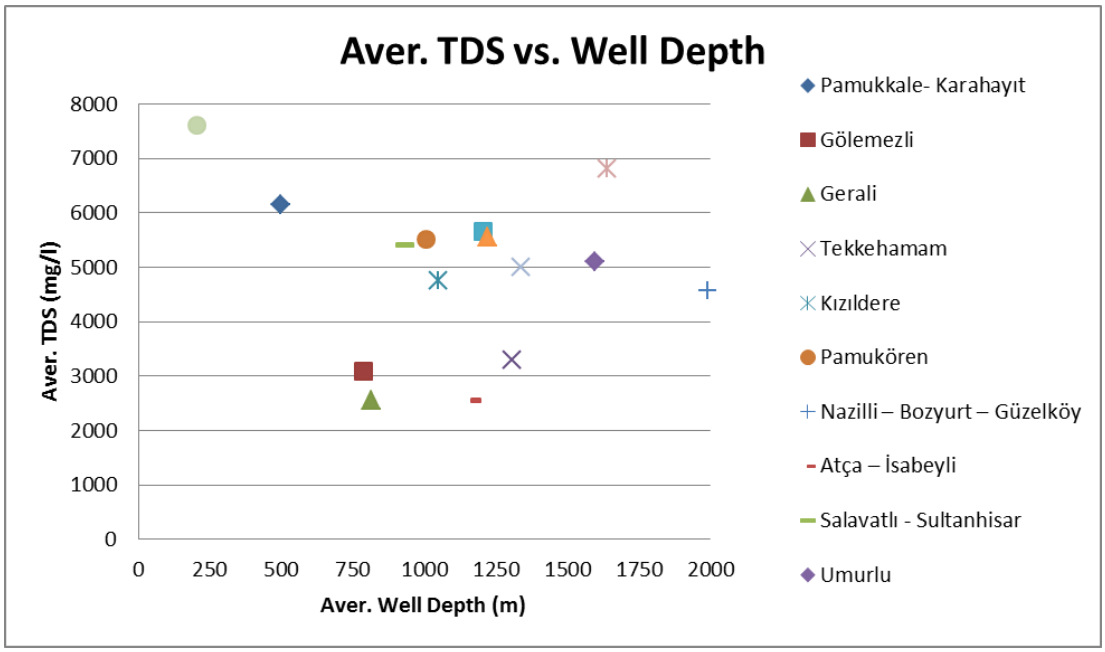

Figure 4-67: The change of average TDS geothermal fields with average well depth.

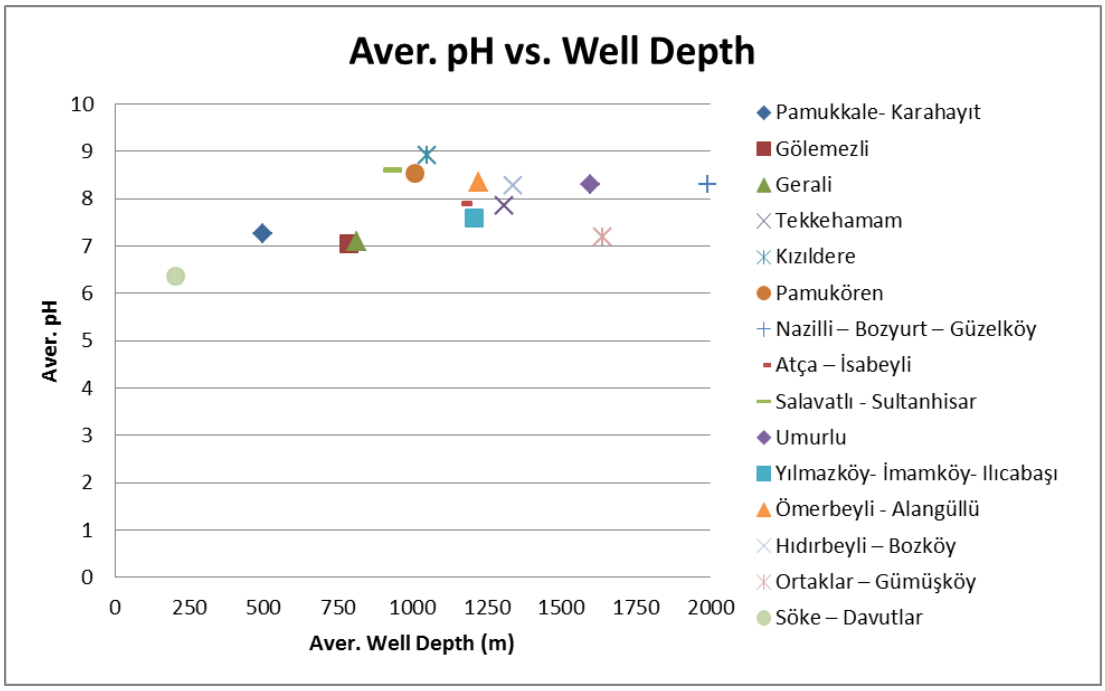

Figure 4-68: The change of average pH geothermal fields with average well depth.

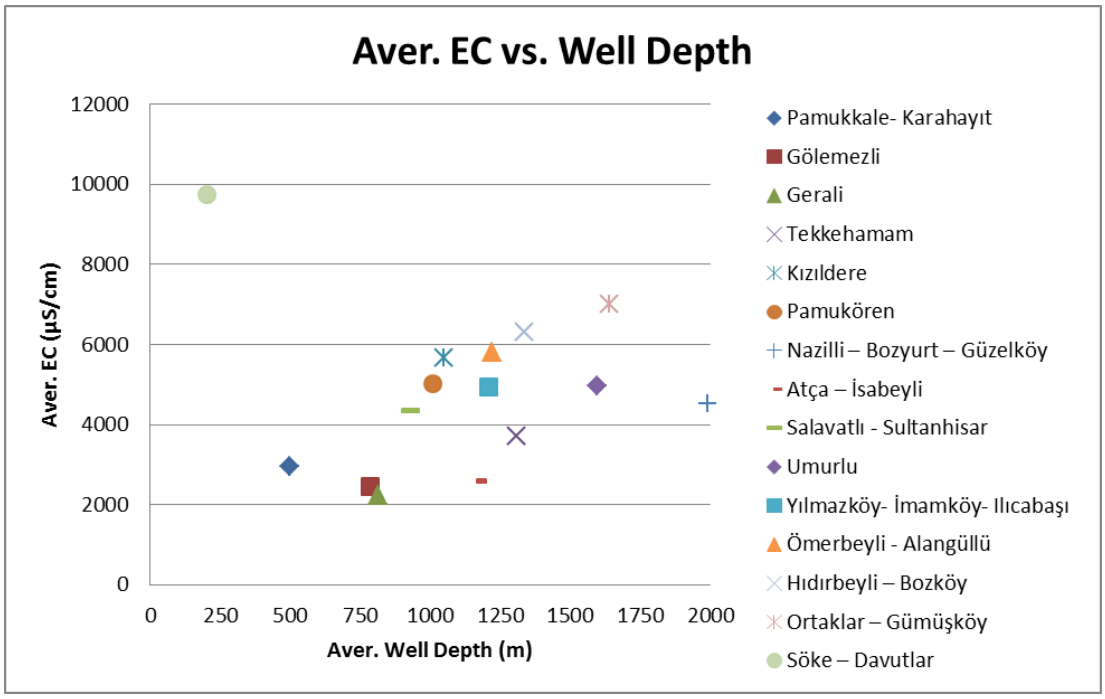

Figure 4-69: The change of average EC geothermal fields with average well depth.

4.4.2.3 Analyses of Average Chemical Compounds with Well Distance to Sea

Na^+ average amounts in the wells increase, as the well location gets closer to sea while the other cation average amounts vary irregularly as the well distance to sea increases. High concentration of Ca^{2+} and Mg^{2+} ions in Pamukkale-Karahayıt geothermal field can be related to water- rock (karstic units) interaction. High concentration of Ca^+ in Söke-Davutlar geothermal field must be due to mixing of sea water. Moreover, average NH_4^+ concentrations show a slight decrease as the well distance to sea increases.

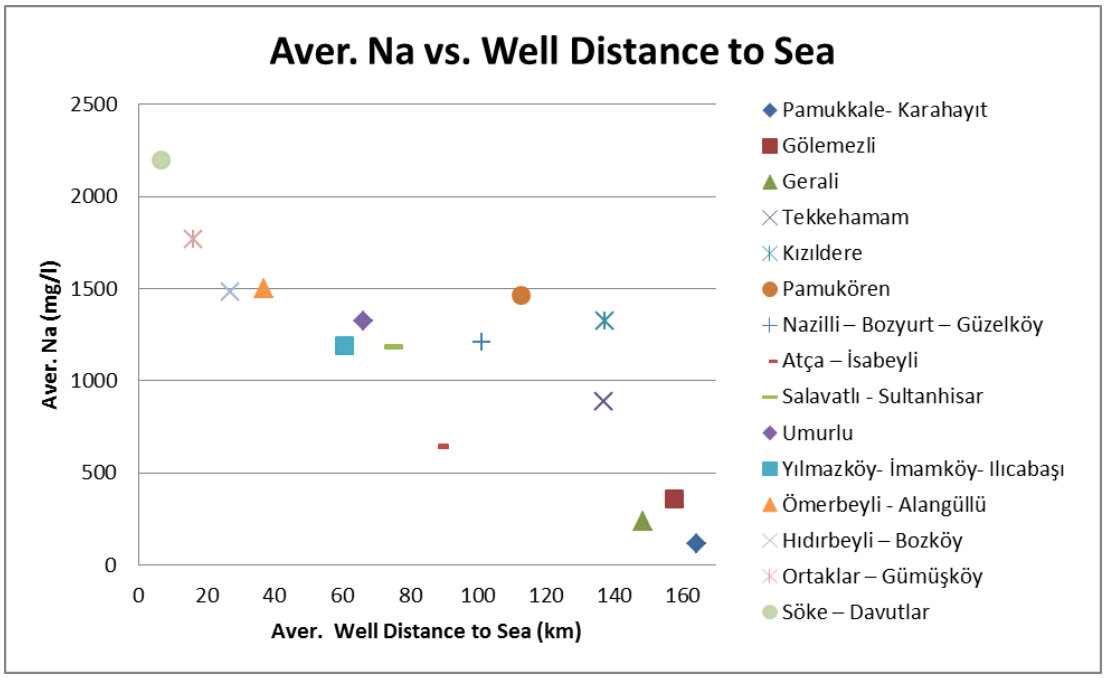

Figure 4-70: The change of average Na geothermal fields with average well distance to sea.

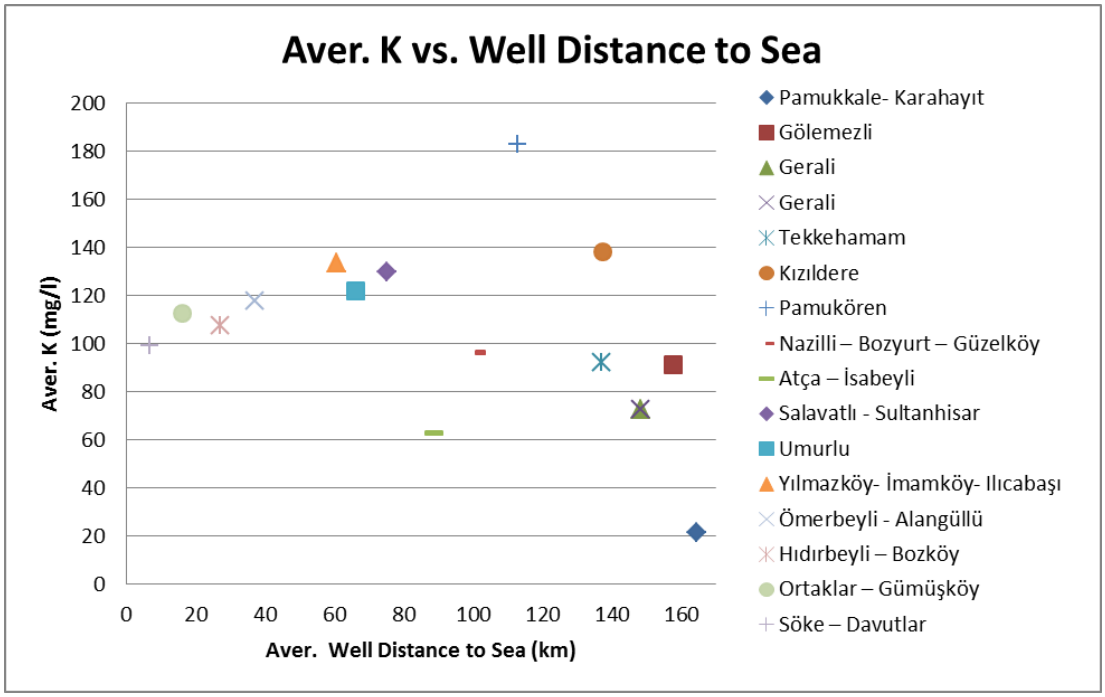

Figure 4-71: The change of average K geothermal fields with average well distance to sea.

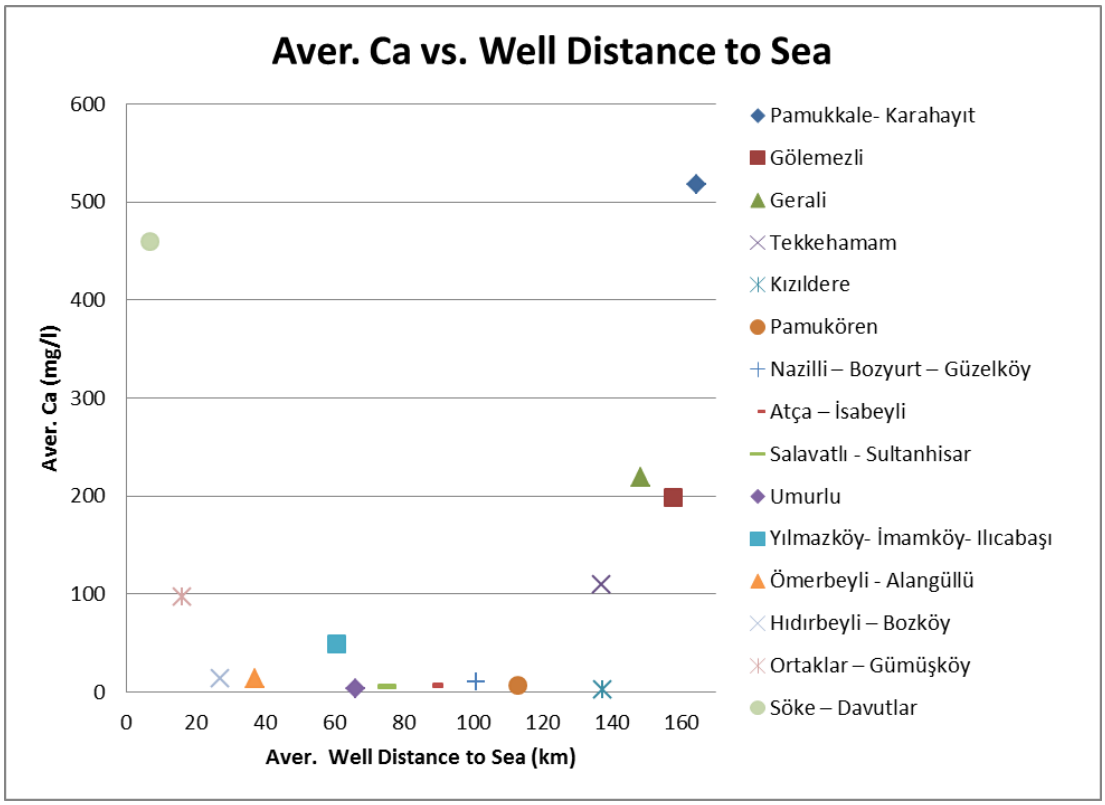

Figure 4-72: The change of average Ca geothermal fields with average well distance to sea.

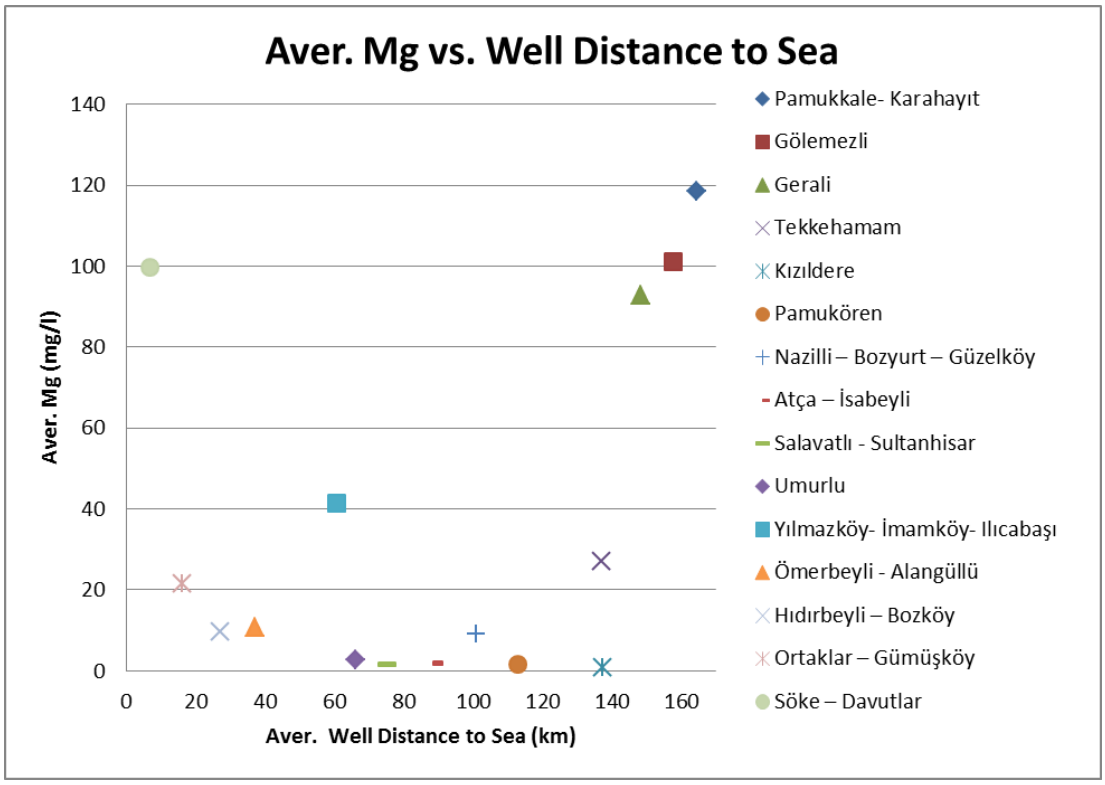

Figure 4-73: The change of average Mg geothermal fields with average well distance to sea.

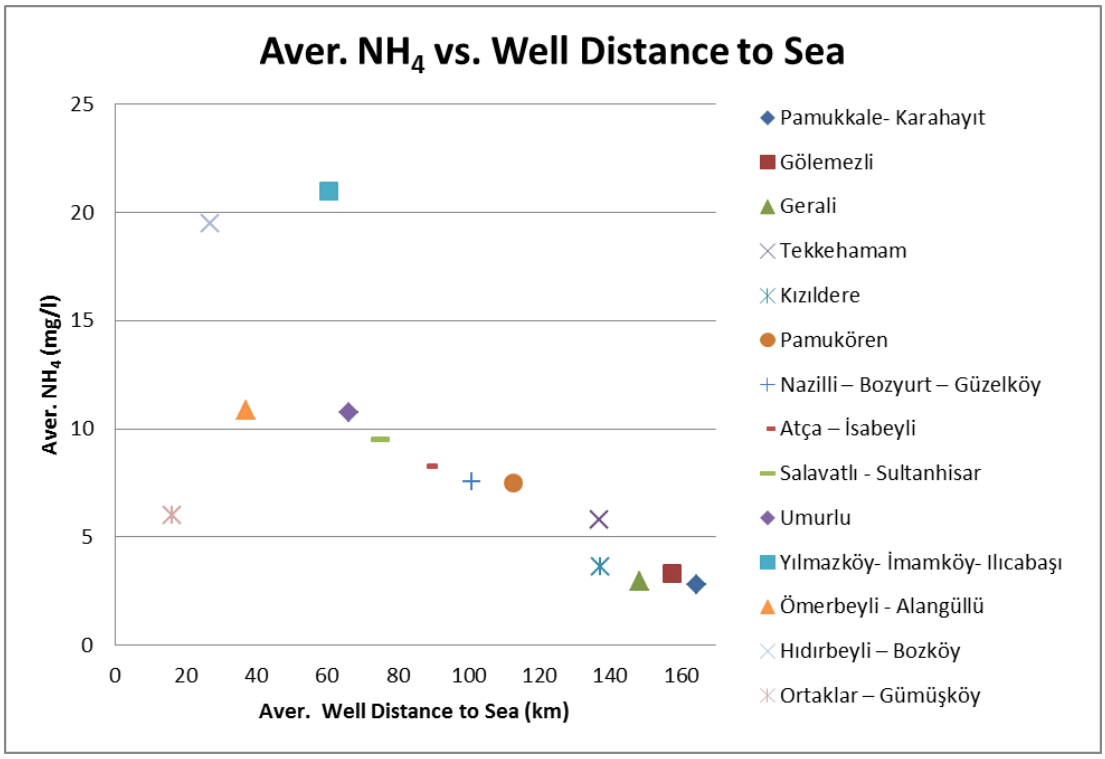

Figure 4-74: The change of average NH_4 geothermal fields with average well distance to sea.

Cl^- average amounts in the wells increase as the well location gets closer to sea. High Cl^- concentrations in the wells close to sea are the result of sea water mixing Moreover SO_4^{2-} average concentrations are high in amount at the east of the graben while it decreases as the distances of the wells get closer to sea. The anayses results of these two anions, Cl^- and SO_4^{2-}, show good correlation while HCO_3^- average concentrations vary irregularly according to well distance to sea. The variations of average anion values according to well distance to sea are shown in Figure 4.75 to Figure 4.77.

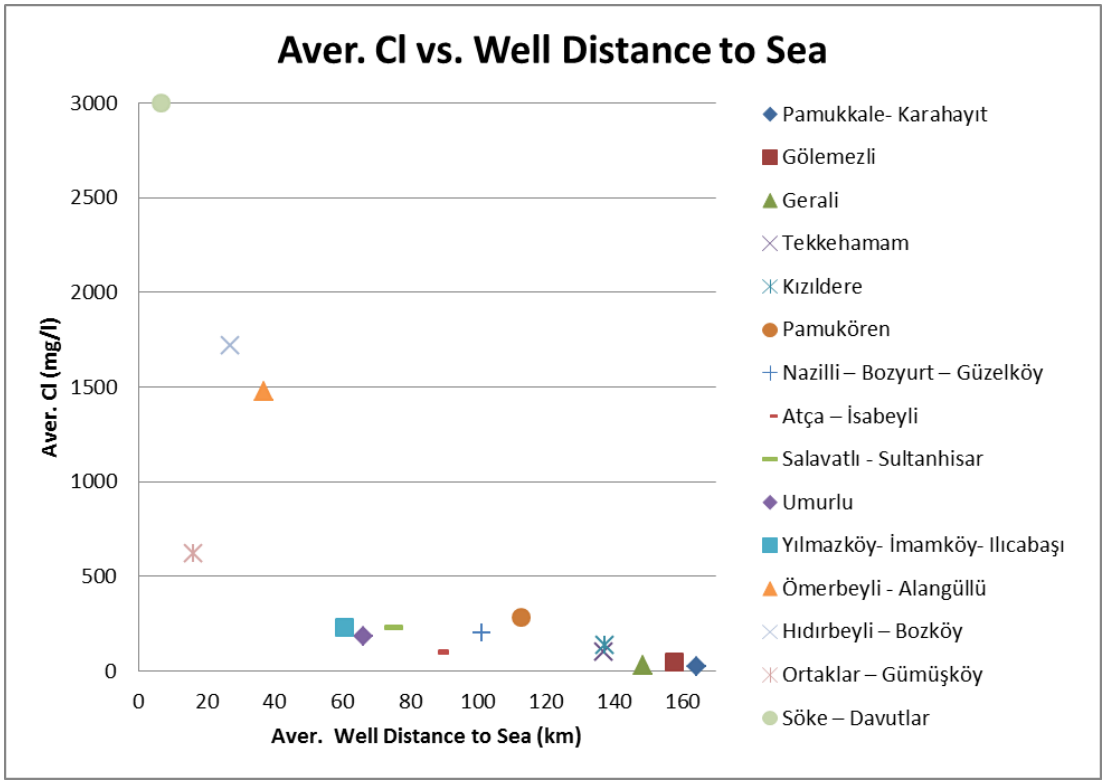

Figure 4-75: The change of average Cl geothermal fields with average well distance to sea.

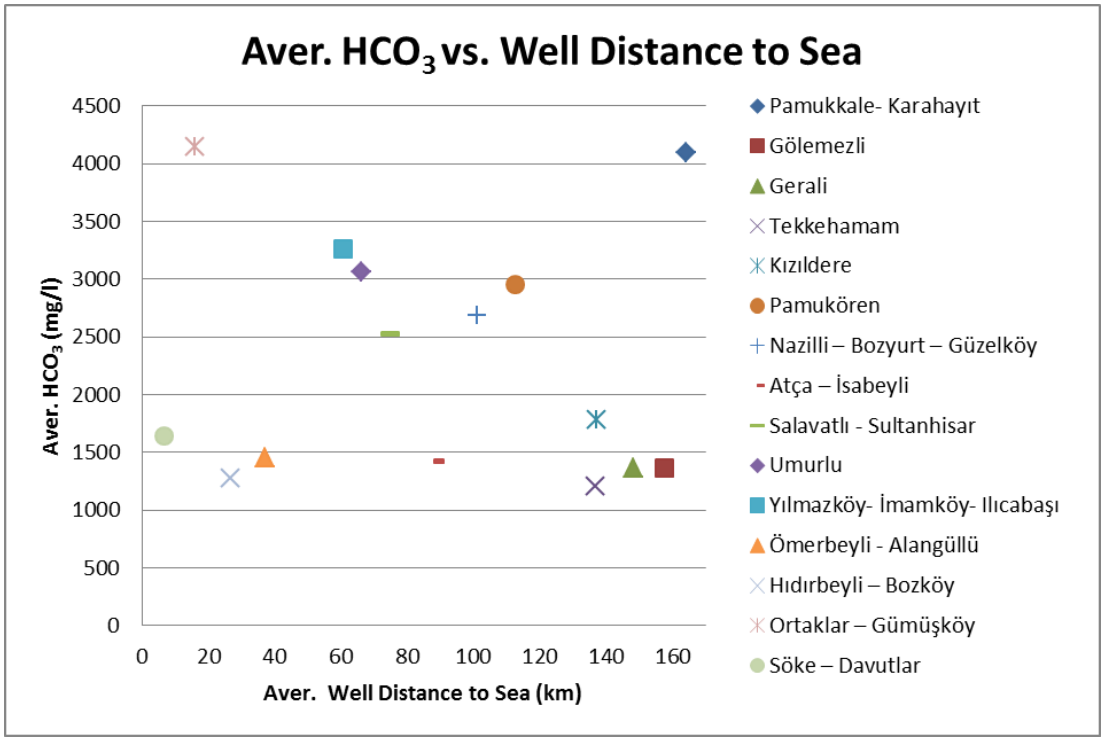

Figure 4-76: The change of average HCO_3 geothermal fields with average well distance to sea.

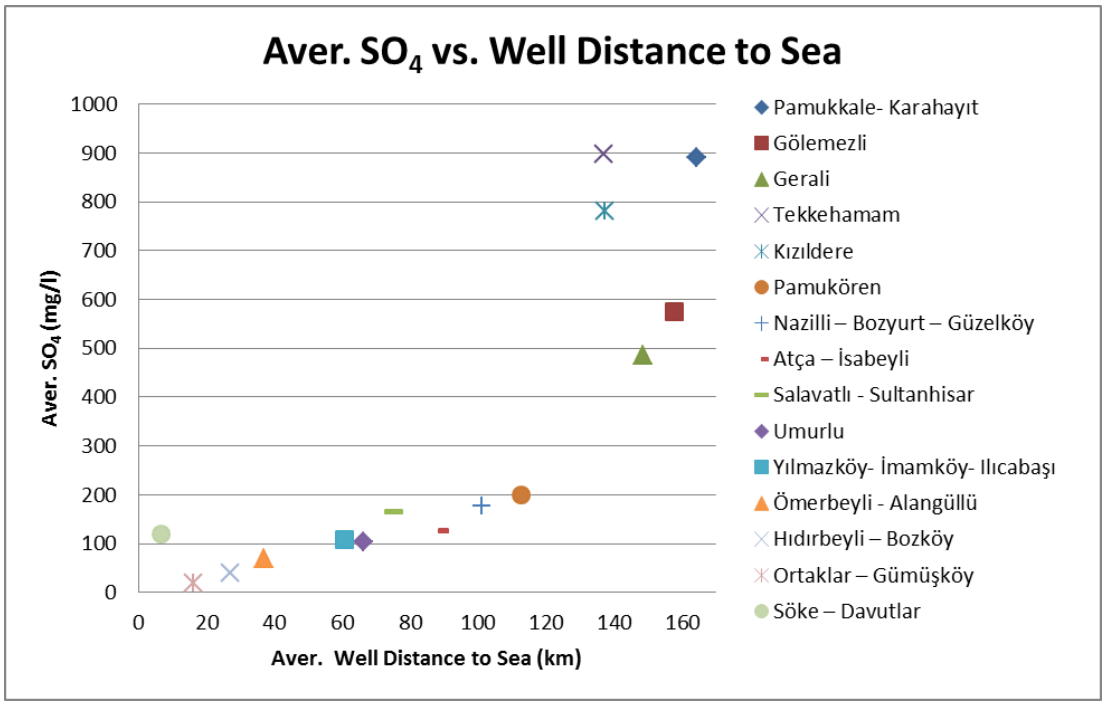

Figure 4-77: The change of average SO_4 geothermal fields with average well distance to sea.

Moreover, average Boron (B), TDS and EC contents were seen in high amounts in the wells close to sea. Good correlation of EC analysis can be related to mixing of sea water and salinity. Boron (B), TDS and EC analyses are shown in Figure 4.78, 4.80 and 4.82 respectively. The variabilities of average SiO_2 and pH values are very high according to well distances to the sea.

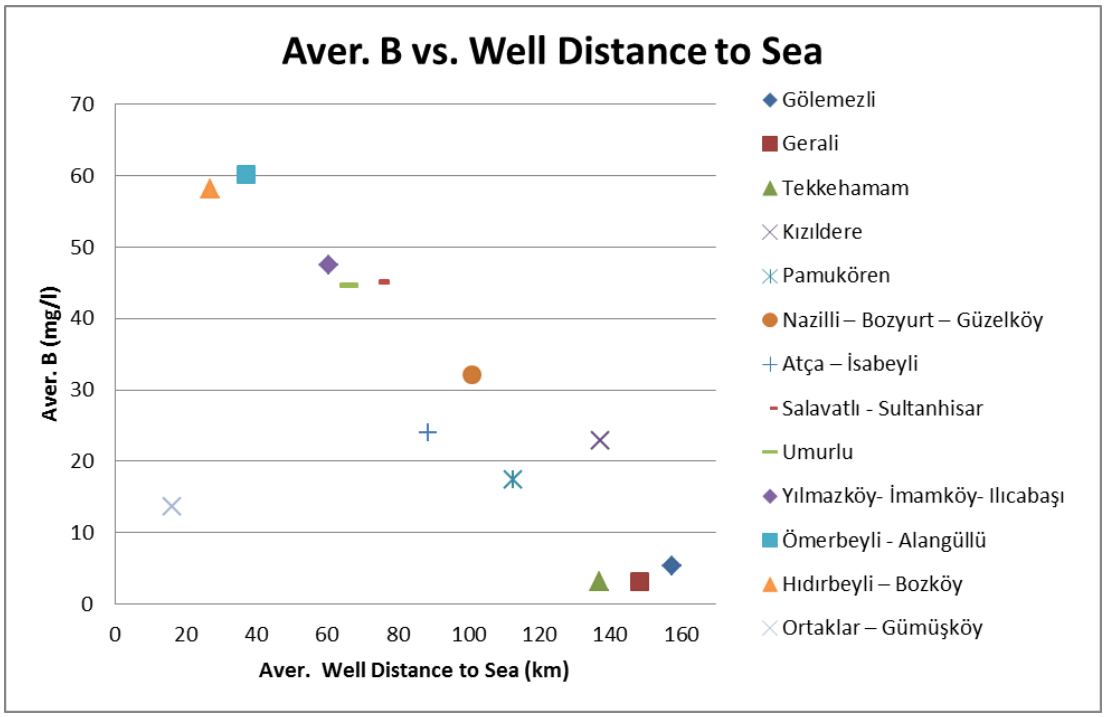

Figure 4-78: The change of average B geothermal fields with average well distance to sea.

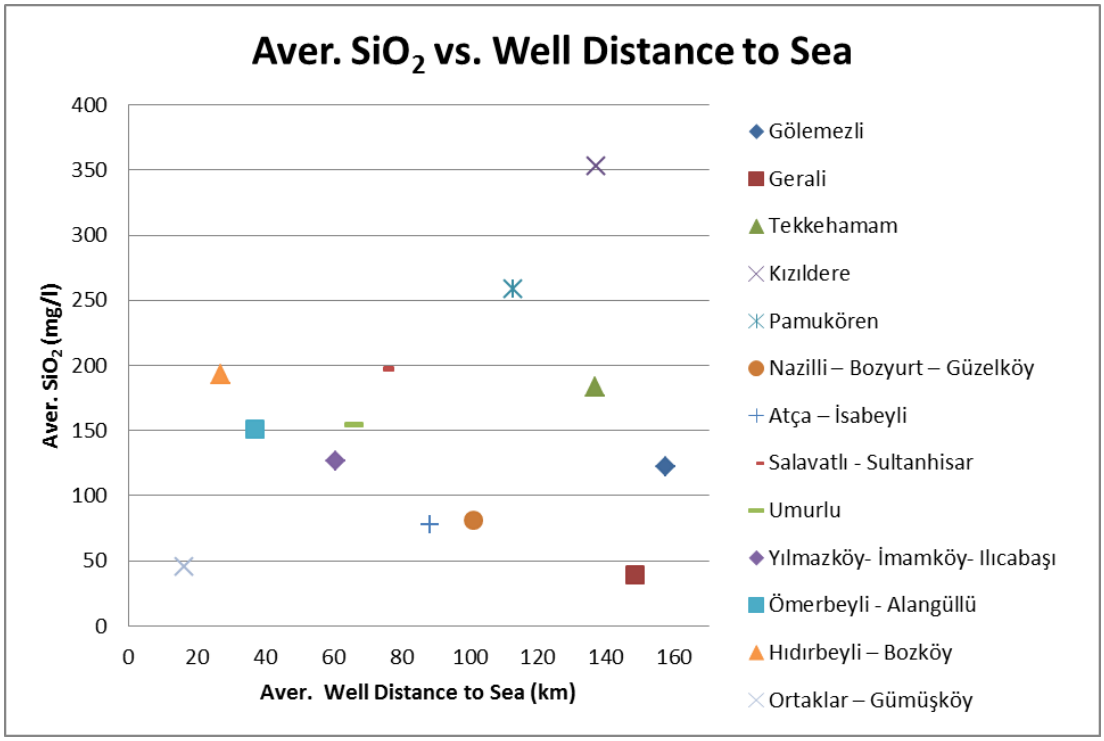

Figure 4-79: The change of average SiO_2 geothermal fields with average well distance to sea.

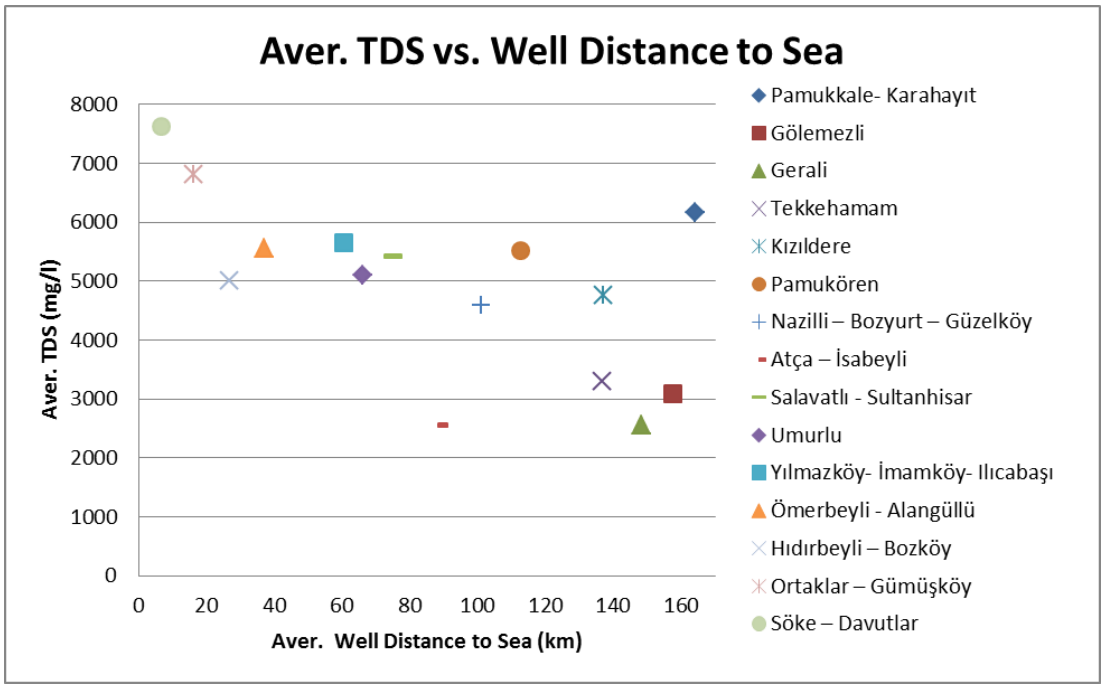

Figure 4-80: The change of average TDS geothermal fields with average well distance to sea.

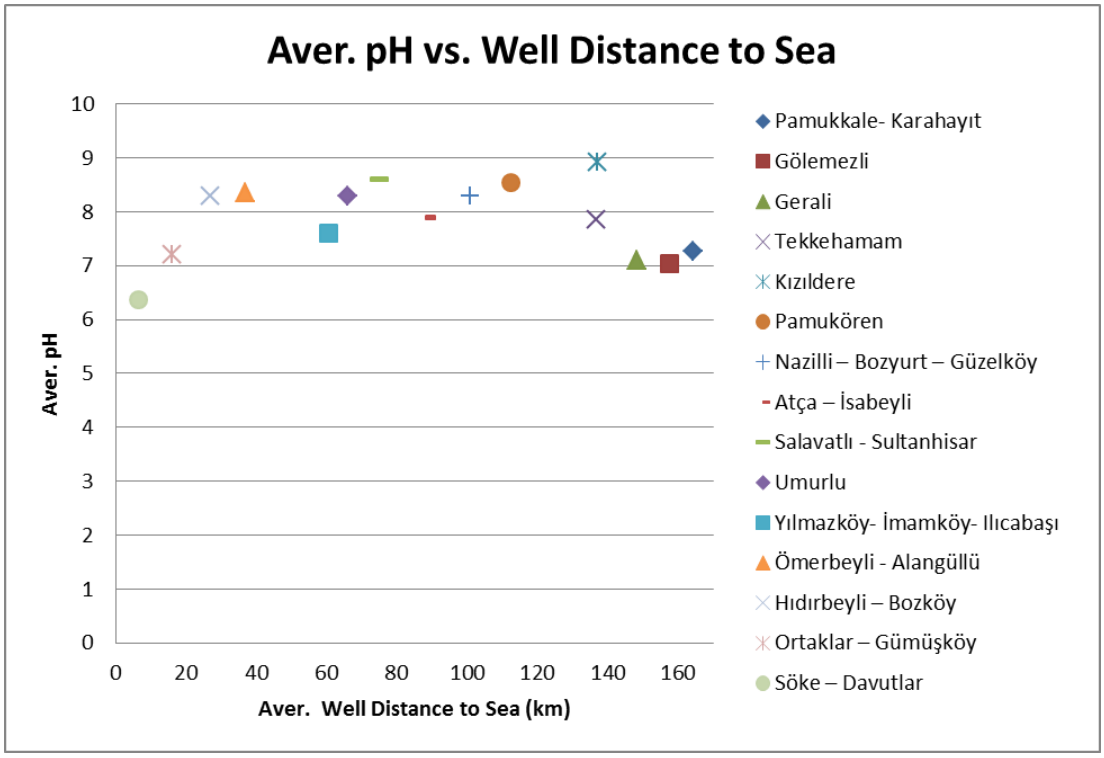

Figure 4-81: The change of average pH geothermal fields with average well distance to sea.

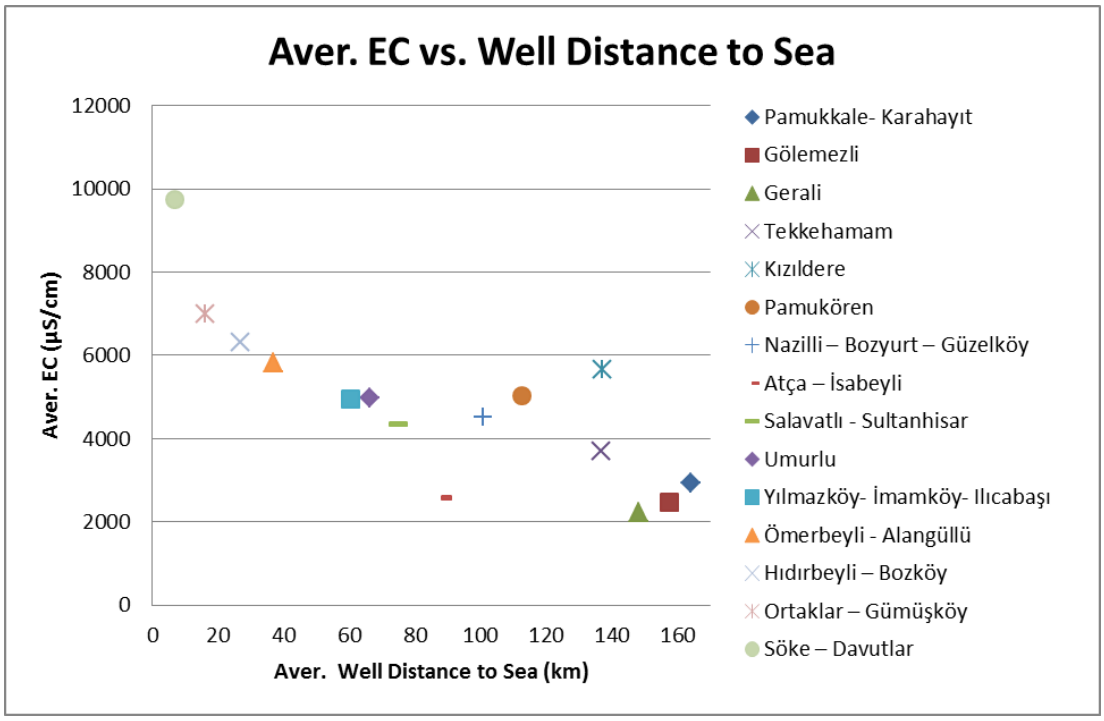

Figure 4-82: The change of average EC geothermal fields with average well distance to sea.

4.4.3 Analyses Based on Geothermal Water Type

The geothermal fields in the graben are fed by meteoric waters generally. The meteoric waters in the drainage area percolate at fault zones and permeable clastic sediments into the reaction zone where meteoric fluids are heated and ascend to the surface due to their lower density caused by convection cells. The origins of most of the waters are meteoric. Only, Söke–Davutlar geothermal field waters are mixed with sea waters.

All of the geothermal fields mainly contain Na-HCO_3 type geothermal waters. The geothermal waters in the Aydın region are mainly of the Na-Ca-HCO_3 type and Na-Ca-HCO_3-SO_4 type in the Denizli region (Şimşek, 2003b). Moreover, some systems have mixed compositions, like Na-Cl-HCO_3 (Vengosh et al., 2002).

At east of the Büyük Menderes Graben, Ca-Na-(SO_4)-HCO_3 type waters are dominant. The waters are also seen in Denizli geothermal fields, from Pamukkale–Karahayıt geothermal field on the east to Kızıldere geothermal field. The HCO_3 nature of the Denizli area is a consequence of an interaction between waters and

carbonate rocks inside the geothermal reservoir (Mutlu & Güleç, 1985). These waters compose abundantly Ca^{2+} and SO_4^{2-} ions. Pamukkale–Karahayıt and Gölömezli geothermal fields also contain Mg^{2+} ions.

Na-Ca-HCO_3 type waters are seen in the middle part of the graben in Aydın province. But there are some exceptions like Yılmazköy–İmamköy–Ilıcabaşı–Kalfaköy geothermal field in Aydın. The thermal waters of Yılmazköy–İmamköy–Ilıcabaşı–Kalfaköy can be classified as Na-Ca-HCO_3 type, but these waters also consist of SO_4^{2-} ions.

The geothermal waters of the fields on the west of the Aydın province can be classified as Na-Cl-HCO_3 type. These type thermal waters are seen in the regions from Ömerbeyli–Alangüllü geothermal field to Söke–Davutlar geothermal field. Furthermore, Hıdırbeyli–Bozköy geothermal field waters are Na-Cl-Mg-HCO_3 type. The chemical analyses show that the thermal water is of the Na-HCO_3 type which suggests water rock interaction is an important process for most of the chloride hot springs and deep geothermal well fluids in the Germencik reservoirs (Şimşek, 2003a). In addition, Cl^- enrichment is probably due to the presence of connate fossil waters in the rocks (Mutlu & Güleç, 1985). Söke–Davutlar geothermal fluid of the system is a mixture of meteoric and sea origin at different proportions. Thermal water type of the field is Na-Cl-HCO_3 type.

4.4.4 Analyses Based on Non-condonsable Gas Content

The high concentration of the non-condensable gas content is a major problem because it triggers scaling and decreases generator output. The non-condensable gas content (mainly carbon dioxide) in well R-1 fluids (extracted from the third reservoir) is about 3% (by weight); in other wells, producing from the first and second reservoirs, it is about 1–1.8% in Kızıldere geothermal field (Şimşek et al., 2005). The geothermal fluid in Salavatlı-Sultanhisar geothermal field contains an average of 1% of CO_2 (the non-condensable gas content) by weight (Serpen et al., 2006). The geothermal fluid of Germencik-Ömerbeyli geothermal field contains an average of 2.5 % of CO_2 (the non-condensable gas content) (Batscha, 2011).

CHAPTER 5

RESULTS AND DISCUSSION

In this thesis, the geothermal fields located in the Büyük Menderes graben system have been examined and seventeen of them are studied to investigate their similar and distinct features. Geological, hydrogeological and geochemical data from these geothermal fields are analyzed to form a dataset and to characterize the fields. In this chapter, the results of the processed data are given and the results are discussed.

The lithological units and their stratigraphic relations of the fields have been analyzed as the geological parameters. Generally, the lithological sequences of all of the fields are more or less similar to each other. Moreover, depositional ages of these sequences are also similar. In addition, it can be said that the fields have formed at the same time frame of tectonic evolution. Mainly, the basement rocks of the all the fields are Paleozoic Menderes metamorphics, which are commonly gneiss, schist, marble and quartzite. Neogene (Miocene and Pliocene) sedimentary rocks are conglomerate, sandstone, siltstone, claystone, marl, and lignite layers and overlie the basement. The Quaternary units are composed of terrace deposits, alluvium, slope debris, alluvial fans and travertine. A different lithological sequence is exposed in Söke–Davutlar geothermal field due to presence of volcanic units. Like the lithology, fault and fold patterns of the fields also show similar caharacteristics. There are mainly two fault types trending in north–south and in east–west directions. E–W-trending graben bounding faults characterize the whole graben. Considering the similarities of the lithology and the structural patterns, the Büyük Menderes Graben can be thought as forming a single and a huge geothermal system.

Reservoir characteristics, aquifer and cap rocks, well temperature, well depth and water origin are the hydrogeological parameters analyzed. Most of the fields contain two reservoir units. Only the Kızıldere geothermal field has proven three reservoir units. The shallowest reservoir units are Neogene sedimentary rocks for all of the fields. Limestone layers often host as shallowest reservoir. Besides, conglomerate and sandstone layers are the other aquifer members of the shallowest reservoirs. The second and deeper reservoir is formed of the rocks of the Menderes Massif metamorphics which are generally karstic marbles, quartzites and types of schists and gneisses. These units are fractured due to active tectonism and they gain high fracture permeability and porosity. Menderes metamorphics also serve as the third reservoir units in the Kızıldere geothermal field and are comprised of gneisses. The cap rocks of these fields are clay and silty units of Neogene rocks and schists of the Menderes metamorphics. To sum up, the reservoir lithologies of the fields have more or less same aquifer and cap rock characteristics.

Moreover, presence of the fault cut in the reservoir was analyzed. The average temperature of the wells cut by a fault is about 162 ^{o}C while the average temperature of the wells without a fault cut is about 125 ^{o}C. So, higher temperatures were obtained from the wells which cut a fault. Although reservoir and cap rock characteristics of the fields and wells are similar to each other the wells with fault cut produce fluid at higher temperatures. Hence, it can be concluded that the fault cut is an essential parameter to obtain high enthalpy from the geothermal systems.

Study on all the temperature observations at the wells shows that fluid temperature generally increases with depth. This is somehow following the general knowledge of the fluid temperatures in the fields. This knowledge is verified by the temperature-well depth analysis.

Temperature variation is also studied with respect to locations of the fields in the graben system. In doing this the temperatures are correlated with distances of the wells to the sea, which are taken as the reference points. Analyses of the correlations between the temperatures and the distances to the sea indicate that the temperatures

are not affected by the location of the fields. This means the fluid temperatures vary independently with respect to distance to sea along E-W direction.

Chemical components of the geothermal fluids have been analysed based on fluid temperature, well depth and well distance to sea. The results indicate that the temperature is an important parameter affecting the chemical concentrations. Additionally, the origin of the geothermal fluid and the host rock affect the chemical types of the geothermal fluids.

According to temperature analyses, Ca^{2+} and Mg^{2+} concentrations decrease significantly as the temperature rises. Generally, Ca^{2+} and Mg^{2+} solubilities decrease when the temperature increases. So, drop of Ca^{2+} and Mg^{2+} concentrations in the wells with high reservoir temperature are expected results. However, it must be indicated that CO_2 which is a non-condensable gas affects the dissolution and precipitation of $CaCO_3$. The solution loses the temperature, pressure, and CO_2 on its way to the surface. CO_2 becomes free at lower fluid temperature (degassing is more effective at lower water temperatures) leading to precipitation of $CaCO_3$. The fluid temperatures of Ca^{2+} ions used in the analyses were cooler than the actual reservoir temperatures. So, the Ca^{2+} concentrations in the analysis can not be reliable. Moreover, the analyses based on average values of Ca^{2+} and Mg^{2+} concentrations with respect to individual ion-temperature analyses gave more promising results. Apart from these two cation concentrations, temperature affects the Na^+ and K^+ concentrations. Na^+ and K^+ concentrations increase with increasing temperature.

Furthermore study of the cation concentrations with respect to well depth does not yield any relation. On the other hand the cation concentrations change independently with respect to well location. However, the study of average cation concentrations shows some trends with respect to well location and well depth. These trends are seen in the analyses of average Na^+, Ca^{2+} and Mg^{2+} concentrations. Average Na^+ concentration increases as the well location gets closer to the sea. In addition, average Ca^{2+} and Mg^{2+} concentrations indicate similar results based on average well depth. Average Ca^{2+} and Mg^{2+} concentrations decrease with average well depth

significantly though in the analyses of all the wells, decrease of Ca^{2+} and Mg^{2+} concentrations with well depth can be considered negligible.

All of the anions, Cl^-, HCO_3^-, SO_4^{2-}, do not present reliable results and it is found that they are not related to temperature change. It means that the examined anions are not affected by temperature. Moreover, inspection of the concentrations shows high Cl – concentrations probably due to sea water intrusion in the fields located closer to the sea.

Furthermore, SO_4^{2-} –distribution in the graben indicate that the temperature has no effect on this distribution. It can be remarkable that TH1, Tekkehamam, and KD 9, Kızıldere, wells have high SO_4^{2-} concentration while AGG 16, Ortaklar–Gümüşköy, well has low SO_4^{2-} concentration. It is known that the west of the graben have SO_4^{2-} type geochemical water while the fields close to sea have very low SO_4^{2-} concentrations. Furthermore, the avarege concentrations of anions do not show significant variance with average temperature change.

The analyses of Cl^-, HCO_3^- and SO_4^{2-} concentrations in all wells and average values of them with respect to well depth and/or average well depth do not yield suggestive results. It can be concluded that of Cl^-, HCO_3^- and SO_4^{2-} concentrations do not depend on the well depth.

Moreover, Cl^- and SO_4^{2-} concentrations change with well locations significantly while HCO_3^- concentration distribution is not significant according to the result of the analyses. Cl^- concentration increases and SO_4^{2-} concentration decreases as the well distance to sea decreases. However, HCO_3^- concentration does not change regularly. The analyses of average Cl^-, SO_4^{2-} and HCO_3^- concentrations with respect to average well distance to sea also support the results which are obtained based on all of the wells' analyses. High Cl^- concentrations in the wells close to sea is the result of sea water mixing.

SiO_2 concentration is another parameter that was analyzed. SiO_2 concentration of 60 wells and average value of the all fields were examined with respect to temperature.

According to results, SiO_2 concentrations increase as the temperature increases. This is an expected result due to fact that the concentration of SiO_2 increases with increasing temperature.

Besides, analyses of pH values gave similar result with SiO_2 concentration. pH of all the wells and average pH values of all the fields increase when the temperature increases. Because the activity of the H^+ ions is dependent on temperature, so the temperature influences the pH value.

Additionally, B concentration, TDS and EC values and average values of them were analyzed with respect to temperature change. They give sensible results; these values increase with increasing temperature. It can be assessed that B concentration, TDS and EC values do not depend on the temperature change.

SiO_2 and B concentrations, TDS, EC and pH values of all wells were examined with respect to well depth. It is observed that there is no dependency between these parameters and well depth.

Moreover, average Boron (B), TDS and EC contents were analyzed based on well distance of well locations to sea. These values were seen in high amounts in the fields close to sea. Moreover high TDS and EC contents are the result of sea water mixing and salinity. However, the variabilities of average SiO_2 and pH values are very high according to well distances to the sea.

CHAPTER 6

CONCLUSION

In this thesis study, the geothermal fields in the Büyük Menderes Graben which is a promising region due to the highest potential of geothermal energy in Turkey were studied. Büyük Menderes Graben region has been studied for relatively long years by institutions, companies and researchers. There are several and complicated information about the graben. However, the region has not been completely handled in terms of geology, geochemical, hygdogeological and tectonic activity variables.

In this study, the parameters of these variables has been handled and interpreted. The temperature and pressure of reservoirs, the thermal water origin and type, water content have analyzed. The relations among them and tectonic activity, faults and reservoir relations have been compared and contrasted.

The following conclusions can be drawn from the results of the thesis study,

1. Geothermal fields in the Büyük Menderes Graben system have generally same lithological sequence. Menderes Massif metamorphics, Neogene (Miocene and Pliocene) fluvial and lacustrine sedimentary rocks and Quaternary loose and unconsolidated units form the graben lithology.
2. All of the geothermal fields have at least two reservoir units. Menderes metamorphics comprise the deeper reservoir which produces liquid at higher temperature. The shallower reservoir is composed of permeable sedimentary units.

3. Reservoir and cap rock units of the fields are similar to each other in terms of lithology. The deeper reservoir rocks are Menderes Massif metamorphics which are generally karstic marbles, quartzites and types of schists and gneisses. The upper reservoir rocks are sedimentary units such as limestone, sandstone and conglomerate. The cap rocks are schists of the Menderes metamorphics and impermeable units of the sedimentary rocks.
4. The deeper reservoir rocks, Menderes Massif metamorphics, are highly fractured and faulted which result in secondary permeability and lead to high temperature gothermal fluid.
5. Although the reservoir features are more or less the same in the entire graben, the wells with fault cut yield high temperatured fluid.
6. Generally, the temperature increases with increasing well depth.
7. Geochemical analyses show that well fluid temperature affects the Ca^{2+}, Mg^{2+} and SiO_2 concentrations and pH values while well locations affect the Cl^- and SO_4^{2-} concentrations. Ca^{2+} and Mg^{2+} concentrations decrease significantly and SiO_2 concentration and pH value increase as the temperature rises. High Cl^- concentration is the result of sea water mixing.
8. The geothermal parameters cations, anions, SiO_2 and trace element B (Boron) concentrations, TDS (Total Dissolved Solids), EC (electrical conductivity) do not depend on well depth.
9. B, TDS and EC contents were observed in high amounts in the fields close to sea.
10. It is verified that all of the geothermal fields generally constitute Na-HCO_3 type geothermal waters. Aydın region has mainly of the Na-Ca-HCO_3 type and Denizli region has Na-Ca-HCO_3-SO_4 type geothermal water based on their chemical composition. Moreover, the fields on the west of Aydın province have mixed compositions of geothermal water type which is Na-Cl-HCO_3.
11. High concentration of Cl^- ion in Söke–Davutlar geothermal field is due to mixing of seawater.

REFERENCES

[1] Aksoy, N. and Serpen, U., (2005). Reinjection Management in Balçova Geothermal Field. Proceedings World Geothermal Congress, Antalya, Turkey.

[2] Alçiçek, H., Varol, B. and Özkul, M., (2007). Sedimentary facies, depositional environments and palaeogeographic evolution of the Neogene Denizli Basin, SW Anatolia, Turkey. Sedimentary Geology, 202, 596–637.

[3] Armstead, H.C.H., (1983). Geothermal Energy, (E. & F. Nn Spon, London), 404.

[4] Atmaca, İ., (2010). Resource Assessment in Aydın – Pamukören Geothermal Field. M.Sc. Thesis, Middle East Technical University, Ankara, Turkey.

[5] Avigad, D., Garfunkel, Z., Jolivet, L. and Azañón, J. M., (1997). Back-arc extension and denudation of Mediterranean eclogites. Tectonic, 16, 924–41.

[6] Bali, T., (2010). Aydın-Kuşadası-Davutlar AKD 2010/2 Kuyusu Kamp Bitirme Raporu. MTA report (in Turkish).

[7] Batscha, D., (2011). Türkiye'nin Batısındaki Jeotermal Sahalar İçin Jeotermal Güç Santrallarinin Karşılaştırılması. X. Ulusal Tesisat Mühendisliği Kongresi, Nisan 2011, İzmir.

[8] Bates, R. J. and Jackson, J. A., (1984). Dictionary of Geological Terms (3. ed.). American Geological Institute, 299.

[9] Beyazıt, H., Değer, İ. and Başıkara, M., (2010). Denizli-Sarayköy-Gerali Jeotermal Sondaj Kampı DSG 2010/4 Kuyusu Bitirme Raporu. MTA report (in Turkish).

[10] Bozkurt, E., (2000). Timing of Extension on the Büyük Menderes Graben, Western Turkey, and Its Tectonic Implications. Geological Society, London, Special Publications, 173, 385.

[11] Bozkurt, E. and R. Oberhänsli., (2001). Menderes Massif (western Turkey):structural, metamorphic and magmatic evolution – a synthesis. International Journal of Earth Sciences, 89, 679-708.

[12] Bozkurt, E., (2004). Granitoid rocks of the southern Menderes Massif (southwestern Turkey): field evidence for Tertiary magmatism in an extensional shear zone. International Journal of Earth Sciences, 93, 52–71.

[13] Bozkurt, E. and Sözbilir, H., (2004). Tectonic evolution of the Gediz Graben: field evidence for an episodic, two-stage extension in western Turkey. Geological Magazine, 141, 63–79.

[14] Bozkurt, E. and Rojay, B., (2005). Episodic, two-stage Neogene extension and short-term intervening compression in western Anatolia: field evidence from the Kiraz basin and Bozdağ Horst. Geodinamica Acta, 18/3-4, 295–312.

[15] Bozkurt, E., (2007). Extensional v. contractional origin for the southern Menderes shear zone, SW Turkey: tectonic and metamorphic implications. Geological Magazine, 144 (1), 191–210.

[16] Bülbül, E., (2008). Aydın-Salavatlı ASR-3 Reenjeksiyon Kuyusu Bitirme Raporu. MTA report, No. 11087 (in Turkish).

[17] Çağlayan, İ. and Dünya, H., (2012). Aydın-Germencik-Gümüşköy AGG 2010/16 Jeotermal Enerji Araştırma Sondajı Kuyu Bitirme Raporu. MTA report, No. 11499 (in Turkish).

[18] Çakın, A., (2003). Environmental Effects of Geothermal Applications.Case Study: Balçova Geothermal Field. M.Sc. Thesis, İzmir Institute of Technology, İzmir, Turkey.

[19] Ceyhan, S., (2000). Aydın Alangüllü Boğazköy Sıcaksu Sondajı A 2 Kuyu Bitirme Raporu. MTA report, No. 10469 (in Turkish).

[20] Dağıstan, H., Doğdu, N. and Karadağlar, M., (2010). Geothermal Explorations and Investigations by MTA in Turkey. Proceedings World Geothermal Congress 2010, Bali, Indonesia.

[21] Demirel, V. and Beker, K., (2005). Aydın-Salavatlı ASR-2 Reenjeksiyon Kuyusu Kuyu Bitirme Raporu. MTA report, No. 10797 (in Turkish).

[22] Demirel, Y., Yolal, A. and Beker, K., (2007). Denizli Kizildere R-3 No'lu Reenjeksion Kuyu Bitirme Raporu. MTA report, No. 10963 (in Turkish).

[23] Dewey, J. F. and Şengör, A. M. C., (1979). Aegean and Surrounding Regions: Complex Multiplate and Continuum Tectonics in a Convergent Zone. Geological Society of America Bulletin, 90, 84–92.

[24] Dünya, H., (2009). Aydın-Umurlu AU-2 Jeotermal Sondajı Kuyu Bitirme Raporu. MTA report, No. 11186 (in Turkish).

[25] Eşder, T., Çağlav, F. and Pekatan, R., (1994). Kızıldere Jeotermal Sahasındaki KD-20, KD-21, KD-22 Üretim Kuyuları (1985-1986) ve Sistemin Yeni Verilerle Yorumlanması. MTA Report (in Turkish).

[26] Filiz. S., Tarcan. G. and Gemici. Ü., (1999). Germencik (Aydın) Jeotermal Alanlarının Hidrojeokimyasal Açıdan İncelenmesi. Dokuz Eylül Üniversitesi Mühendislik Fakültesi, Fen ve Mühendislik Dergisi, 1(1), 41–64.

[27] Filiz. S., Tarcan. G. and Gemici. Ü., (2000). Geochemistry of the Germencik Geothermal Fields, Turkey. Proceedings World Geothermal Congress, Kyushu-Tohoku, Japan.

[28] Flerit, F., Armijo, R., King, G. and Meyer, B., (2004). The mechanical interaction between the propagating North Anatolian Fault and the back-arc extension in the Aegean. Earth and Planetary Science Letters, 224, 347–62.

[29] Gessner, K., Piazolo, S., Güngör, T., Ring, U., Kröner, A. and Passchier, C. W., (2001). Tectonic significance of deformation patterns in granitoid rocks

of the Menderes nappes, Anatolide belt, southwest Turkey. International Journal of Earth Sciences, 89, 766–80.

[30] Giggenbach, W. F., (1980). Geothermal Gas Equilibria. Geochimica et Cosmochimica Acta, 44, 2021-2032.

[31] Gökgöz, A., Yılmazlı, İ. E., Güngör, İ. and Yavuzer, İ., (2010). Hydrogeology and Environmental Study at the Karahayit Geothermal Field (Western Turkey). Proceedings World Geothermal Congress 2010, Bali, Indonesia.

[32] Gunnlaugsson, E., (2008). Importance of Chemistry in Geothermal Exploration and Utilization. Workshop for Decision Makers on Direct Heating Use of Geothermal Resources in Asia, China.

[33] Güdücü, A., (2008). Aydın Atça AT-1 Sıcaksu Sondajı Kuyu Bitirme Raporu. MTA report, No. 11086 (in Turkish).

[34] Güleç, N., (2005). Aplications of Geothermometery, Geothermal Geochemistry and Some New Geothermal Approaches, Dokuz Eylül University, Geohermal Energy Research and Application Center (GERAC).

[35] Güner, İ. N. and Elhatip, H., (1999). Pamukkale Yöresi (Denizli) Termal Kaynaklarının Hidrokimyasal ve İzotopik İncelenmesi. Nigde Üniversitesi Mühendislik Bilimleri Dergisi, 3-1, 35-47.

[36] Gürer, Ö. F., Sarıca-Filoreau, N., Öburan, M., Sangu, E. and Doğan, B., (2009). Progressive Development of the Büyük Menderes Graben Based on New Data, Western Turkey. Geological Magazine, Cambridge University Pres, 1- 22.

[37] Hamendi, A., (2009). Numerical Simulation of Germencik Geothermal Field. M.Sc. Thesis, Middle East Technical University, Ankara, Turkey.

[38] Hochstein, M. P., (1990). Classification and Assessment of Geothermal Resources. In: Dickson MH and Fanelli M (eds) Small geothermal resources, UNITAR/UNDP Centre for Small Energy Resources, Rome, Italy.

[39] Kahraman, S., (2003). Denizli Gölemezli Jeotermal Alanı DG-3 ve DG-5 Sondajları Kuyu Bitirme Raporu. MTA report, No. 10660 (in Turkish).

[40] Kara, İ., (2003). Aydın Yılmazköy AY 1 Sondaj Kuyu Bitirme Raporu. MTA report, No. 10496 (in Turkish).

[41] Karaca, S. and Destur, M., (2012). Aydın-Kuşadası-Davutlar Sahası Jeotermal Etüt (Jeoloji-Jeofizik) Raporu. MTA report, (in Turkish, unpublished).

[42] Karahan, Ç., (2007). Aydın Sultanhisar SH-1 ve SH-2 Sıcak Su Sondajları Kuyu Bitirme Raporu. MTA report, No. 10957 (in Turkish).

[43] Karahan, Ç., (2008). Aydın-Hıdırbeyli HB-1 ve HB-2 Sıcak Su Sondajlari Kuyu Bitirme Raporu. MTA report, No. 11065 (in Turkish).

[44] Karahan, Ç. and Güdücü, A., (2008a). Aydın Atça AT-1 Sıcaksu Sondajı Kuyu Bitirme Raporu. MTA report, No. 11086 (in Turkish).

[45] Karahan, Ç. and Güdücü, A., (2008b). Aydın Serçeköy ASK-1 Sıcaksu Sondajı Kuyu Bitirme Raporu. MTA report, No. 11151 (in Turkish).

[46] Karahan, Ç. and Dönmez, H., (2009). Aydın-Umurlu AU-1 Jeotermal Sondajı Kuyu Bitirme Raporu. MTA report, No. 11185 (in Turkish).

[47] Karahan, Ç., Dünya, H. and Gökmenoğlu, O., (2009). Aydın-Umurlu AU-2 Jeotermal Sondajı Kuyu Bitirme Raporu. MTA report, No. 11186 (in Turkish).

[48] Karahan, Ç., (2010a). Aydın-Nazilli Güzelköy NG–1 Jeotermal Sondajı Kuyu Bitirme Raporu. MTA report, No. 11294 (in Turkish).

[49] Karahan, Ç., (2010b). Aydın-İsabeyli İS-1 Sıcak Su Sondajı Kuyu Bitirme Raporu. MTA report, No. 11295 (in Turkish).

[50] Karakuş, H., (2010). Investigation of Geothermal Systems in Büyük Menderes Graben by Using Geochemical and Isotopic Techniques. Ph.D. Thesis, Hacettepe University, Ankara, Turkey.

[51] Karamanderesi, İ. H., (1987). Aydın Sultanhisar Salavatlı Jeotermal Sahası AS 1 ve AS 2 Kuyularının Bölgesel Değerlendirme Raporu. MTA report, No. 9956 (in Turkish).

[52] Karamanderesi, İ. H., Çağlav, F., Işık, E., Ölçenoğlu, K., Pekatan, R. and Yıldırım, N., (1990). Ayter A.Ş. Adına Açılmış Olan Ayter 1 Ayter 2 Sıcaksu Arama Kuyularının Kuyu Bitirme Raporu. MTA report, No. 9052 (in Turkish).

[53] Karamanderesi, İ. H. and Helvacı, C., (2003). Geology and Hydrothermal Alteration of the Aydın-Salavatlı Geothermal Field, Western Anatolia, Turkey. Turkish Journal of Earth Sciences (Turkish J. Earth Sci.), 12, 175-198.

[54] Karamanderesi, İ. H. and Ölçenoğlu, K., (2005). Geology of the Denizli Sarayköy (Gerali) Geothermal Field, Western Anatolia, Turkey. Proceedings World Geothermal Congress 2005, Antalya, Turkey.

[55] Kaya, M. and Gökgöz, A., (2005). Ortakçı (Buharkent-Aydın) Sıcak ve Mineralli Su Kaynağının Hidrojeokimyasal İncelemesi. Pamukkale Üniversitesi Mühendislik Fakültesi, Mühendislik Bilimleri Dergisi, 11(2), 257-266.

[56] Kaya, T. and Kindap, A., (2009). Kızıldere – New Geothermal Power Plant in Turkey. Proceedings of the International Conference on National Development of Geothermal Energy Use and International Course/EGEC Business Seminar on Organization of Successful Development of a Geothermal Project.

[57] Keskin, B., (1972). Kuşadası-Germencik-Aydın Arası Büyük Menderes Grabeninin Jeotermal Değerlendirilmesi Hakkında Detay Jeolojik Rapor. MTA report, No. 5734 (in Turkish).

[58] Kindap, A., Kaya, T., Tut Haklıdır, F. S. and Alpagut Bükülmez, A., (2010). Privatization of Kizildere Geothermal Power Plant and New Approaches for

Field and Plant. Proceedings World Geothermal Congress 2010, Bali, Indonesia.

[59] Koçyiğit, A., Yusufoğlu, H. and Bozkurt, E., (1999). Evidence from the Gediz graben for episodic two-stage extension in western Turkey. Geological Society, London, 156, 605–616.

[60] Lagat, J., (2010). Hydrothermal Alteration Mineralogy in Geothermal Fields with Case Examples From Olkaria Domes Geothermal Field, Kenya. Short Course V on Exploration for Geothermal Resources, Kenya.

[61] Ledru, P. and Frottier, G. F., (2010). Geothermal Energy Systems: Exploration, Development, and Utilization. Wiley-VCH.

[62] Lund, J. W., (2007). Characteristics, Development and Utilization of Geothermal Resources. Geo-Heat Center Quarterly Bulletin.

[63] Mcclusky, S., Balassania, S., Barka, A., Demir, C., Ergintav, S., Georgiev, I., Gürkan, O., Hamburger, M., Hurst, K., Kalhe, H., Kastens, K., Kekelidze, G., King, R., Kotzev, V., Lenk, O., Mahmoud, S., Mishin, A., Adariya, M., Ouzounis, A., Paradissis, D., Peter, Y., Prilepin, M., Reilinger, R., Sanli, I., Seeger, H., Tealeb, A., Toksöz, M. N. and Veis, G., (2000). Global positioning system constraints on plate kinematics and dynamics in the eastern Mediterranean and Caucasus. Journal of Geophysical Research 105, 5695–719.

[64] Mckenzie, D., (1978). Active Tectonics of the Alpine–Himalayan Belt: the Aegean Sea and Surrounding Regions. Geophysical Journal of the Royal Astronomical Society, 55, 217–52.

[65] Mertoğlu, O., Şimşek, Ş., Dağıstan, H., Bakır, N. and Doğdu, N., (2010), Geothermal Country Update Report of Turkey (2005-2010). Proceedings World Geothermal Congress 2010, Bali, Indonesia.

[66] Michard, G., (1991). The Physical Chemistry of Geothermal Systems. In: F. D'Amore (co-ordinator) Application of Geochemistry in Geothermal Reservoir Development. UNITAR-UNDP Publication, Rome, 197-214.

[67] Mutlu, H. and Güleç N., (1998). Hydrogeochemical Outline of Thermal Waters and Geothermometry Applications in Anatolia (Turkey). Journal of Volcanology and Geothermal Research, 85, 495–515.

[68] Okay, A. I. and Satır, M., (2000). Coeval plutonism and metamorphism in a latest Oligocene metamorphic core complex in northwest Turkey. Geological Magazine, 137, 495–516.

[69] Ozan, Z. Ö., (2007). Kızıldere (Denizli) ve Ömerbeyli (Aydın) Jeotermal Alanında Gelişen Hidrotermal Alterasyon Minerallerinin İncelenmesi. Hacettepe Üniversitesi Fen Bilimleri Enstitüsü Yüksek Lisans Tezi, Ankara, Türkiye.

[70] Öngür, T., (2010). Geologic and Thermal Evolution of Turkeys Wealthy Geothermal Region, MMM. Proceedings World Geothermal Congress 2010, Bali, Indonesia.

[71] Özdemir, K., Babaeren, F., Göçmez, A., Çetinkaya, Z. and Saygılı, U., (2012). Jeotermal Enerjinin Seracılıkta Kullanımının Önündeki Engellerin Tespiti Projesi Araştırma Raporu 2012. T.C. Güney Ege Development Agency.

[72] Özgür, N., Pekdeğer, A., Wolf, M., Stichler, W., Seiler, K.P. and Satir, M., (1998). Hydrogeochemical and Isotope Geochemical Features of the Thermal Waters of Kizildere, Salavatli, and Germencik in the Rift Zone of the Büyük Menderes, Western Anatolia, Turkey: Preliminary studies. Water-Rock Interaction, Arehart & Hutston(eds), Balkema, Rotterdam.

[73] Özgür, N., (2003). Active Geothermal Systems in the Rift Zone of the Büyük Menderes, Western Anatolia, Turkey. European Geothermal Conference, Szeged, Hungary.

[74] Özgür, N., (2010). Hydrogeological, Hydrogeochemical and Isotope Geochemical Modeling of the Thermal Waters in the Continental Rift Zones of the Menderes Massif, Western Anatolia, Turkey. Proceedings World Geothermal Congress 2010, Bali, Indonesia.

[75] Özkaya, M., (2007). Numerical Modelling of Kızıldere Geothermal Field. M.Sc. Thesis, Middle East Technical University, Ankara, Turkey.

[76] Özler, H. M., (2000). Hydrogeology and geochemistry in the Çürüksu (Denizli) hydrothermal field, Western Turkey. Environmental Geology, 39 (10), 1169–1180.

[77] Purtul, E., (2010). Aydın-Nazilli-Bozyurt NB-1 Sıcak Su Sondajı Kuyu Bitirme Raporu. MTA report, No. 11308 (in Turkish).

[78] Rojay, B., Toprak, V., Demirci, C. and Süzen, L., (2005). Plio-Quaternary evolution of the Küçük Menderes Graben (Southwestern Anatolia, Turkey). Geodinamica Acta 18/3-4, 317–331.

[79] Satman, A., Serpen, U. and Mihcakan, İ, M., (2000). Assessment of Reinjection Trials in Kızıldere Geothermal Reservoir. Proceedings World Geothermal Congress, Kyushu-Tohoku, Japan.

[80] Serpen, U., Yamanlar, Ş. and Karamanderesi, İ. H., (2000). Estimation of Geothermal Potential of Büyük Menderes Region in Turkey. Proceedings World Geothermal Congress, Kyushu-Tohoku, Japan.

[81] Serpen, U., Balat, M. and Aksoy, N., (2006). Assessment of Well Tests in Salavatlı-Sultanhisar Geothermal Field of Turkey. Proceedings, 31st Workshop on Geothermal Reservoir Engineering, Stanford University, Stanford, California.

[82] Serpen, U. and Aksoy, N., (2010). Reassessment of Reinjection in Salavatli-Sultanhisar Field of Turkey. Proceedings World Geothermal Congress 2010, Bali, Indonesia.

[83] Seyitoğlu G. and Scott B., (1992). The Age of the Büyük Menderes Graben (Western Turkey) and Its Tectonic Implications. Geological Magazine, 129, 239–242.

[84] Seyitoğlu G., Işık, V. and Çemen, İ., (2004). Complete Tertiary exhumation history of the Menderes Massif, Western Turkey: an alternative working hypothesis. Terra Nova, 16, 358–63.

[85] Söğüt, A. R., (2011). Source, Characterictics and Some Geological Features of the Thermal Waters of Hıdırbeyli Region, Aydın, Turkey. International Journal of the Physical Sciences, 6(8), 2027-2036.

[86] Stefansson, V. and Fridleifsson, I. B., (1998). Geothermal Energy - European and Worldwide Perspective. Presented at Expert hearing on Assessment and Prospects for Geothermal Energy in Europe, SubCommittee on Technology Policy and Energy of the Parliamentary Assembly of the Council of Europe, Strasbourg, France, 10.

[87] Süer, S., (2010). Geochemical Monitoring of the Seismic Activities and Noble Gas Characterization of the Geothermal Fields Along the Eastern Segment of the Büyük Menderes Graben. Ph.D. Thesis, Middle East Technical University, Ankara, Turkey.

[88] Şimşek, Ş., (1984). Denizli, Kızıldere-Tekkehamam-Tosunlar-Buldan-Yenice alanının jeolojisi ve jeotermal enerji olanakları. MTA report, No. 7846 (in Turkish).

[89] Şimşek, Ş., (2003a). Hydrogeological and Isotopic Survey of Geothermal Fields in the Büyük Menderes Graben, Turkey. Geothermics, 32, 669-678.

[90] Şimşek, Ş., (2003b). Present Status and Future Development Possibilities of Aydın-Denizli Geothermal Province. International Geothermal Conference, Reykjavík.

[91] Şimşek, S., Yıldırım, N. and Gülgör, A., (2005). Development and Environmental Effects of the Kızıldere Geothermal Power Project, Turkey. Geothermics, 34, 239-256.

[92] Tamgaç, Ö. F., (2010). Denizli-Gölemezli DG-1 Sıcak Su Sondajı Kuyu Bitirme Raporu. MTA report, No. 11257 (in Turkish).

[93] Tarcan, G., Filiz, S. and Gemici, Ü., (2000). Davutlar Kaplıcası (Kuşadası-Aydın) Çevresinin Hidrojeolojisi ve Hidrojeokimyası. Dokuz Eylül University Mühendislik Fakültesi, Fen ve Mühendislik Dergisi, 2(1), 91–110.

[94] Tarcan, G., (2005). Mineral Saturation and Scaling Tendencies of Waters Discharged from Wells (>150 ^{o}C) in Geothermal Areas of Turkey. Journal of Volcanology and Geothermal Research, 142, 263–283.

[95] Taymaz, T., Jackson, J. and Mckenzie, D., (1991). Active Tectonics of the North and Central Aegean Sea. Geophysical Journal International, 106, 433–90.

[96] Tekin, S., (2010). Estimation of the Formation Temperature from the Inlet and Outlet Mud Temperatures While Drilling Geothermal Formations. M.Sc. Thesis, Middle East Technical University, Ankara, Turkey.

[97] Toka, B. and Parlaktuna, M., (2010). On the Renewability of Geothermal Resources in Turkey. Proceedings World Geothermal Congress 2010, Bali, Indonesia.

[98] Toksoy, M. and Aksoy, N., (2003). Aydın Jeotermal Gelişme Projesi. İzmir Institute of Technology, Geocen, Report No. 8 (in Turkish).

[99] Turalı, Ü. and Karahan, Ç., (2009). Aydın Atça AT-2 Sıcaksu Sondajı Kuyu Bitirme Raporu. MTA report, No. 11184 (in Turkish).

[100] Uysal, E., (2002). Kuşadası (Aydın) Çevresinin Hidrojeolojik İncelenmesi. Dokuz Eylül Üniversitesi Fen Bilimleri Enstitüsü Yüksek Lisans Tezi, İzmir, Türkiye.

[101] Vengosh, A., Helvacı, C. and Karamanderesi, İ. H., (2002). Geochemical Constraints for the Origin of Thermal Waters from Western Turkey. Applied Geochemistry, 17, 163-183.

[102] Whitney, D. L. and Bozkurt, E., (2002). Metamorphic history of the southern Menderes Massif, western Turkey. Geol. Soc. Am. Bull., 114(7), 829–838.

[103] Yeltekin, K., Parlaktuna, M. and Akın, S., (2002). Modeling of Kızıldere Geothermal Reservoir, Turkey. 27th Workshop on Geothermal Reservoir Engineering, Stanford University, Stanford, California.

[104] Yeltekin, K. and Parlaktuna, M., (2006). Interpretation of Reinjection Tests in Kızıldere Geothermal Field, Turkey. Proceedings, 31st Workshop on Geothermal Reservoir Engineering, Stanford University, Stanford, California.

[105] Yeltekin, K. and Akın, S., (2006). Analysis of Long Term Tracer Test in Kızıldere Geothermal Field, Turkey. Proceedings, 31st Workshop on Geothermal Reservoir Engineering, Stanford University, Stanford, California.

[106] Yılmaz, Y., Genç, S.C., Gürer, O.F., Bozcu, M., Yılmaz, K., Karacık, Z., Altunkaynak, I. and Elmas, A., (2000). When did the western Anatolian grabens begin to develop?. in Bozkurt, E., Winchester, J.A., and Piper, J.D.A., eds., Tectonics and magmatism in Turkey and the surrounding area: Geological Society of London Special Publication, 173, 353–384.

[107] Yıldırım, N., Uygur, N., Ölmez, E., Çiçekli, K. and Akıllı, H., (2001). Denizli Kızıldere R 2 No'lu Reenjeksiyon Kuyu Bitirme Raporu. MTA report, No. 10527 (in Turkish).

[108] Yıldırım, N., Önc, S. and Akman, U. A., (2010). High Enthalpy Geothermal Potential Possibility in SW of Büyük Menderes Graben, Turkey. Proceedings World Geothermal Congress 2010, Bali, Indonesia.

[109] Yolal, A., (2010). Aydın Pamukören AP-2 Jeotermal Sondajı Kuyu Bitirme Raporu. MTA report, No. 11281 (in Turkish).

[110] Yolal, A. and Karahan, Ç., (2010a). Aydın Pamukören AP-3 Jeotermal Sondajı Kuyu Bitirme Raporu. MTA report, No. 11280 (in Turkish).

[111] Yolal, A. and Karahan, Ç., (2010b). Aydın Yılmazköy AY 2 Jeotermal Sondajı Kuyu Bitirme Raporu. MTA report, No. 11350 (in Turkish).

[112] Yurttaş, Ö., (2008). Ilıcabaşı Jeotermal Alanının (Aydın) Hidrojeolojisi. Dokuz Eylül Üniversitesi Fen Bilimleri Enstitüsü Yüksek Lisans Tezi, İzmir, Türkiye.

APPENDIX A

ANALYZED DATA OF WELL DEPTH AND TEMPERATURE

Table A 1: Analyzed data of well depth and temperature.

Data Compiled From	Geothermal Field	City	Well Name	Drilling Year	Well Depths (m)	Well Dist. to Sea (km)	Res. Tem. (°C)	Bottomhole Temp. (°C)
Gökgöz, et al., (2010). Hydrogeology and Environmental Study at the Karahayit Geothermal Field (Western Turkey).	Karahayıt	Denizli	KH 1	2007	**452**	**165,00**	**58**	
Gökgöz, et al., (2010). Hydrogeology and Environmental Study at the Karahayit Geothermal Field (Western Turkey).	Karahayıt	Denizli	KH 2	2007	**468**	**164,33**	**58**	
Gökgöz, et al., (2010). Hydrogeology and Environmental Study at the Karahayit Geothermal Field (Western Turkey).	Karahayıt	Denizli	KH 3	2007	**570**	**163,67**	**61.5**	
Tamgaç,(2010). Denizli-Gölemezli DG-1 Sıcak Su Sondaji Kuyu Bitirme Raporu.	Gölemezli	Denizli	DG 1	2001	1500	**156,67**	**95,48 (static temp. At 1289 m)**	
Tamgaç,(2010). Denizli-Gölemezli DG-1 Sıcak Su Sondaji Kuyu Bitirme Raporu.	Gölemezli	Denizli	DG 2	2002	**596,8**	**157,73**	**73,00**	
Kahraman, (2003). Denizli Gölemezli Jeotermal Alanı DG-3 ve DG-5 Sondajları Kuyu Bitirme Raporu.	Gölemezli	Denizli	DG 3	2003	**549**	**157,80**	**66,00**	
Tamgaç,(2010). Denizli-Gölemezli DG-1 Sıcak Su Sondaji Kuyu Bitirme Raporu.	Gölemezli	Denizli	DG 4	2003	**750**	**157,83**	**70,00**	
Kahraman, (2003). Denizli Gölemezli Jeotermal Alanı DG-3 ve DG-5 Sondajları Kuyu Bitirme Raporu.	Gölemezli	Denizli	DG 5	2003	**750**	**157,77**	**62,00**	
Şimşek, (2003). Present Status and Future Development Possibilities of Aydın-Denizli Geothermal Province.	Yenice	Denizli	Yenice	2002	**54,00**	**149,00**	**53,00**	
Şimşek, (2003). Present Status and Future Development Possibilities of Aydın-Denizli Geothermal Province.	Yenice	Denizli	Yenice	2002	**238,00**	**149,00**	**63,00**	
Şimşek, (2003). Present Status and Future Development Possibilities of Aydın-Denizli Geothermal Province.	Yenice	Denizli	Yenice	2002	**250,00**	**149,00**	**38,00**	
Karamanderesi & Ölçenoğlu, (2005). Geology of the Denizli Sarayköy (Gerali) Geothermal Field, Western Anatolia, Turkey.	Gerali	Denizli	MDO-1	2003	2401	**148,33**	**96 (1st reservoir) at 814 m**	125 °C
Karamanderesi & Ölçenoğlu, (2005). Geology of the Denizli Sarayköy (Gerali) Geothermal Field, Western Anatolia, Turkey.	Gerali	Denizli	MDO-1a	2003	2401	**148,33**	**125 (2nd reservoir) at 1143 m**	125 °C
Beyazıt, et al., (2010). Denizli-Sarayköy-Gerali Jeotermal Sondaj Kampı DSG 2010/4 Kuyusu Bitirme Raporu.	Gerali	Denizli	DSG 4	2010	2202	**146,67**	**117,98 (static temp. At 2171 m)**	
Süer, (2010). Geochemical Monitoring of the Seismic Activities and Noble Gas Characterization of the Geothermal Fields Along the Eastern Segment of the Büyük Menderes Graben.	Tekkehamam-Sarayköy	Denizli	TH1	1968	**615,5**	**136,67**		**116**
Süer, (2010). Geochemical Monitoring of the Seismic Activities and Noble Gas Characterization of the Geothermal Fields Along the Eastern Segment of the Büyük Menderes Graben.	Tekkehamam-Sarayköy	Denizli	TH2	1997	**2001**	**137,00**		**170**
Süer, (2010). Geochemical Monitoring of the Seismic Activities and Noble Gas Characterization of the Geothermal Fields Along the Eastern Segment of the Büyük Menderes Graben.	Tekkehamam-Sarayköy	Denizli	KB 1	2001	**115**	**136,67**		**120**
Süer, (2010). Geochemical Monitoring of the Seismic Activities and Noble Gas Characterization of the Geothermal Fields Along the Eastern Segment of the Büyük Menderes Graben.	Tekkehamam-Sarayköy	Denizli	KB 2	2001	**202**	**136,67**		**100**
Süer, (2010). Geochemical Monitoring of the Seismic Activities and Noble Gas Characterization of the Geothermal Fields Along the Eastern Segment of the Büyük Menderes Graben.	Tekkehamam-Sarayköy	Denizli	KB 3	2002	**161**	**136,67**		**100**
Süer, (2010). Geochemical Monitoring of the Seismic Activities and Noble Gas Characterization of the Geothermal Fields Along the Eastern Segment of the Büyük Menderes Graben.	Tekkehamam-Sarayköy	Denizli	KB 4	2002	**253**	**136,67**		**100**

Bold writtens are used in the analyses.

Table A 1: Continued.

Data Compiled From	Geothermal Field	City	Well Name	Drilling Year	Well Depths (m)	Well Dist. to Sea (km)	Res. Tem. (°C)	Bottomhole Temp. (°C)
Özkaya, (2007). Numerical Modelling of Kızıldere Geothermal Field.	Kızıldere	Denizli	KD-1	1968	**540**	**137,18**		**203**
a) Kindap, et al., (2010). Privatization of Kizildere Geothermal Power Plant and New Approaches for Field and Plant. b) Özkaya, (2007). Numerical Modelling of Kızıldere Geothermal Field.	Kızıldere	Denizli	KD-2	1968 (a)	**706,5 (a)**	**136,87**		**175 (b)**
Kindap, et al., (2010). Privatization of Kizildere Geothermal Power Plant and New Approaches for Field and Plant.	Kızıldere	Denizli	KD-3	1969	**370**	**136,83**	**158**	
a) Kindap, et al., (2010). Privatization of Kizildere Geothermal Power Plant and New Approaches for Field and Plant. b) Özkaya, (2007). Numerical Modelling of Kızıldere Geothermal Field.	Kızıldere	Denizli	KD-4	1969 (a)	**486 (a)**	**138,19**		**166 (b)**
a) Kindap, et al., (2010). Privatization of Kizildere Geothermal Power Plant and New Approaches for Field and Plant. b) Özkaya, (2007). Numerical Modelling of Kızıldere Geothermal Field.	Kızıldere	Denizli	KD-1A	1969 (a)	**571,1 (a)**	**137,19**		**198 (b)**
Kindap, et al., (2010). Privatization of Kizildere Geothermal Power Plant and New Approaches for Field and Plant.	Kızıldere	Denizli	KD-111	1969	**504,85**	**137,19**	**164**	
Özkaya, (2007). Numerical Modelling of Kızıldere Geothermal Field.	Kızıldere	Denizli	KD-6	1970	**851**	**137,20**		**196**
a) Kindap, et al., (2010). Privatization of Kizildere Geothermal Power Plant and New Approaches for Field and Plant. b) Özkaya, (2007). Numerical Modelling of Kızıldere Geothermal Field.	Kızıldere	Denizli	KD-7	1971 (a)	**667 (a)**	**137,20**		**204 (b)**
a) Kindap, et al., (2010). Privatization of Kizildere Geothermal Power Plant and New Approaches for Field and Plant. b) Özkaya, (2007). Numerical Modelling of Kızıldere Geothermal Field.	Kızıldere	Denizli	KD-8	1970 (a)	**576,5 (a)**	**137,22**		**193 (b)**
Özkaya, (2007). Numerical Modelling of Kızıldere Geothermal Field.	Kızıldere	Denizli	KD-9	1970	**1241**	**137,17**		**170**
a) Kindap, et al., (2010). Privatization of Kizildere Geothermal Power Plant and New Approaches for Field and Plant. b) Özkaya, (2007). Numerical Modelling of Kızıldere Geothermal Field.	Kızıldere	Denizli	KD-12	1970 (a)	**404,7 (a)**	**138,17**		**160 (b)**
a) Kaya & Kindap, (2009). Kızıldere – New Geothermal Power Plant in Turkey. b) Kindap, et al., (2010). Privatization of Kizildere Geothermal Power Plant and New Approaches for Field and Plant.	Kızıldere	Denizli	KD-13	1971(b)	**763 (a)**	**137,20**		**195 (a)**
a) Kaya & Kindap, (2009). Kızıldere – New Geothermal Power Plant in Turkey. b) Kindap, et al., (2010). Privatization of Kizildere Geothermal Power Plant and New Approaches for Field and Plant.	Kızıldere	Denizli	KD-14	1970 (b)	**597 (a)**	**137,21**		**207 (a)**
a) Kaya & Kindap, (2009). Kızıldere – New Geothermal Power Plant in Turkey. b) Kindap, et al., (2010). Privatization of Kizildere Geothermal Power Plant and New Approaches for Field and Plant.	Kızıldere	Denizli	KD-15	1971(b)	**510 (a)**	**137,22**		**205 (a)**
a) Kaya & Kindap, (2009). Kızıldere – New Geothermal Power Plant in Turkey. b) Özkaya, (2007). Numerical Modelling of Kızıldere Geothermal Field.	Kızıldere	Denizli	KD16	1973(b)	**666 (a)**	**137,21**		**207 (b)**
Kindap, et al., (2010). Privatization of Kizildere Geothermal Power Plant and New Approaches for Field and Plant.	Kızıldere	Denizli	KD-17	1975	**365,2**	**137,22**	**157**	
a) Kaya & Kindap, (2009). Kızıldere – New Geothermal Power Plant in Turkey. b) Kindap, et al., (2010). Privatization of Kizildere Geothermal Power Plant and New Approaches for Field and Plant.	Kızıldere	Denizli	KD-20	1986(b)	**810 (a)**	**137,20**		**201 (a)**
a) Kaya & Kindap, (2009). Kızıldere – New Geothermal Power Plant in Turkey. b) Kindap, et al., (2010). Privatization of Kizildere Geothermal Power Plant and New Approaches for Field and Plant.	Kızıldere	Denizli	KD-21	1985(b)	**898 (a)**	**137,21**		**202 (a)**
a) Kaya & Kindap, (2009). Kızıldere – New Geothermal Power Plant in Turkey. b) Kindap, et al., (2010). Privatization of Kizildere Geothermal Power Plant and New Approaches for Field and Plant.	Kızıldere	Denizli	KD-22	1985(b)	**888 (a)**	**137,20**	**201 (b)**	

Table A 1: Continued.

Data Compiled From	Geothermal Field	City	Well Name	Drilling Year	Well Depths (m)	Well Dist. to Sea (km)	Res. Tem. (°C)	Bottomhole Temp. (°C)
Kindap, et al., (2010). Privatization of Kizildere Geothermal Power Plant and New Approaches for Field and Plant.	Kızıldere	Denizli	R1	1998	**2260**	**137,00**	**242**	
Yeltekin & Akın, (2006). Analysis of Long Term Tracer Test in Kızıldere Geothermal Field, Turkey.	Kızıldere	Denizli	R-2	1999	**1371,89**	**137,20**		**204**
Demirel, et al., (2007). Denizli Kizildere R-3 No'lu Reenjeksion Kuyu Bitirme Raporu.	Kızıldere	Denizli	R3		**2250**	**137,20**	**241**	
Yolal, (2010). Aydın Pamukören AP-2 Jeotermal Sondaji Kuyu Bitirme Raporu.	Pamukören	Aydın	AP 2	2008	1150 m	**112,60**	**182,41(dynamic temp. At 1090 m)**	171,32 °C at 1000 m (thermic log)
Yolal & Karahan, (2010). Aydın Pamukören AP-3 Jeotermal Sondaji Kuyu Bitirme Raporu.	Pamukören	Aydın	AP 3	2009	1052 m	**112,67**	**182,79 (dynamic temp. At 925 m)**	161, 4 at 1010 m (thermic log)
Karahan, (2010). Aydın-Nazilli Güzelköy NG–1 Jeotermal Sondaji Kuyu Bitirme Raporu.	Güzelköy	Aydın	NG 1	2008	2200 m	**102,67**	**127,36 (dynamic temp. At 2152 m)**	122,5 °C at 2197 m (thermic log)
Purtul, (2010). Aydın-Nazilli-Bozyurt NB-1 Sıcak Su Sondaji Kuyu Bitirme Raporu.	Bozyurt	Aydın	NB 1	2009	1900 m	**99,33**	**140,31 (dynamic temp. At 1829 m)**	135,7 °C at 1899 m (thermic log)
Karahan & Güdücü, (2008). Aydın Atça AT-1 Sıcaksu Sondaji Kuyu Bitirme Raporu.	Atça	Aydın	AT 1		1200	**88,33**	**123,64 at 1186 m (static temp.)**	
Turalı & Karahan, (2009). Aydın Atça AT-2 Sıcaksu Sondaji Kuyu Bitirme Raporu.	Atça	Aydın	AT 2		782	**88,33**	**122,90 at 700 m (static temp.)**	
Karahan, (2010). Aydın-İsabeyli İS-1 Sıcak Su Sondaji Kuyu Bitirme Raporu.	İsabeyli	Aydın	İS 1	2008	1150 m	**88,67**	**88,3 at 1150 m (static temp.)**	90,2 (thermic log)
Karahan, (2007). Aydın Sultanhisar SH-1 ve SH-2 Sıcak Su Sondajları Kuyu Bitirme Raporu.	Sultanhisar	Aydın	SH 1	2005	**988,00**	**80,00**	**144,86**	
Karahan, (2007). Aydın Sultanhisar SH-1 ve SH-2 Sıcak Su Sondajları Kuyu Bitirme Raporu.	Sultanhisar	Aydın	SH 2	2005	**986,00**	**81,33**	**146,01**	
Serpen & Aksoy, (2010). Reassessment of Reinjection in Salavatli-Sultanhisar Field of Turkey.	Salavatlı	Aydın	ASR 1	2007	**1430**	**71,67**	**150**	
(a) Serpen & Aksoy, (2010). Reassessment of Reinjection in Salavatli-Sultanhisar Field of Turkey. (b) Demirel & Beker, (2005). Aydın-Salavatlı ASR-2 Reenjeksiyon Kuyusu Kuyu Bitirme Raporu.	Salavatlı	Aydın	ASR 2	2007	1300 (a)	**71,33**	**165 (static Temp. at 900 m) (b)**	
Bülbül, (2008). Aydın-Salavatlı ASR-3 Reenjeksiyon Kuyusu Bitirme Raporu.	Salavatlı	Aydın / Sultanhisa	ASR 3	2008	1250,5 m	**73,67**	**169,42 (static temp. At 900 m)**	max. 140
(a) Serpen & Aksoy, (2010). Reassessment of Reinjection in Salavatli-Sultanhisar Field of Turkey. (b) Karamanderesi, (1987). Aydın Sultanhisar Salavatlı Jeotermal Sahası AS 1 ve AS 2 Kuyularının Bölgesel Değerlendirme Raporu.	Salavatlı	Aydın	AS 1	1987	1500 (a)	**73,00**	**169,77 (static temp. At 850 m) (b)**	
(a) Serpen & Aksoy, (2010). Reassessment of Reinjection in Salavatli-Sultanhisar Field of Turkey. (b) Karamanderesi, (1987). Aydın Sultanhisar Salavatlı Jeotermal Sahası AS 1 ve AS 2 Kuyularının Bölgesel Değerlendirme Raporu.	Salavatlı	Aydın	AS 2	1988	**960 (a)**	**70,33**		**175,5 (b)**
Mineral Research & Exploration General Directorate, Department of Energy Raw Material Research and Exploration. Annual Report of 2011.	Sultanhisar	Aydın	ASMM 5	2011	**750**	**83,33**	**128**	
Karahan & Dönmez, (2009). Aydın-Umurlu AU-1 Jeotermal Sondajı Kuyu Bitirme Raporu.	Umurlu	Aydın	AU 1	2008	1223	**66,17**	**154,39 (static temp. At 1211 m)**	
Karahan,et al., (2009). Aydın-Umurlu AU-2 Jeotermal Sondajı Kuyu Bitirme Raporu.	Umurlu	Aydın	AU 2	2008	1602	**66,33**	**149,58 (dynamic temp. At 1582 m)**	130,6 (Termik prob)
Karahan & Güdücü, (2008). Aydın Serçeköy ASK-1 Sıcaksu Sondaji Kuyu Bitirme Raporu.	Umurlu	Aydın	ASK 1	2008	2054	**66,00**	**154,48 (static temp. At 2000 m)**	
Candaş, (2002). Hydrogeochemical Study of Aydın Geothermal Fields.	İmamköy	Aydın	İmamköy		**1300**	**61,67**	**160,00**	
Candaş, (2002). Hydrogeochemical Study of Aydın Geothermal Fields.	Yılmazköy	Aydın	Yılmazköy		**1100**	**60,00**	**160,00**	
Toksoy & Aksoy, (2003). Aydın Jeotermal Gelişme Projesi.	Yılmazköy	Aydın	AY 1	1999	**1501**	**60,67**	**142**	
Yolal & Karahan, (2010). Aydın Yılmazköy AY 2 Jeotermal Sondaji Kuyu Bitirme Raporu.	Yılmazköy	Aydın	AY 2	2009	**2500**	**61,00**	**190**	
Candaş, (2002). Hydrogeochemical Study of Aydın Geothermal Fields.	Ilıcabaşı	Aydın	Ayter 1	1989	**471**	**60,00**	**84,50**	
Candaş, (2002). Hydrogeochemical Study of Aydın Geothermal Fields.	Ilıcabaşı	Aydın	Ayter 2	1989	**355**	**60,33**	**101,50**	
Candaş, K. M., 2002, Hydrogeochemical Study of Aydın Geothermal Fields.			DSİ 1		**200**	**59,67**	**100**	
Candaş, (2002). Hydrogeochemical Study of Aydın Geothermal Fields.			DSİ 2		**200**	**59,33**	**100**	
Ceyhan, (2000). Aydın Alangüllü Boğazköy Sıcaksu Sondajı A 2 Kuyu Bitirme Raporu.	Alangüllü	Aydın	A 2	2000	488 m	**38,33**	**102,8 at 480 m (thermic log)**	102,8
Filiz, et al., (2000). Geochemistry of the Germencik Geothermal Fields, Turkey.	Ömerbeyli	Aydın	OB1	1982	**1000**	**36,67**	**203**	
Filiz, et al., (2000). Geochemistry of the Germencik Geothermal Fields, Turkey.	Ömerbeyli	Aydın	OB2	1982	**975,5**	**37,00**	**231**	

Table A 1: Continued.

Data Compiled From	Geothermal Field	City	Well Name	Drilling Year	Well Depths (m)	Well Dist. to Sea (km)	Res. Tem. (°C)	Bottomhole Temp. (°C)
a) Karakuş, (2010), Investigation of Geothermal Systems in Büyük Menderes Graben by Using Geochemical and Isotopic Techniques b) Filiz, et al., (2000). Geochemistry of the Germencik Geothermal Fields, Turkey.	Ömerbeyli	Aydın	OB3	1983	**1196,7 (b)**	**36,33**	**232 (a)**	
Filiz, et al., (2000). Geochemistry of the Germencik Geothermal Fields, Turkey.	Ömerbeyli	Aydın	OB4	1984	**285**	**37,33**	**213**	
Filiz, et al., (2000). Geochemistry of the Germencik Geothermal Fields, Turkey.	Ömerbeyli	Aydın	OB5	1984	**1302**	**37,67**	**221**	
Filiz, et al., (2000). Geochemistry of the Germencik Geothermal Fields, Turkey.	Ömerbeyli	Aydın	OB6	1984	**1100**	**36,60**	**221**	
a) Karakuş, (2010), Investigation of Geothermal Systems in Büyük Menderes Graben by Using Geochemical and Isotopic Techniques b) Filiz, et al., (2000). Geochemistry of the Germencik Geothermal Fields, Turkey.	Ömerbeyli	Aydın	OB7	1985(b)	**2398 (b)**	**36,20**	**227 (a)**	
a) Karakuş, (2010), Investigation of Geothermal Systems in Büyük Menderes Graben by Using Geochemical and Isotopic Techniques b) Filiz, et al., (2000). Geochemistry of the Germencik Geothermal Fields, Turkey.	Ömerbeyli	Aydın	OB8	1986	**2000 (a)**	**36,83**	**219.87 (b)**	
Filiz, et al., (2000). Geochemistry of the Germencik Geothermal Fields, Turkey.	Ömerbeyli	Aydın	OB9	1986	**1464,7**	**36,90**	**223.8**	
Tekin, (2010). Estimation of the Formation Temperature from the Inlet and Outlet Mud Temperatures While Drilling Geothermal Formations.	Ömerbeyli	Aydın	ÖB-10	between 2007 and 2008	**1524**	**36,67**	**224**	
Tekin, (2010). Estimation of the Formation Temperature from the Inlet and Outlet Mud Temperatures While Drilling Geothermal Formations.	Ömerbeyli	Aydın	ÖB-11	between 2007 and 2008	**965**	**36,00**	**210**	
Tekin, (2010). Estimation of the Formation Temperature from the Inlet and Outlet Mud Temperatures While Drilling Geothermal Formations.	Ömerbeyli	Aydın	ÖB-14	between 2007 and 2008	**1205**	**35,33**	**228**	
Tekin, (2010). Estimation of the Formation Temperature from the Inlet and Outlet Mud Temperatures While Drilling Geothermal Formations.	Ömerbeyli	Aydın	ÖB-17	between 2007 and 2008	**1706**	**34,67**	**228**	
Tekin, (2010). Estimation of the Formation Temperature from the Inlet and Outlet Mud Temperatures While Drilling Geothermal Formations.	Ömerbeyli	Aydın	ÖB-19	between 2007 and 2008	**1651**	**33,33**	**227**	
Tekin, (2010). Estimation of the Formation Temperature from the Inlet and Outlet Mud Temperatures While Drilling Geothermal Formations.	Alangüllü	Aydın	AG-22	between 2007 and 2008	**2260**	**31,67**	**205**	
Tekin, (2010). Estimation of the Formation Temperature from the Inlet and Outlet Mud Temperatures While Drilling Geothermal Formations.	Alangüllü	Aydın	AG-24	between 2007 and 2008	**1252**	**31,33**	**199**	
Tekin, (2010). Estimation of the Formation Temperature from the Inlet and Outlet Mud Temperatures While Drilling Geothermal Formations.	Alangüllü	Aydın	AG-25	between 2007 and 2008	**1838**	**30,33**	**191**	
Tekin, (2010). Estimation of the Formation Temperature from the Inlet and Outlet Mud Temperatures While Drilling Geothermal Formations.	Alangüllü	Aydın	AG-26	between 2007 and 2008	**2432**	**30,00**	**195**	
Karahan, (2008). Aydın-Hıdırbeyli HB-1 ve HB-2 Sıcak Su Sondajlari Kuyu Bitirme Raporu	Hıdırbeyli	Aydın	HB 1	2007	882 m	**27,00**	**120,54 at 873 m(dynamic temp.)**	
Karahan, (2008). Aydın-Hıdırbeyli HB-1 ve HB-2 Sıcak Su Sondajlari Kuyu Bitirme Raporu	Hıdırbeyli	Aydın	HB 2	2007	596,30 m	**26,67**	**141,78 at 280m (dynamic temp.)**	
Maren A.Ş. 2011. Personal communication.	Hıdırbeyli	Aydın	HB 7		**2149,39**	**26,83**	**169,10**	
Maren A.Ş. 2011. Personal communication.	Gümüşköy	Aydın	GM 1		**1934,45**	**26,77**	**174,00**	
Maren A.Ş. 2011. Personal communication.	Gümüşköy	Aydın	GM 2		**2046,00**	**27,10**	**167,73**	
MTA report	Gümüşköy	Aydın	GK 1		**2100,00**	**24,00**	**178,00**	
Çağlayan & Dünya, (2012). Aydın-Germencik-Gümüşköy AGG 2010/16 Jeotermal Enerji Araştırma Sondajı Kuyu Bitirme Raporu.	Gümüşköy	Aydın	AGG 16	2011	1252,5	**8,33**	**66,15 at 1180 (dynamic T)**	63,4
Uysal, (2002). Kuşadası (Aydın) Çevresinin Hidrojeolojik İncelenmesi.	Davutlar	Aydın	Davutlar		**203,00**	**6,67**	**43,00**	
Bali, (2010). Aydın-Kuşadası-Davutlar AKD 2010/2 Kuyusu Kamp Bitirme Raporu.	Davutlar	Aydın	AKD 2	2010	815 m	**6,67**	**58 (dynamic temp. At 785 m)**	

APPENDIX B

ANALYZED DATA OF GEOCHEMICAL COMPOUNDS

Table B 1: Analyzed data of geochemical compounds.

Well Name	Na (mg/l)	K (mg/l)	Ca (mg/l)	Mg (mg/l)	NH_4 (mg/l)	Cl (mg/l)	HCO_3 (mg/l)	SO_4 (mg/l)	B (mg/l)	SiO_2 (mg/l)	TDS (mg/l)	pH	EC (µS/cm)	Water Type	Water origin
KH 1	108,00	17,80	484,40	105,60	3,89	26,90	1329,80	971,70			3671,320	7,00	3110,00	Ca-HCO_3-SO_4	meteoric
KH 2	120,00	22,40	563,00	132,40	3,50	25,30	1305,40	837,60			3217,385	7,80	2990,00	Ca-HCO_3-SO_4	meteoric
KH 3	116,80	23,60	505,20	117,20	1,00	24,50	9644,00	863,00			11602,243	7,00	2730,00	Ca-SO_4-HCO_3	meteoric
DG 1	750,00	140,00	66,50	71,70	1,50	32,80	2006,00	634,00	6,80	48,00	3957,83	7,22	4227,25	Na-HCO_3-SO_4	meteoric
DG 2	245,00	50,50	106,00	111,00	0,00	54,70	544,00	651,00	6,30	73,10	1864,74	7,60	2030,00	Mg-Na-HCO_3-SO_4	meteoric
DG 3	240,00	72,60	219,00	92,80	2,96	31,40	1361,00	485,00	3,10	39,00	2719,83	7,10	2220,00	Mg-Ca-Na-HCO_3-SO_4	meteoric
DG 4	243,00	112,00	222,00	76,90	2,60	27,50	1243,00	471,00	4,30	396,82	2850,82	6,70	695,85	Mg-Ca-Na-HCO_3-SO_4	meteoric
DG 5	315,00	80,10	377,00	152,50	9,42	87,40	1653,00	635,00	6,50	53,50	4033,76	6,60	3120,00	Mg-Ca-Na-HCO_3-SO_4	meteoric
MDO-1	240,00	72,60	219,00	92,80	2,96	31,40	1361,00	485,00	3,10	39,00	2556,86	7,10	2220,00		meteoric
TH 1	530,00	64,00	217,00	53,00	5,80	90,00	1068,00	1070,00		190,00	3291,20	6,30	2600,00	Na-(SO_4)-HCO_3	meteoric
TH 2	1240,00	120,00	2,00	1,20		112,00	1335,00	727,00	3,10	177,00		9,40	4800,00		
KD-1	1468,00	174,30	2,77	0,70		120,50	2183,00	847,00	29,70	227,00	5436,47	8,80			meteoric
KD-6	1220,00	116,00	1,20	0,36		124,00	1586,00	560,00	20,40	364,00	1859,00	8,97	5830,00		
KD-9	1260,00	80,00	8,00	5,80		137,00	1342,00	1180,00	3,60	277,00		8,80	4810,00		
KD-13	1125,00	132,50	2,00	0,25		128,00	1525,00	773,00	26,50	364,00	4264,12	8,89	5940,00		
KD-14	1342,00	143,00	1,00	0,00		144,00	2403,00	737,00	24,40	392,00	3698,00	8,96	6160,00		
KD-15	1364,00	136,00	2,00	0,00		140,00	1464,00	730,00	24,60	393,00	3764,00	8,82	5780,00		
KD-16	1400,00	148,00	2,20	0,10	3,60	122,00	1525,00	714,00	28,00	398,00	9684,77	8,80	5835,00		meteoric
KD-20	1375,00	140,00	1,60	0,15		140,00	1159,00	710,00	24,10	367,00		8,92	6180,00		
KD-21	1318,00	133,00	2,00	1,00		140,00	1220,00	710,00	24,60	387,00		9,02	5940,00		
KD-22	1296,00	132,00	2,00	0,00		136,00	1586,00	729,00	25,00	392,00		9,20	5830,00		
R1	1556,00	245,00	2,67	0,23		134,00	3074,00	792,00	30,00	416,00		8,80	5820,00		
R2	1290,00	110,00	1,60	0,80		137,00	2257,00	810,00	20,40	380,00		9,30	5320,00	HCO_3 constituting CO_2	meteoric
R3	1225,00	104,00	2,48	1,00		140,00	1787,00	850,00	17,00	227,00	4545,18	8,70	4600,00	Na-HCO_3 constituting B	meteoric
AP 2	1272,00	196,00	3,27	1,00	7,70	276,00	2519,00	180,00	30,00	336,00	5041,12	8,50	5100,00	Na-HCO_3 constituting B and F	meteoric
AP 3	1660,00	170,00	9,50	2,45	7,30	293,00	3378,00	222,00	4,80	182,00	5975,13	8,60	4970,00	Na-HCO_3 constituting F	meteoric
NG 1	1014,00	94,30	5,88	9,79	0,10	150,00	2531,00	180,00	24,00	29,00	4078,67	8,30	3890,00	Na-HCO_3 constituting B, K and Si	meteoric
NB 1	1400,00	98,10	15,40	8,31	15,00	256,00	2830,00	176,00	40,30	133,00	5079,73	8,30	5120,00	Na-HCO_3 constituting B, F and Si	meteoric
AT 1	1074,00	111,00	3,66	1,61	15,40	190,00	2384,00	130,00	48,00	107,00	4207,12	8,40	4280,00	Na-HCO_3 constituting B and Si	meteoric
İS 1	215,00	14,40	10,20	2,21	1,10	16,70	463,00	125,00	0,10	48,60	908,90	7,40	901,00	Na-Cl-HCO_3	meteoric
SH 1	1134,00	117,00	6,30	1,00	9,65	263,00	2361,00	243,00	57,00	176,00	4619,70	8,70	4710,00	Na-HCO_3 constituting B and Si	meteoric
SH 2	1156,00	96,00	4,70	1,00	18,20	205,00	2111,00	182,00	50,00	162,00	4310,90	8,70	4480,00	Na-HCO_3 constituting B and Si	meteoric
ASR 2	1420,00	109,00	11,80	0,27	8,00	238,00	2705,00	193,00	6,50	191,00	9415,10	8,60	4350,00	Na-HCO_3	meteoric
ASR 3	1047,00	180,00	3,59	2,14	10,00	245,00	2628,00	117,00	50,00	223,00	4505,73	8,30	4390,00	Na-HCO_3 constituting B and Si	meteoric
AS 1	1159,00	144,00	4,36	2,89	5,90	228,00	2658,00	133,00	46,90	203,00	4966,94	8,70	3499,00		meteoric
AS 2	1175,00	133,00	4,00	2,20	5,30	216,00	2706,00	130,00	60,40	227,00	4668,07	8,60	4600,00		meteoric
AU 1	1602,00	131,00	3,80	1,00	5,90	74,40	3731,00	106,00	15,40	161,00	6086,70	8,50	5610,00	Na-HCO_3 constituting B and Si	meteoric
AU 2	1250,00	99,00	4,10	3,50	14,70	233,00	2840,00	101,00	52,50	144,00	4758,20	8,20	5000,00	Na-HCO_3 constituting B, F and Si	meteoric
ASK 1	1123,00	136,00	2,02	3,58	11,70	237,00	2607,00	105,00	66,20	159,00	4478,30	8,20	4300,00	Na-HCO_3 constituting B, F and Si	meteoric
AY 1	1002,00	103,00	104,00	49,00		290,00	3019,00	117,00	62,00	240,00	6865,00	6,50	5150,00	Na-HCO_3 -H_2CO_3 constituting B and Si	
AY 2	1130,00	160,00	10,00	40,00		220,00	3010,00	100,00	43,70		4610,00				
Ayter 1	1560,00	144,00	60,00	34,00	23,00	220,00	4058,00	104,00	45,00	64,00	6441,00	8,07	6000,00	Na-HCO_3-SO_4	meteoric
Ayter 2	1080,00	128,00	22,00	43,00	19,00	203,00	2952,00	117,00	39,00	75,00	4684,00	8,20	3700,00	Na-HCO_3-SO_4	meteoric
A 2	1085,00	78,00	23,40	56,50	16,90	954,00	1914,00	148,00	48,40	71,00	4459,51	7,71	4894,00	Na-Cl-HCO_3	meteoric
OB1	1355,00	45,00	50,00	16,00	3,81	1586,00	1172,00	37,00	45,00	140,00	7034,40		7000,00	Na-Cl-HCO_3	meteoric
OB2	1830,00	189,00	1,60	0,00	8,74	1359,00	1525,00	71,00	71,00	160,00	7277,40	9,00	7200,00	Na-Cl-HCO_3	meteoric
OB3	1775,00	170,00	1,60	0,50	4,80	1818,00	1342,00	74,00	68,00	55,00	4720,00	8,70	7100,00		
OB4	1420,00	135,00	12,00	1,70	32,10	1500,00	1440,00	37,00	55,00	53,00		7,70	5400,00		
OB5	1387,00	128,00	8,40	6,80	9,60	1454,00	1409,00	46,00	56,00	209,00		8,40	3000,00		

Table B 1: continued.

Well Name	Na (mg/l)	K (mg/l)	Ca (mg/l)	Mg (mg/l)	NH_4 (mg/l)	Cl (mg/l)	HCO_3 (mg/l)	SO_4 (mg/l)	B (mg/l)	SiO_2 (mg/l)	TDS (mg/l)	pH	EC (µS/cm)	Water Type	Water origin
OB6	1775,00	180,00	3,60	0,10	9,30	1882,00	1202,00	64,00	74,00	41,00	6319,02	8,70	6200,00	Na-HCO_3-Cl	meteoric
OB7	1100,00	132,00	19,00	6,10	1,00	855,00	1837,00	51,00	56,00	214,00		7,53	4200,00		
OB8	1550,00	15,00	8,00	2,43		1528,00	1317,00	45,00		286,00	4607,14	8,80	6600,00		
OB9	1750,00	105,00	4,80	1,20	11,30	1819,00	1376,00	133,00	68,00	286,00	4485,80	8,60	6500,00		
HB 1	1554,00	104,00	6,03	18,10	19,50	1501,00	1699,00	43,60	56,10	64,00	5197,47	8,30	6040,00	HCO_3 constituting B and Si	meteoric
HB 2	1369,00	97,90	16,20	1,21	0,00	1399,00	1541,00	25,09	50,00	201,00	4745,40	8,10	5510,00	HCO_3 constituting B and Si	meteoric
HB 7	1352,00	126,40	6,33	7,24		1436,80	1140,00	44,00	62,84	253,30	4621,67	8,61	6760,00		
GM 2	1654,00	100,80	23,81	11,54		2550,42	700,00	50,11	63,43	255,22	5425,35	8,13	6930,00		
GK 1	516,00	40,60	177,00	35,00	2,68	667,00	960,00	24,00	6,10	64,00	2430,00	6,80	3568,00		meteoric and sea water
AGG 16	3014,00	185,00	16,40	8,00	9,30	575,00	7320,00	16,40	21,20	25,90	11202,80	7,60	10430,00	Na-HCO_3 constituting B and F	
Davutlar	2200,00	99,00	460,00	99,60		3000,00	1637,00	119,80			7615,40	6,36	9730,00	Na-Cl-HCO_3	meteoric and sea water